NTNU – Trondheim
Norwegian University of
Science and Technology

Small Water Plane Area Solutions for Access of Offshore Wind Turbines

Heine Grøtting

Marine Technology
Submission date: June 2015
Supervisor: Jørgen Ranum Krokstad, IMT

Norwegian University of Science and Technology
Department of Marine Technology

NTNU – Trondheim
Norwegian University of
Science and Technology

Small Water Plane Area Solutions for Access of Offshore Wind Turbines

Heine Grøtting

June 10, 2015

MASTER THESIS

Department of Marine Technology
Norwegian University of Science and Technology

Supervisor: Professor 2 Jørgen Ranum Krokstad

NTNU – Trondheim
Norwegian University of Science and Technology

MASTER THESIS IN MARINE TECHNOLOGY

SPRING 2015

FOR

STUD.TECHN. HEINE GRØTTING

Small Water Plane Area Solutions for Access of Offshore Wind Turbines

Department of Marine Technology
Norwegian University of Science and Technology

Many new and novel access vessel designs have evolved during the last years as a consequence of an innovation push towards more cost efficient offshore wind turbine operation and maintenance. One of the challenges in addition to cost reduction is to develop safe and weather robust access and entrance solutions with the ability to efficiently operate far offshore. Statkraft and Statoil are investigating the robustness of access systems for the Dogger Bank offshore wind parks using a combination of mother- and standalone vessels. The transfer system or gangway may be crucial for the operability of such systems but will in reality be designed as a balance between vessels motion capability and the need to safely compensate all dangerous loads and motions of the transfer system. In addition to personal transport there are a functional need to transport increasingly heavy equipment and turbine parts without using high capacity and expensive jack-ups.

The thesis will investigate novel developments of small water plane vessels due to its robustness against complex weather conditions. With emphasize on cost efficient semis, swaths or other means of small water plane vessels a concept will be developed and investigated thoroughly by comprehensive hydrodynamic analysis to document weather robustness against complex directional sea and conditions.

The thesis will both address functional requirements and modelling of accept criteria by performing frequency and possible time domain hydrodynamic analysis. Possible novel design of access vessel will be simulated against the wave environment at Dogger Bank. This is aiming to model the complexity of the directional interaction and demonstrate robustness against such. The thesis will involve:

1. Functional specification of access vessels with small water plane and selection of one concept for further in depth studies.
2. Establish a suitable coupling system balancing the cost and capabilities of the vessel.
3. Establish weather constrains and discuss what parameters that needs to be included.
4. Establish a hydrostatic and hydrodynamic numerical basis by using SESAM HYDRODYN or ShipX tools. Analyze limiting sea states with different number of parameters with either Matlab developed frequency domain tools and/or SIMO time domain tools. Investigate the effects of some key parameters.
5. Investigate possible benefits of more complex accept criterias including several parameters.
6. Investigate the relevance and accuracy of frequency versus time domain hydrodynamic analysis including transfer system.
7. Verify different numerical approaches by comparisons.
8. Compare any small water plane vessel designs against state of the art catamaran access vessel performance

The work scope may prove to be larger than initially anticipated. Subject to approval from the supervisor, topics may be deleted from the list above or reduced in extent.

In the thesis the candidate shall present her personal contribution to the resolution of problems

within the scope of the thesis work. Theories and conclusions should be based on mathematical derivations and/or logic reasoning identifying the various steps in the deduction. The candidate should utilise the existing possibilities for obtaining relevant literature.

The thesis should be organised in a rational manner to give a clear exposition of results, assessments, and conclusions. The text should be brief and to the point, with a clear language. Telegraphic language should be avoided.

The thesis shall contain the following elements: A text defining the scope, preface, list of contents, summary, main body of thesis, conclusions with recommendations for further work, list of symbols and acronyms, references and (optional) appendices. All figures, tables and equations shall be numbered.

The supervisor may require that the candidate, in an early stage of the work, presents a written plan for the completion of the work. The plan should include a budget for the use of computer and laboratory resources which will be charged to the department. Overruns shall be reported to the supervisor.

The original contribution of the candidate and material taken from other sources shall be clearly defined. Work from other sources shall be properly referenced using an acknowledged referencing system.

The thesis shall be submitted in electronic form:

- Signed by the candidate
- The text defining the scope included
- Drawings and/or computer prints which cannot be bound should be organised in a separate folder.

Supervisor: Professor 2 Jørgen Ranum Krokstad

Deadline: June 10th 2015

Preface

This report is submitted to fulfill the requirement to the degree of Master of Science in Marine Technology at the Norwegian University of Science and Technology (NTNU). The scope of the work is developed together with my supervisor Professor II Jørgen Ranum Krokstad. The background of the project is the development of offshore wind turbine parks at Dogger Bank outside of England.

The thesis has introduced me to practical applications of my knowledge in hydrodynamics, as well as new knowledge in fields I was not familiar with before. The workload has been heavy and from time to time quite demanding. Especially the task of obtaining quality information has been challenging. However, not a lot of research has been done in the area of fender docking onto an offshore wind turbine, and I hope that some of the ideas presented in this thesis can be a little contribution to make the offshore wind industry competitive without subsidies in the future.

A lot of people have helped me throughout this thesis. I would like to thank the educational personnel at the NTNU department of marine technology for having patience and knowledge enough to answer my questions, the library staff for being very helpful in the search for literature as well as the technical staff that makes a great effort to lay the conditions for a great learning environment. A well deserved thanks also goes to my colleagues at office A1.019, commonly known as " Hydrodynamisk Hjørnekontor", whom have helped me through the long nights and weekends at the university.

Last but not least, I thank Professor Dag Myrhaug for his guiding in the field of statistics and Statkraft for financing a excursion to the Smøla wind farm. Finally, a special thanks to my supervisor Professor II Jørgen Ranum Krokstad for helping and guiding me through this thesis.

Trondheim June 10, 2015
Heine Grøtting

Summary

In 2014, 536 offshore wind turbines were installed on European shelf, connecting an average of 5.9 MW to the grid every day. About two thirds of this were installed in the North Sea. This new and emerging market represents an opportunity for Norway to make use of our knowledge about marine operations in the North Sea from the petroleum industry. In this thesis the operation of accessing the wind turbine to transfer personnel and parts is investigated. Due to maintenance and unexpected repair the wind turbine needs to be accessed by technicians about three times per year.

Hence, for a wind farm of some size, the access operation is done a significant amount of times per year. The lack of a sufficient robust and cheap way to do this has proven a costly problem for the industry. Another problem is how to analyse and compare different access concepts. Time domain simulations as widely used in the offshore petroleum industry are time consuming and expensive, as you in principle should find one limiting H_s for all combinations of peak period and wave direction each concept will encounter to do a fair comparison. Therefore, MARINTEK's MingKang Wu in 2014 proposed a efficient way to calculate the limiting significant wave height for all combinations of peak period and wave direction in the frequency domain.

At Dogger Bank location two, the moderate sea states where access is realistic have peak periods in the area of 5 to 9 seconds. Having a small water plane area vessel designed to have low responses in this frequency area, such as a SWATH or a mini semi-submersible might be a good access solution on such a location. There is different strategies on how to access the wind turbine, fender docking is a popular choice today due to its simplicity and lack of vulnerable expensive parts. Considering its superior velocity to the semi-submersible, a SWATH concept with fender docking was chosen for further analysis. The concept was inspired by the FOB SWATH used by Oddfjell Wind AS and has been created and analysed in VERES. Further, fender docking with this vessel was analysed with a MATLAB program containing the frequency domain method proposed by Wu (2014) and in the time domain simulation software SIMO.

This thesis have three focus points, which this SWATH concept has been used to investigate. Firstly, to explore what parameters that should be included in the accept criteria for initiating the access operation. It was found that the limiting significant wave height depend on both peak period and direction of the wave environment. Hence, it is recommended to step away

from the industry standard of considering limiting H_s as a constant value, and consider limiting H_s as a function of T_p andβ.

The second were to explore the potential of small water plane area solutions. It was found that it is feasible to design a SWATH to maximize its performance in a specific wave environment. The producers of classical work boat catamarans claims that their vessels can access an offshore wind turbine in H_s up to 1.5 m without considering T_p nor wave direction. Comparing this with the results from the Matlab program and SIMO, the SWATH concept analysed can not outperform this. One should nevertheless have in mind that as this is not a design thesis, the concept investigated is not optimized and that a optimized vessel surely would outperform the SWATH considered here. As well there is a chance that the limit of 1.5 m H_s typically given by the manufacturers is somewhat optimistic. It might for instance only be valid in favorable combinations of T_p and β, this belief is supported by wind farm owners reporting of work boats not being able to perform as promised in all sea states.

The last focus point was to verify the method proposed by Wu (2014) by time domain simulation in SIMO. The method has not been verified, the results obtained by the use of Wu (2014) and time domain simulation in SIMO had large deviations. It was found that the simplification done by Wu that the propeller thrust works in the global x-direction directly in the fender point, at least is one of the reasons why the method underestimate the risk of slip. In the end of chapter three a frequency domain method where the propeller thrust is directed along the local x-axis is proposed.

To improve the modelling of fender docking, one should improve the understanding of how the fenders dynamic and static coefficient depend on pressure, temperature, slip velocity and humidity. Another improvement would be to investigate whether diffraction effects from the wind turbine needs to be included in the analysis.

Sammendrag

I 2014, 536 vindturbiner ble installert på europeisk sokkel. I gjennomsnitt ble daglig 5.9 MW installert. De fleste av disse ble installert i Nordsjøen. Dette nye markedet i sterk vekst er en mulighet for Norge til å benytte ekspertisen om marine operasjoner i Nordsjøen som har bygget seg opp takket være oljeindustrien. I denne oppgaven er det fokus på operasjonen å koble seg til vindturbinen for å overføre personell og deler. Grunnet vedlikehold og uforutsette reperasjonsbehov er det behov for å overføre teknikere til vindturbinen rundt tre ganger årlig.

For en vindfarm av en viss størrelse, vil det årlig være behov for et stor antall tilkoblinger. Mangelen på en tilstrekkelig robust og rimelig måte å gjøre dette på er et kostbart problem for industrien. Et annet problem er hvordan å analysere og sammenligne forskjellige løsninger og fartøy. Tidsdomeneanalyser som er utbredt i oljeindustrien er tidkrevende og dyre fordi man strengt tatt bør finne en begrensende H_s for alle kombinasjoner av topp-periode og bølgeretning fartøyene vil møte for å kunne gjøre en rettferdig sammenlikning. Som et svar denne problematikken foreslo Wu (2014) en effektiv metode for å beregne begrensende H_s for alle kombinasjoner av topp-periode og bølgeretning i frekvensdomenet.

På Doggerbank lokasjon 2 har de moderate sjøtilstandene hvor tilkobling til vindturbinen er realistisk en topp-periode på mellom 5 og 9 sekunder. Et fartøy med lite vannlinjeareal designet til å ha lav respons i dette frekvensområdet, slik som en såkalt SWATH eller en mini semi-sub vil kunne være et godt valg som fartøy i dette området. Det finnes forskjellige strategier på hvordan å koble seg til vindturbinen, tilkobling med fender er utbredt idag trolig på grunn av metodens enkelhet og at ingen kostbare skjøre deler er involvert. Grunnet den overlegne hastigheten en SWATH har i forhold til en mini semi-sub er det SWATH-konseptet som ble valgt for videre analyse. Et SWATH-konsept inspirert av Oddfjell Wind AS sin FOB SWATH er blitt designet og analysert i VERES. Videre, ble tilkobling med fender analysert i MATLAB med metoden foreslått av Wu (2014) og i tidsdomenet med simulasjonsverktøyet SIMO.

Denne oppgaven har 3 hovedpunkter, som dette SWATH-konseptet har blitt brukt til å utforske. Det første, hvilke parametere som bør bli inkludert i aksepkriteriet for å starte tilkoblingsoperasjonen. Det ble kommet frem til at begrensende H_s avhenger av både topp-perioden og retningen til sjøtilstanden. Dermed er det anbefalt å gå vekk ifra bransjestandarden med å se på begrensende H_s som en konstant verdi, og heller se på begrensende H_s som en funksjon av T_p og β.

Dernest var det et mål å utforske potensialet til fartøy med lite vannlinjeareal. Det ble funnet at å tilpasse disse til å yte maksimalt i et spesifikt bølgemiljø er fullt mulig. Produsenter av arbeidskatamaraner som er utbred i bransjen idag hevder at deres båter kan operere i en H_s opp til 1.5 m, uten tanke på hverken T_p og β. Når man sammenlikner dette med resultatene ifra analysene i SIMO og i MATLAB, presterer SWATH-konseptet brukt her dårligere. Dog bør man tenke på at dette ikke er en designoppgave, SWATH-designet som er benyttet er ikke optimert og et optimert SWATH-konsept ville uten tvil ha utkonkurrert konseptet som brukes i denne oppgaven. I tillegg er det en viss risiko for at grensen på H_s=1.5 m typisk gitt av produsentene av arbeidskatamaraner er noe optimistisk. For eksempel at den kun gjelder i fordelaktige kombinasjoner av T_p og β, dette synet støttes av vindfarmeiere som rapporterer om arbeidsbåter som ikke er i stand til å prestere som lovet.

Det siste hovedpunktet var å verifisere metoden foreslått av Wu (2014) med simulasjoner i SIMO. Metoden har ikke blitt verifisert , resultatene funnet med denne metoden viste store avvik med resultatene ifra SIMO. Det ble funnet at forenklingen gjort av Wu at kraften ifra propulsjonssystemet virker i global x-retning, i det minste er en av grunnene til at hans metode undervurderer risikoen for slip. I 3.4 er det foreslått en frekvensdomenemetode hvor kraften ifra propulsjonssystemet er antatt å virke langs den lokale x-aksen.

For å forbedre evnen til modellere tilkobling med fender, er det viktig å øke forståelsen av hvordan fenderen sin statiske og dynamiske friksjonskoeffisient avhenger av trykk på fenderen, temperatur , glidehastighet og fuktighet. En annen forbedring ville vært å øke kunnskapen rundt betydningen av diffraksjonseffekter ifra selve vindturbinen.

Contents

List of Figures

List of Tables

Nomenclature

$\alpha(\omega, \beta)$ Variable measuring if upwards slip will happen

$\alpha_{transf}(\omega, \beta)$ Transfer function of the variable α, measuring if upwards slip will happen

β Wave direction[deg]

β_s Wave direction of swell[deg]

β_w Wave direction of wind generated sea[deg]

$\chi(\omega, \beta)$ Variable measuring if rightwards slip will happen

$\chi_{transf}(\omega, \beta)$ Transfer function of the variable χ, measuring if rightwards slip will happen

$\eta(\omega, \beta)$ Variable measuring if downwards slip will happen

$\eta_{transf}(\omega, \beta)$ Transfer function of the variable η, measuring if downwards slip will happen

γ Peakedness factor in the JONSWAP spectrum

μ Friction coefficient between wind turbine and fender

ω Wave frequency[rad/s]

$\psi(\omega, \beta)$ Variable measuring if leftwards slip will happen

$\psi_{transf}(\omega, \beta)$ Transfer function of the variable ψ, measuring if leftwards slip will happen

ρ Sea water density $[kg/m^3]$

θ_{max} Maximum acceptable roll angle[deg]

ζ_a Wave amplitude[m]

$A(\omega)$ Frequency dependent added mass matrix

A_{2specW} Total winter availability obtained by dividing each sea state into swell and wind generated waves[-]

A_{2spec} Total availability obtained by dividing each sea state into swell and wind generated waves[-]

A_{jonW} Total winter availability with use of JONSWAP spectrum[-]

A_{jon} Total availability with use of JONSWAP spectrum[-]

A_{tmaW} Total winter availability with use of TMA spectrum[-]

A_{tma} Total availability with use of TMA-spectrum[-]

B Width of Ship [m]

$B(\omega)$ Frequency dependent damping matrix

B_{visc} Additional linearized viscous damping in heave and pitch[N]

C Hydrostatic stiffness matrix

C_d Drag coefficient [-]

$D(x)$ Width of SWATH pontoon

D_{CAT} Draft of ship in catamaran mode [m]

D_{SWATH} Draft of ship in SWATH mode [m]

$disA$ Part of sea states approved by the TMA-spectrum approach that was not approved by the two spectrum approach[-]

$F(\omega, \beta)$ Vector containing excitation forces

F_{3visc} Viscous excitation force [N/m]

F_b Bollard push force [N]

F_{visc} Additional viscous excitation force[N]

F_{zc} Constant vertical force working in the fender

h Water depth[m]

H_s Significant wave height [m]

H_sS Significant wave height of swell part of sea[m]

H_sW Significant wave height of wind generated part of sea[m]

k Wave number[rad/m]

k_x X part of wave number[rad/m]

k_y Y part of wave number[rad/m]

L_t Vertical distance between propeller thrust and fender point

L_{oa} Length overall of Ship[m]

L_{wl} Length in waterline of Ship[m]

M Mass matrix

N_{acc1yr} Number of access operations during a year[-]

$P(\omega, \beta)$ Vector containing forces and moments in fender point

P_{1cycle} Acceptable probability of incident during one cycle[-]

P_{apf} Part of wind industry fatalities caused by access[-]

P_{facc} Acceptable expected number of slips during one access operation[-]

P_{ffa} Probability of fatality for a fender slip[-]

P_{inc} Probability of incident during one cycle[-]

$r(\omega, \beta)$ response vector

$r_{1point}(\omega, \beta)$ Translational motion at fender point

R_{acc} Acceptable risk of fatalities in power production[fatalities/TWh]

$R_{transf}(\omega, \beta)$ Roll transfer function with vessel coupled to turbine

RAO Response amplitude operator

T_p Peak period [s]

T_pS Peak period of swell part of sea[s]

T_pW Peak period of wind generated part of sea[s]

t_{acc} Length of access operation [s]

t_{expinc} Expected time to first incident in time domain[s]

t_{exp} Expected time to first incident from frequency domain calculations [s]

t_{inc} Time to first incident in time domain[s]

TOW_{1yr} Total 1 year power production of offshore wind in Europe [TWh]

v Vertical velocity $[m/s]$

WS Wave seed

X_{acc} Distance from center center of gravity to fender

Chapter 1

Introduction

In Europe 2014, 536 wind turbines were erected offshore, an average of 5.9 MW per day. 63.3% of the installed capacity were installed in the North Sea ,Corbetta and Mbistrova (2015). This new and emerging market represents an opportunity for Norway to make use of our knowledge about marine operations in the North Sea from the oil and gas industry. This thesis will take a look into the problem of transferring personnel and equipment to offshore wind turbines with relatively small vessels using fender docking. The downtime of wind turbines while waiting for weather windows is one of the major contributors to loss of production, and hence income. The potential for savings with the development of new and innovative access systems is therefore significant.

The current practice when specifying weather windows for access of an offshore wind turbine is not based on the vessel behaviour during the operation, but simply the significant wave height (H_s). Given acceptable H_s the captain of the service vessel decides whether safe access can be made or not, this is of course a subjective decision no matter how competent and experienced the captain is. One might argue that a better solution would be to define the accept criteria as the probability of failure for the specific vessel in the specific sea state.

For an access system with fender docking, the seakeeping of the vessel is a key factor. One strategy to avoid large motions is to design the vessel to have natural periods away from typical wave periods. This is the strategy behind small water plane area concepts, which is investigated further in this thesis. To do this the proposed method by Wu (2014) is used to numerically analyse the access operation. The frequency domain method is written in a MATLAB script. The results are validated by time domain analysis in SIMO.

This thesis will have three focus points, to explore the potential of small water plane area solutions for access of offshore wind turbines, to explore what parameters a accept criteria should contain and to validate the frequency domain method proposed by Wu (2014) with time domain simulations in SIMO. Emphasis will be made on making the thesis as structured and orderly as possible. In chapter one, the problem is introduced together with how it is investigated. Chapter two contain background information about the offshore wind industry in general, discussion on what specifications a access concept must have and the relevance of small water plane area concepts regarding this. In chapter 3, the methods for obtaining the results are described. Chapter 4 contain the results together with some simple observations. Interpretation and discussion of the results is saved for chapter 5. Finally, the conclusion and proposals for future work is the topic for chapter 6.

Chapter 2

Background

2.1 The offshore wind market

In eleven countries across Europe , at 74 different offshore wind farms the total number of wind turbines connected to the electricity grid reached 2488 in 2014. A total installed capacity of 8045.3 MW, with a predicted production of 29.6 TWh in a normal wind year. About 1% of the EU's total electricity consumption. This is according to Corbetta and Mbistrova (2015). The level of annual installed capacity is showed in the following figure.

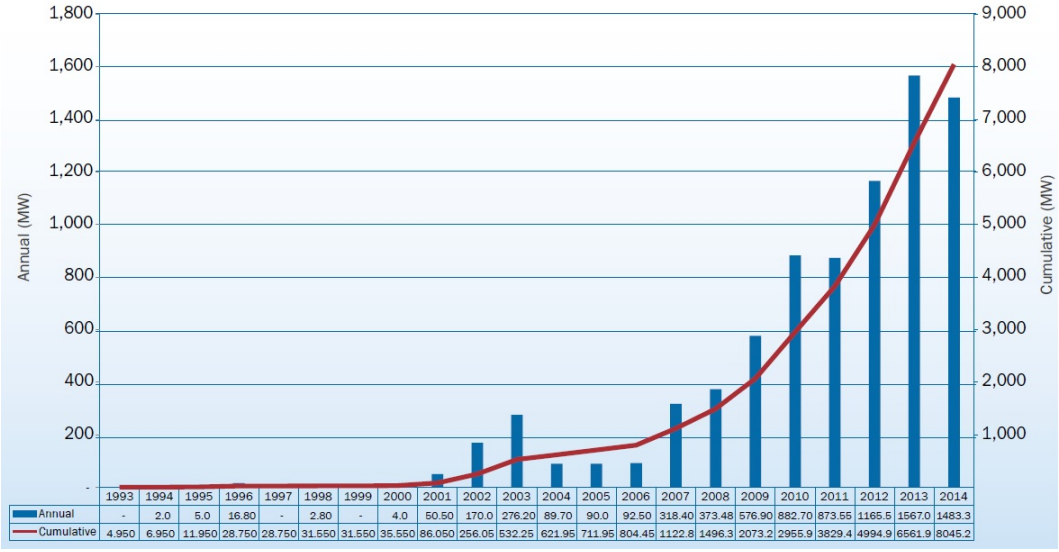

	1993	1994	1995	1996	1997	1998	1999	2000	2001	2002	2003	2004	2005	2006	2007	2008	2009	2010	2011	2012	2013	2014
Annual	-	2.0	5.0	16.80	-	2.80	-	4.0	50.50	170.0	276.20	89.70	90.0	92.50	318.40	373.48	576.90	882.70	873.55	1165.5	1567.0	1483.3
Cumulative	4.950	6.950	11.950	28.750	28.750	31.550	31.550	35.550	86.050	256.05	532.25	621.95	711.95	804.45	1122.8	1496.3	2073.2	2955.9	3829.4	4994.9	6561.9	8045.2

Figure 2.1: Cumulative and annual offshore wind installations(MW), Corbetta and Mbistrova (2015)

One can see that the annual installed capacity reached a top in 2013, it is expected to be at the same level in 2015 as in 2014 while a reduction is anticipated in 2016.

Looking further forward, the European Wind Energy Association has identified consented plans for a total of 26.4 GW installed capacity, Corbetta and Mbistrova (2015). It is nevertheless important to have in mind that per today the offshore wind industry depend on subsidies, and that cutting costs through innovation is an absolute necessity for the industry to develop further. As can be seen from the figure to the right, the main players in the offshore wind industry are Denmark, Germany and Great Britain. Norway is involved through Statkraft and Statoils role as wind farm owners, but only with a total 3.5% ownership of the total installed capacity today according to Corbetta and Mbistrova (2015). Hence in Europe, Norway is per today not a significant player in the offshore wind industry.

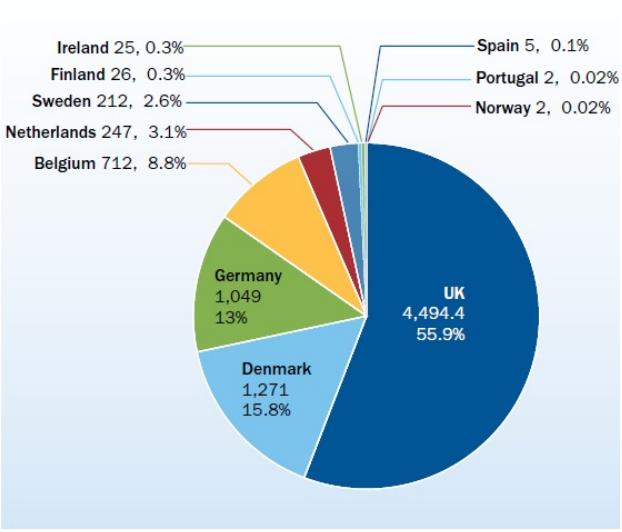

Figure 2.2: Installed capacity by country, Corbetta and Mbistrova (2015)

2.2 O&M of offshore wind farms

With several moving parts and high cyclic loads, a wind turbine demands carefully planned maintenance and inspection. Land based wind turbines has planned maintenance 3 times a year, in addition comes unexpected needs for repairs and so on. Experience from Sheringham Shoal shows that even though the ambition was to only access the mill 2 times a year, according to Nielsen (2014) the need is about three in reality. With the need of three yearly accesses and 2488 offshore wind turbines in Europe, the annual number of accesses is around 7500. This indicates the market potential of robust and cost efficient access systems. As well, it indicates the benefits of improving the maintenance intervals.

2.3 Operational criteria of access systems

Ocean waves is a stochastic process and for a given sea state and vessel one can in principle not guarantee towards failure, one can only calculate the probability for failure. To define the operational criteria is therefore to decide on a acceptable probability for failure. This is more a ethical than technical issue and well beyond the scope of this thesis, nevertheless some general thoughts will be given.

As an accident during access will have a significant risk of fatalities, the operational criteria should be defined by the governing authorities, and not by each wind farm owner. No company should have a competitive advantage by exposing their technicians to more danger. As can be seen by the figure to the right, all kinds of power production involves some kind of risk for fatalities. Major accidents of the hole world are included. The column for hydro power is so high due to a few very major events, mainly the Henan disaster in China where the estimate of fatalities range between 30 000 and 230 000.

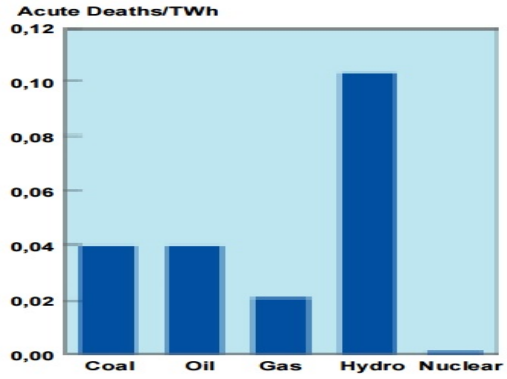

Figure 2.3: Deaths from major accidents per TWh 1969-1996 Starfelt et al. (2005)

A more natural number to compare with would be the number of deaths per TWh caused by severe accidents in OECD countries in the natural gas industry, which in the period 1969-2000 is 0.01, claimed by the World Nuclear Association. As natural gas is a direct competitor of offshore wind it seems reasonable to compare. Still, safety levels in the natural gas industry is likely to have improved during the years. Number of fatal work related accidents in Norway have according to Brekken (2012) been reduced by around 50% since the 1980s , as a coarse assumption one might assume that this improvement is representative for the natural gas industry as well. Further, as discussed in Tveiten (2011), other operations than access are causing accidents in the offshore wind industry. Such as diving accidents, falling objects and capsizing of jack-up vessels as examples.

The author has not been able to find data about the percentage of offshore wind industry

fatalities that are caused by accidents due to failed access, so as a coarse approximation 60% is assumed. From Corbetta and Mbistrova (2015) one have that a total of 2488 wind turbines produces 29.6 TWh in a normal wind year, it is reasonable that the same accept criteria should apply no matter the effect of the turbine so average numbers needs to be used. Working under the condition that the the same level off risk is acceptable in the offshore wind industry as in other power producing industries one get the following relation

$$R_{acc} = \frac{P_{facc} * N_{acc1yr} * P_{ffa}}{TOW_{1yr} * P_{apf}} \tag{2.1}$$

And then deduce an expression for acceptable probability of failure during one access operation is an easy task.

$$P_{facc} = \frac{R_{acc} * TOW_{1yr} * P_{apf}}{N_{acc1yr} * P_{ffa}} \tag{2.2}$$

The following table shows the acceptable probability for failure during access given assumed acceptable fatality rate for power producing industries (R_{acc}), probability of fatality given fender slip (P_{ffa}) and part of fatalities in offshore wind industry caused by failed access(P_{apf}).

	R_{acc}[fatalities/TWh]	P_{ffa}[-]	P_{apf}[-]	P_{facc}[-]
Best estimate	0.005	0.01	0.6	0.00119
Conservative	0.001	0.05	0.3	0.00002
Non-conservative	0.0338	0.005	1	0.02681

Table 2.1: Calculation of acceptable probability for failure during access operation, given different assumptions

The best estimate is based on the R_{acc} discussed, the conservative estimate is based on the R_{acc}standard of nuclear power production and the non-conservative by having a expected value of one fatality during access in the offshore wind industry each year with the current installed capacity.

One should have in mind that the discussion is quite hypothetical, with the R_{acc} taken from the natural gas industry and the current level of offshore wind power production one should experience a fatal accident in Europe every seventh year or so. The risk level today in the offshore wind industry are not close to this at the moment with fatal accidents yearly, Tveiten (2011). Nevertheless this is something that has to improve as the industry matures, probably

as a combination of increased production and improved safety procedures. The P_{ffa} and P_{apf} are estimated after the authors best ability, as offshore wind is a novel industry it proved hard to find data about this. Better data will be available as the industry matures.

2.4 Small water plane area concepts

2.4.1 General

The idea behind small water plane marine crafts is to have natural periods much larger than the wave periods and hence minimize the response. One is also able to design a cancellation period where one find it beneficial by appropriately designing the difference in wet area over and beneath the pontoons.The strategy has proven successful as semi-submersibles are the preferred concept for several applications in the oil and gas industry. To the right one can see a Canadian mini semi-submersible wind farm service concept developed by ExtremeOcean Innovation. However, such a concept has a low transit speed and is dependent on having a offshore maintenance base. The internal distances in a offshore wind farm is also large enough that it limits the efficiency of such a concept. It is desired that that the vessel has a higher transit speed than a mini semi-submersible can offer.

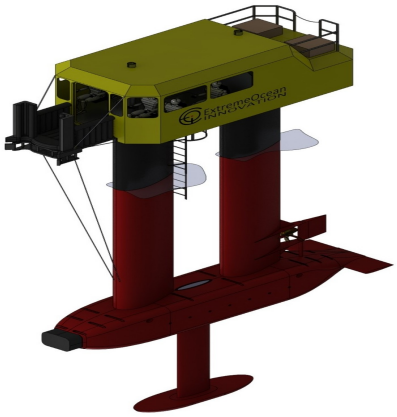

Figure 2.4: ExtremeOcean Innovations TransSPAR concept

With small water plane area twin hull vessels(SWATH) that is able to operate in catamaran-mode during transit, then change draft and enter SWATH-mode for the operation phase one might have a vessel that both have sufficient seakeeping capabilities and transit speed. The following figure illustrates the difference between SWATH-mode and catamaran-mode.

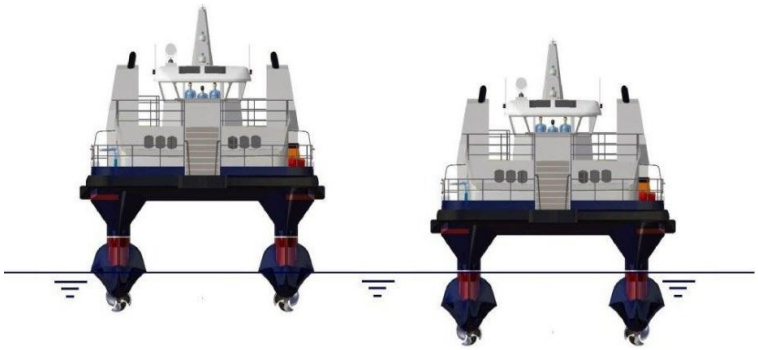

Figure 2.5: FOB Swath. Left: Catamaran mode. Right: SWATH mode. From http://www.odfjellwind.com/

2.4.2 Functional Specifications

This thesis is written with the sea conditions at Dogger Bank in mind, where the data for location 2 is used in this thesis. All wave statistics mentioned in this thesis will be taken from this location. The data is from the NORA10 hindcast made by the Norwegian Meteorological Institute. The following figure shows the joint distribution of significant wave heights and peak periods.

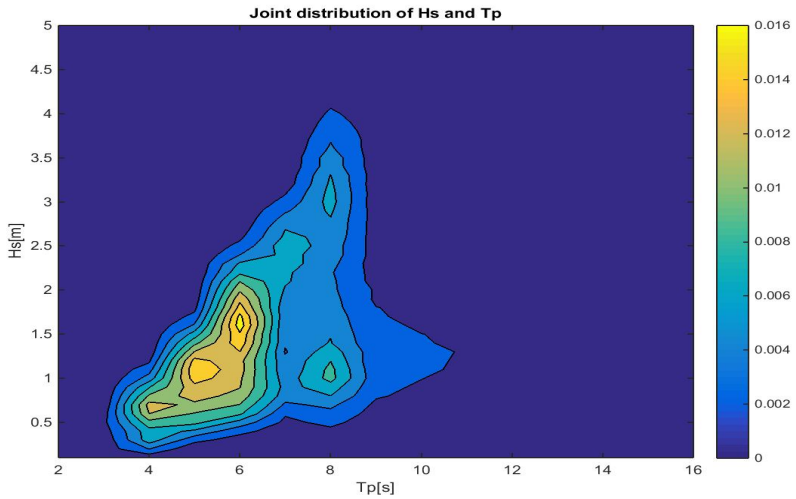

Figure 2.6: Joint distribution of significant wave heights and peak periods at Dogger Bank location 2

What one want is obviously to have a vessel that is able to do access for as large parts of the year as possible, for a cost as low as possible. It lies in the nature of the access problem that there is no need to have 100 percent availability, but one should be able to do unplanned maintenance and repairs all year round. From November to February the mean significant wave height is above 2.1 m. Novel vessel designs should be able to cope with significant wave heights of such magnitude for the most common types of sea states to make sure one have a real all-year access possibility.

It seems reasonable to assume that for all sea states with significant wave heights less than 1 m, access is always possible. And that sea states with significant wave heights up to 2.5 m is relevant for access. A access vessel should hence be optimized for sea states in this area. The distribution of peak periods at the location in question for sea states with H_s between 1 and 2.5 m is showed in the following figure.

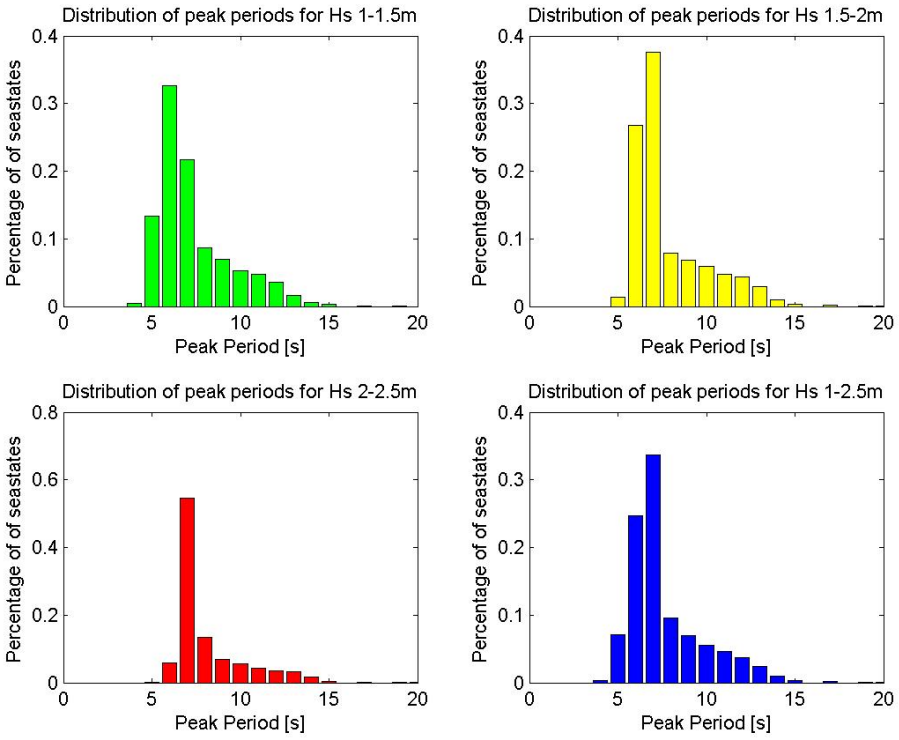

Figure 2.7: Distribution of peak periods of access relevant sea states at Dogger Bank location 2

One can observe that the peak periods are centered around 6 to 9 seconds. A vessel with

little response to waves with peak periods less than 10-12 s would be desirable. The following figure shows the cumulative distribution of peak periods for access relevant sea states.

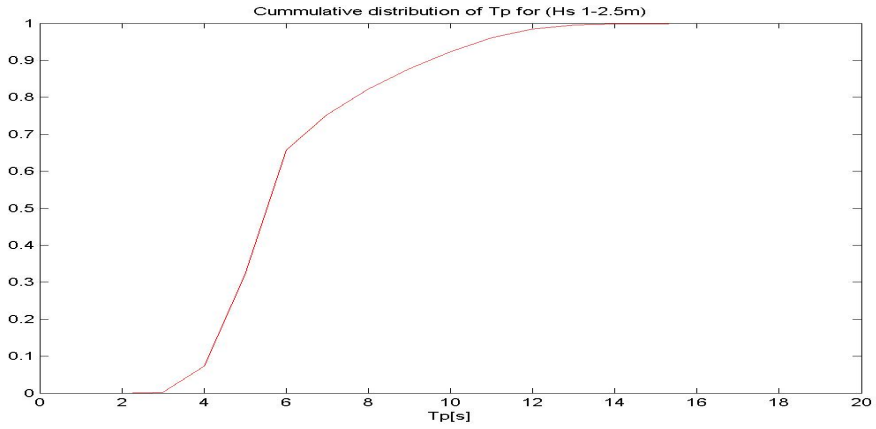

Figure 2.8: Cumulative distribution of peak periods of access relevant sea states at Dogger Bank location 2

One can imagine a system that is able to handle all sea states with Hs less than 1 m, and all sea states with Hs up to 2.5 m given a Tp of less than 12 seconds, which would result in the satisfying overall availability of 80 %.

2.4.3 Concept for further studies

According to Tveiten (2011), 69% of maintenance actions at an offshore wind farm consists of replacement of small part(man carried) or inspection. 23 % of actions involves changing a part too heavy to be carried, but weighing less than 1 ton. This means that a vessel able to perform these two operations can cover 92 % of the maintenance actions needed on a offshore wind farm. One might think of a small semi-submersible as a vessel that could deliver these services, but as it has a limited transit speed the choice for further analysis is a SWATH vessel. This is due that with this kind of vessel one can get a favorable mix between the abilities of a catamaran and those of a semi submersible. A vessel inspired by the FOB SWATH vessel operated by Oddfjell Wind AS will be used as concept vessel and analysed in ShipX. The main particulars will be as described in the following table.

L_{oa}	25 m
L_{wl}	24
B	10.6 m
D_{SWATH}	2.6 m
D_{CAT}	1.6 m

Table 2.2: Main particulars of concept vessel

Figure 2.9: FOB Swath, from http://www.odfjellwind.com/

As fender docking is the most common way to access the offshore wind turbine today as discussed in Cockburn (2010), and as the method proposed by Wu (2014) presumes fender docking. The system for further investigation in this thesis will be fender docking with a SWATH vessel, a fender docking can be seen on the following picture.

Figure 2.10: Fender docking, http://www.windcatworkboats.com/

It is easy to imagine the importance of avoiding fender slips.

Chapter 3

Method

3.1 Establishing the concept vessel

To establish the concept SWATH a function Swathdesign.m was written in MATLAB that writes a .mgf-file, the VERES file format. The function is enclosed in appendix C. To get a concept vessel as realistic as possible the product sheet available on odfjellwind.com, of the Oddfjell FOB SWATH was used as inspiration. To get smooth curves elliptic and sine functions is applied to generate body surface points. A 3-D model from VERES can be seen below.

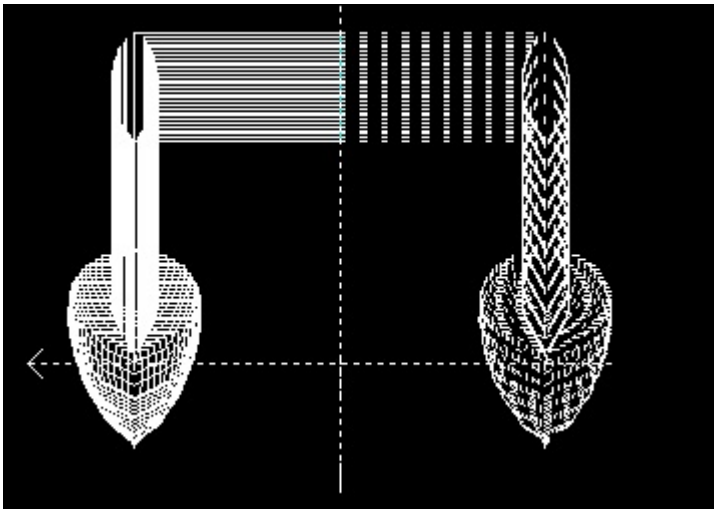

Figure 3.1: SWATH hull lines in VERES

To comply with class rules of DNV (2010), the vertical center of gravity is placed such that a transversal GM of 0.5[m] is obtained. The draft was chosen to 2.6 [m] and the area of the

top of the pontoon covered by strut was chosen to be 35%, this to obtain cancellation periods of the excitation force in heave and moment in pitch around 6 seconds.

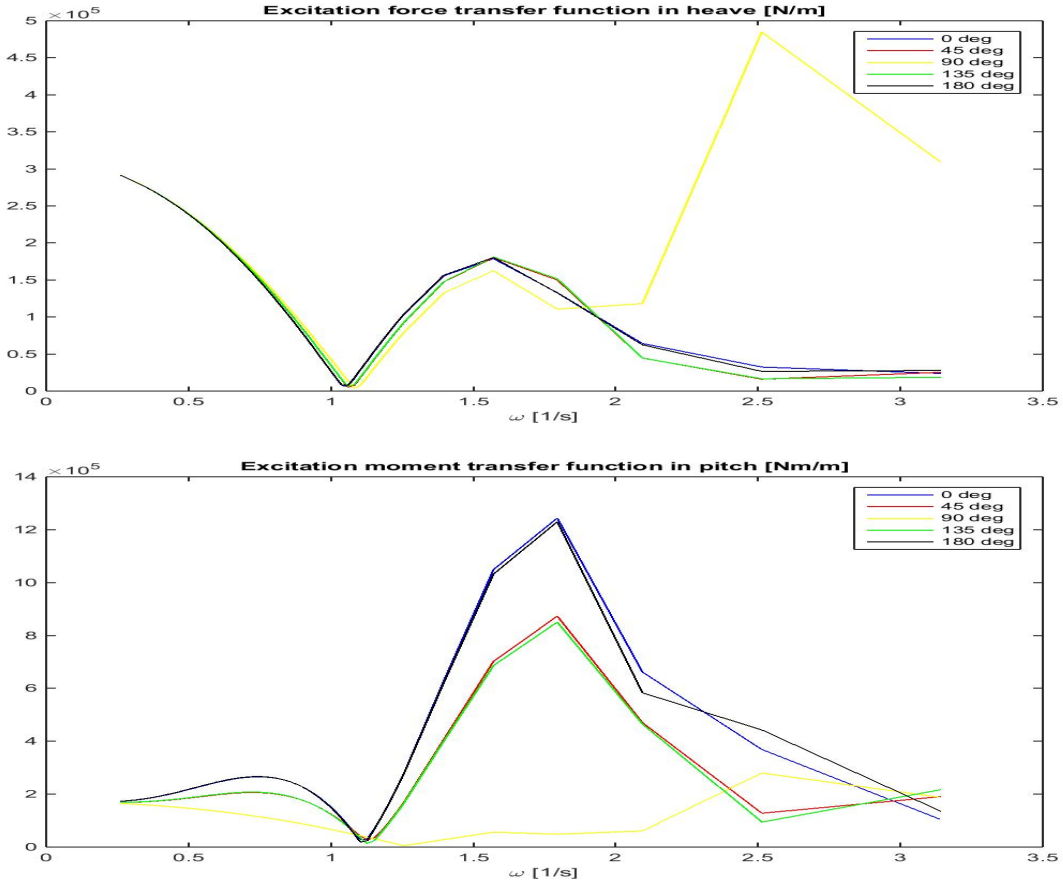

Figure 3.2: Excitation force and moment in heave and pitch

As this is not a design thesis, not many design iterations has been done and surely a optimized SWATH design would outperform the concept SWATH used in this thesis. The strip theory software VERES has been used to establish the hydrodynamical basis of the vessel. Strip theory is basically to divide the ship into a finite number of strips and consider the problem as a sum of 2-D problems. All hydrodynamical softwares are based on some simplifications and assumptions, Fathi (2004) lists the assumptions VERES is based on. The most important ones for a SWATH vessel are the following:

- No 3-D effects
- Linear relation between response and incident wave amplitude

- Potential theory can be applied(However viscous roll damping is included)
- No interactions between the hulls, for multihulls

Whether these simplifications are justifiable or not are more closely discussed in Groetting (2014), where it is concluded that these assumptions are discussable for a small access vessel together with the wave environment at Doggerbank. Although verification through experiments or panel method software seems like a good idea, this is not done in this thesis due to the limited time frame.

3.2 Analyzing fender docking of an offshore wind turbine

The docking between an offshore wind turbine and any access vessel will be executed in an environment consisting of current, wind and waves. As argued in Wu (2014) current and wind forces are relatively small compared to the wave induced forces, therefore it is reasonable to assume that fender docking is dominated by wave forces. Hence both in frequency and time domain, the problem is simplified by neglecting current and wind forces. Further it is assumed that the propulsion system of the vessel is able to give a constant forward thrust, F_b. The coordinate system used in Wu (2014) is shown below.

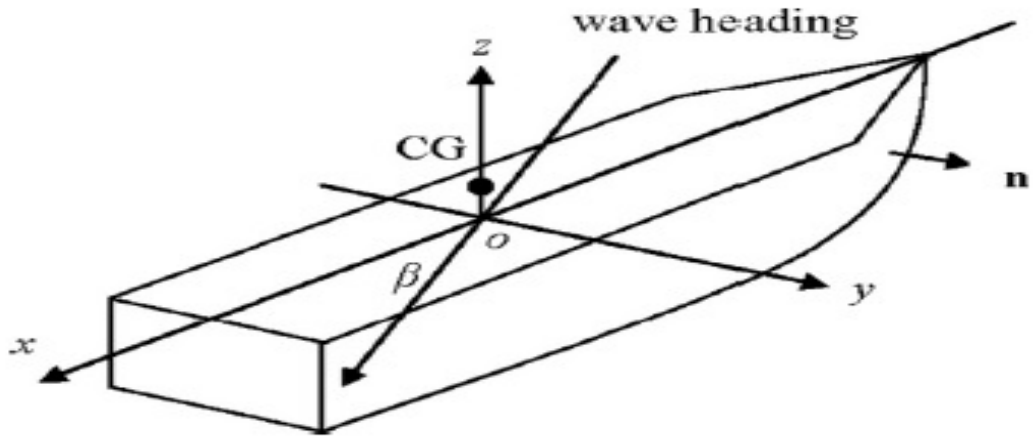

Figure 3.3: Motion coordinate system

3.2.1 Frequency domain

A MATLAB program has been written that uses the method proposed by Wu (2014) to analyse fender docking of an offshore wind turbine in the frequency domain. The code is enclosed in appendix B. Two extensions have been made, the possibility for sideways slip is included and you have the possibility to define a maximum acceptable roll angle. As well, the way you consider acceptable probability has been redefined to consider the total probability for failure instead of considering each failure mode separately. The service vessel bow is assumed to be connected to the wind turbine at a fixed fender point. By doing this it is assumed that the fender deformation is small compared to the ship motion and the dynamic effects of the fender is neglected. The vessel can freely rotate, but not have any translational motion at this point. Having $F(\omega, \beta)$ as the excitation force and $P(\omega, \beta)$ as the coupling force in the fender point one get the following dynamic equilibrium.

$$[-\omega^2(A(\omega) + M) + i\omega B(\omega) + C] * r(\omega, \beta) = F(\omega, \beta) + P(\omega, \beta) \tag{3.1}$$

$\begin{bmatrix} x_p & y_p & z_p \end{bmatrix}$ is the coordinates of the fender point relative to the local body coordinate system. To simplify the following variable is introduced:

$$G(\omega) = [-\omega^2(A(\omega) + M) + i\omega B(\omega) + C] \tag{3.2}$$

The forces and moments working on the vessel from the fender point is written:

$$P(\omega, \beta) = \begin{bmatrix} J_1(\omega, \beta) \\ J_2(\omega, \beta) \\ J_3(\omega, \beta) \\ J_3(\omega, \beta) * y_p - J_2(\omega, \beta) * z_p \\ J_1(\omega, \beta) * z_p - J_3(\omega, \beta) * x_p \\ J_2(\omega, \beta) * x_p - J_1(\omega, \beta) * y_p \end{bmatrix} \tag{3.3}$$

Dividing the response vector into sub-vectors, letting $r_1(\omega, \beta)$ be translational response and$r_2(\omega, \beta)$ be rotational response. Then the dynamic equilibrium can be rewritten to:

$$\begin{bmatrix} G_{11}(\omega) & G_{12}(\omega) \\ G_{21}(\omega) & G_{22}(\omega) \end{bmatrix} * \begin{bmatrix} r_1(\omega, \beta) \\ r_2(\omega, \beta) \end{bmatrix} = \begin{bmatrix} F_1(\omega, \beta) \\ F_2(\omega, \beta) \end{bmatrix} + \begin{bmatrix} P_1(\omega, \beta) \\ P_2(\omega, \beta) \end{bmatrix} \tag{3.4}$$

To help express the moments from the fender point as a function of the forces and the translational motion of the vessel as a function of the rotations, the transformation matrix Q is

introduced:

$$Q = \begin{bmatrix} 0 & -z_p & y_p \\ z_p & 0 & -x_p \\ -y_p & x_p & 0 \end{bmatrix} \tag{3.5}$$

This helps us write the moments from the fender on the vessel as the following:

$$P_2(\omega, \beta) = Q * P_1(\omega, \beta) \tag{3.6}$$

As shown in Faltinsen (1990), the translational motion of any point on the vessel can be expressed:

$$r_{1point} = r_1 + r_2 \times \begin{bmatrix} x_p & y_p & z_p \end{bmatrix} \tag{3.7}$$

As the translational motion at the fixed fender point is zero one get the following expression:

$$r_{1point}(\omega, \beta) = 0 = r_1(\omega, \beta) + \begin{bmatrix} 0 & z_p & -y_p \\ -z_p & 0 & x_p \\ y_p & -x_p & 0 \end{bmatrix} * r_2(\omega, \beta) \tag{3.8}$$

Which allows to express the translational motion of the ship as a function of the rotations:

$$r_1(\omega, \beta) = Q * r_2(\omega, \beta) \tag{3.9}$$

Then equation 3.4 is rewritten by replacing the moments from the fender point and the translations of the vessel with equation 3.6 and 3.9:

$$\begin{bmatrix} G_{11}(\omega) & G_{12}(\omega) \\ G_{21}(\omega) & G_{22}(\omega) \end{bmatrix} * \begin{bmatrix} Q * r_2(\omega, \beta) \\ r_2(\omega, \beta) \end{bmatrix} = \begin{bmatrix} F_1(\omega, \beta) \\ F_2(\omega, \beta) \end{bmatrix} + \begin{bmatrix} P_1(\omega, \beta) \\ Q * P_1(\omega, \beta) \end{bmatrix} \tag{3.10}$$

Solving 3.10 with respect to $P_1(\omega, \beta)$ yields

$$P_1(\omega, \beta) = H(\omega) * \Big[F_2(\omega, \beta) - Q * F_1(\omega, \beta)\Big] - F_1(\omega, \beta) \tag{3.11}$$

Where

$$H(\omega) = \Big[G_{11}(\omega) * Q + G_{12}(\omega)\Big] * \Big[G_{21}(\omega) * Q + G_{22}(\omega) - Q * G_{11}(\omega) * Q - QG_{12}(\omega)\Big]^{-1} \tag{3.12}$$

To avoid horizontally or vertically slips one need the static friction capacity to be larger than the load at any time. So the limit for slip downwards, upwards , to the left and to the right becomes:

$$J_3(t) < \mu * (F_b + J_1(t)) \tag{3.13}$$

$$J_3(t) > -\mu * (F_b + J_1(t)) \tag{3.14}$$

$$J_2(t) < \mu * (F_b + J_1(t)) \tag{3.15}$$

$$J_2(t) > -\mu * (F_b + J_1(t)) \tag{3.16}$$

Physically 3.13 can be understood as that if $J_3(t)$ demands a larger upwards force than the fenders capacity , one get a downwards slip. The same reasoning applies for the other directions of slip. Then by introducing four new variables:

$$\eta(t) = J_3(t) - \mu J_1(t) \tag{3.17}$$

$$\alpha(t) = -(J_3(t) + \mu J_1(t)) \tag{3.18}$$

$$\chi(t) = J_2(t) - \mu J_1(t) \tag{3.19}$$

$$\psi(t) = -(J_2(t) + \mu J_1(t)) \tag{3.20}$$

One get the convenient limits for slip

$$\eta(t) < \mu * F_b \tag{3.21}$$

$$\alpha(t) < \mu * F_b \tag{3.22}$$

$$\chi(t) < \mu * F_b \tag{3.23}$$

$$\psi(t) < \mu * F_b \tag{3.24}$$

These variables will be stationary, ergodic , Gaussian with zero mean. Hence the Rayleigh distribution is suitable to describe the peaks, using the standard deviation which can be found from the transfer functions of $\eta(t)$,$\alpha(t)$, $\chi(t)$ and $\psi(t)$.

$$\eta_{transf}(\omega, \beta) = J_3(\omega, \beta) - \mu J_1(\omega, \beta) \tag{3.25}$$

$$\alpha_{transf}(\omega, \beta) = -(J_3(\omega, \beta) + \mu J_1(\omega, \beta)) \tag{3.26}$$

$$\chi_{transf}(\omega, \beta) = J_2(\omega, \beta) - \mu J_1(\omega, \beta) \tag{3.27}$$

$$\psi_{transf}(\omega, \beta) = -(J_2(\omega, \beta) + \mu J_1(\omega, \beta)) \tag{3.28}$$

For a given wave spectrum then the standard deviations can be found in the following way:

$$\sigma_\eta = \sqrt{\int_0^\infty (J_3(\omega, \beta) - \mu J_1(\omega, \beta))^2 * S(\omega | H_s, T_p) d\omega} \tag{3.29}$$

$$\sigma_\alpha = \sqrt{\int_0^\infty (J_3(\omega,\beta) + \mu J_1(\omega,\beta))^2 * S(\omega|H_s,T_p)d\omega} \tag{3.30}$$

$$\sigma_\chi = \sqrt{\int_0^\infty (J_2(\omega,\beta) - \mu J_1(\omega,\beta))^2 * S(\omega|H_s,T_p)d\omega} \tag{3.31}$$

$$\sigma_\psi = \sqrt{\int_0^\infty (J_2(\omega,\beta) + \mu J_1(\omega,\beta))^2 * S(\omega|H_s,T_p)d\omega} \tag{3.32}$$

Solving 3.10 for $r_2(\omega,\beta)$ gives:

$$r_2(\omega,\beta) = (G_{21}(\omega) * Q + G_{22}(\omega))^{-1} * (F_2(\omega,\beta) + Q * P_1(\omega,\beta)) \tag{3.33}$$

The roll transfer function with the vessel coupled to the wind turbine is then the first term of $r_2(\omega,\beta)$.

$$R_{transf}(\omega,\beta) = r_2(1) \tag{3.34}$$

And the standard deviation of roll angle can be found the same way as for the slip limits.

$$\sigma_{roll} = \sqrt{\int_0^\infty R_{transf}(\omega,\beta)^2 * S(\omega|H_s,T_p)d\omega} \tag{3.35}$$

Then one can use the properties of the Rayleigh distribution as described inForbes (2010), to calculate the probability of slips and exceedance of maximum roll angle. The risk for slip for one cycle in one direction and exceedance of maximum roll angle can be expressed:

$$P_{slip} = e^{\frac{-(\mu * F_b)^2}{2\sigma^2}} \tag{3.36}$$

$$P_{\theta fail} = e^{\frac{-Rollmax^2}{2\sigma_{roll}^2}} \tag{3.37}$$

The acceptable number of incidents during one access operation was defined in 2.2. One can then establish a acceptable probability of a incident during one cycle by assuming a length of the access operation. Throughout this thesis 30 minutes is used.

$$P_{1cycle} = \frac{P_{facc} * T_p}{t_{acc}} \tag{3.38}$$

Then the following accept criteria can be established:

$$P_{1cycle} > P_{inc} \tag{3.39}$$

Where

$$P_{inc} = 1 - (1 - e^{\frac{-\theta_{max}^2}{2\sigma_{roll}^2}}) * (1 - e^{\frac{-(\mu * F_b)^2}{2\sigma_{\dot{\eta}}^2}}) * (1 - e^{\frac{-(\mu * F_b)^2}{2\sigma_{\dot{\alpha}}^2}}) * (1 - e^{\frac{-(\mu * F_b)^2}{2\sigma_{\dot{\chi}}^2}}) * (1 - e^{\frac{-(\mu * F_b)^2}{2\sigma_{\dot{\psi}}^2}}) \tag{3.40}$$

The accept criteria basically states; access is OK if the probability of a incident is less than some defined limit. This way, the program calculates a limiting significant wave height for each combination of peak period and wave direction. Then it compares this to relevant weather information to calculate the availability.

Dividing the sea state into swell and wind generated part

A sea state may not only contain of one type of waves travelling in one main direction, it can very well consist of swell propagating in one direction and wind generated sea propagating in another. One can cope with this by describing each part with a separate wave spectrum, as mentioned in Wu (2014). The standard deviations of our slip variables and roll motion can then be calculated like this.

$$\sigma_\eta = \sqrt{\int_0^\infty ((J_3(\omega,\beta_1) - \mu J_1(\omega,\beta_1))^2 * S_1(\omega|H_{s1},T_{p1}) + (J_3(\omega,\beta_2) - \mu J_1(\omega,\beta_2))^2 * S_2(\omega|H_{s2},T_{p2}))d\omega} \tag{3.41}$$

$$\sigma_\alpha = \sqrt{\int_0^\infty ((J_3(\omega,\beta_1) + \mu J_1(\omega,\beta_1))^2 * S_1(\omega|H_{s1},T_{p1}) + (J_3(\omega,\beta_2) + \mu J_1(\omega,\beta_2))^2 * S_2(\omega|H_{s2},T_{p2}))d\omega} \tag{3.42}$$

$$\sigma_\chi = \sqrt{\int_0^\infty ((J_2(\omega,\beta_1) - \mu J_1(\omega,\beta_1))^2 * S_1(\omega|H_{s1},T_{p1}) + (J_2(\omega,\beta_2) - \mu J_1(\omega,\beta_2))^2 * S_2(\omega|H_{s2},T_{p2}))d\omega} \tag{3.43}$$

$$\sigma_\psi = \sqrt{\int_0^\infty ((J_2(\omega,\beta_1) + \mu J_1(\omega,\beta_1))^2 * S_1(\omega|H_{s1},T_{p1}) + (J_2(\omega,\beta_2) + \mu J_1(\omega,\beta_2))^2 * S_2(\omega|H_{s2},T_{p2}))d\omega} \tag{3.44}$$

$$\sigma_{roll} = \sqrt{\int_0^\infty (R_{transf}(\omega,\beta_1)^2 * S_1(\omega|H_{s1},T_{p1}) + R_{transf}(\omega,\beta_2)^2 * S_2(\omega|H_{s2},T_{p2}))d\omega} \tag{3.45}$$

The expected number of incidents can then be calculated the same way as earlier, and one can determine if the two spectrum sea state is OK for access or not.

Viscous effects

Due to the special hull form of SWATHS, some viscous effects have been investigated. Three viscous effects are included, damping in pitch and heave and excitation force in heave. Viscous roll damping is already included from VERES. Due to the short length and breadth of the vessel compared to wavelengths viscous excitation in pitch and roll is neglected. Here viscous effects is divided into damping, and viscous loads. This is a simplification as it is the relative velocity

that matters for viscous effects. One could argue that stochastic linearization as described in Vada (2013) would be the better choice, but it would have increased the complexity and computational time of the program such that it would loose some of it's benefits. So the method of equivalent linearization as described in Faltinsen (1990) have been applied instead.

As viscous damping is a non-linear effect one have to linearize it in some way to include it in a frequency domain calculation. The method of equivalent linearization have been applied. One weakness of this linearization is that a given wave amplitude has to be assumed. Discussion of viscous flow on various geometries can be found in Cengel and Cimbala (2010). The vertical force on a strip of the swath hull can be expressed:

$$F_3 = \frac{1}{2} * C_d * v * |v| * \rho * D(x) * dx \tag{3.46}$$

And the total pitch moment:

$$F_5 = -F_3(x) * x \tag{3.47}$$

Where v represent the vertical velocity of the strip and x the distance from center of gravity. Then considering viscous heave damping. The total damping force from this motion can be expressed:

$$F_{3damp} = \sum \frac{1}{2} * C_d * \dot{r}(3) * |\dot{r}(3)| * \rho * D(x) * dx * 2 \tag{3.48}$$

The expression is multiplied with two due to the simple fact that there is two pontoons. With the technique of equivalent linearization described in Faltinsen (1990) page 97, the damping force can be written:

$$F_{3damp} = \sum \frac{8\omega}{3\pi} C_d * \dot{r}(3) * |r_{3amp}| * \rho * D(x) * dx \tag{3.49}$$

The motion amplitude is found from the RAO and the assumed wave amplitude:

$$r_{3amp} = \xi_A * RAO(3) \tag{3.50}$$

The RAO of course depends on the F_{3damp}, so this result in a iterative process which continues until the difference between the new and old RAO is less than some limit. The way to estimate pitch damping is analogous to the described method. Linearized, the damping moment per strip in pitch can be written:

$$F_{5damp} = \sum \frac{8\omega}{3\pi} x^3 \frac{1}{2} * C_d * \dot{r}(5) * |r_{5amp}| * \rho * D(x) * dx \tag{3.51}$$

And one get the same iteration procedure as for heave damping. The two contributions is added to the total damping matrix.

When estimating the viscous excitation force the vertical velocity of the wave particles at the given section is considered. The velocity will not only depend on frequency, but also the direction of the waves. Hence, one have to consider each section on each pontoon. The vertical velocity of a wave particle in intermediate water depth can be found from Faltinsen (1990) page 16:

$$v(x,y) = \xi_a \omega \frac{sinh(k(z+h)}{sinh(kh)} * cos(\omega t - k_x x - k_y y) \tag{3.52}$$

The vertical force from each section is given by 3.46, which can be summed into the total viscous excitation force in heave. The total linearized expression becomes:

$$F_{3visc} = \sum^{sections} \frac{8\omega}{3\pi} \xi_a * \frac{1}{2} C_d * v(x,y) * |v(x,y)| * \rho * D(x) * dx \tag{3.53}$$

The linearized viscous heave excitation force is added to the potential theory excitation force in heave calculated by VERES. The phase of the viscous heave excitation force will be 90 degrees, this is due to the orbital motion of water particles, the vertical velocity of the water particles is 90 degrees out of phase with the surface elevation. As can be seen of the figure below, or by inspecting particle velocities calculated by velocity potential as on page 16 Faltinsen (1990).

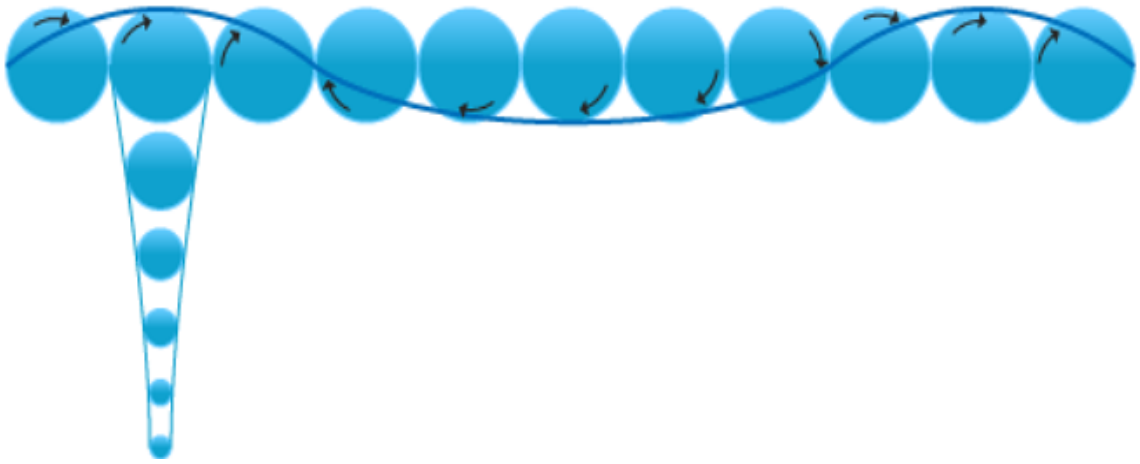

Figure 3.4: Orbital motion of wave particles, picture from yr.no

3.2.2 Time Domain

In order to validate the results obtained by the frequency domain program, a model has been created in the SIMA environment to analyse the access operation in the Marintek software

SIMO. SIMO is a time domain simulation program for study of motions and station keeping of multibody systems, it numerically solves the dynamic equilibrium at each time step. As SIMA does not have the TMA-spectrum built in, the JONSWAP spectrum with $\gamma = 3.3$ is used to describe the different sea states. When modelling misaligned swell and wind seas, one PM spectrum and one JONSWAP with $\gamma = 5$ is applied.

The wind turbine is represented as a globally fixed plane. The contact between the vessel and the wind turbine is modelled as two point fenders, with 40 cm distance between each other. The local body coordinates of the fenders are (12.24, -0.2,3.8) and (12.24,0.2 ,3.8). In the global coordinate system the fenders are positioned at (4,-0.2,3.8) and (4,-0.2,3.8). The friction coefficient applied is the same as in the frequency domain, 0.8, and is assumed to be constant regardless of velocity. To represent a constant bollard push, a specified force is applied through the center of gravity of the vessel in the local positive x-direction. After a preliminary sensitivity analysis a time step of 0.01 seconds was chosen.

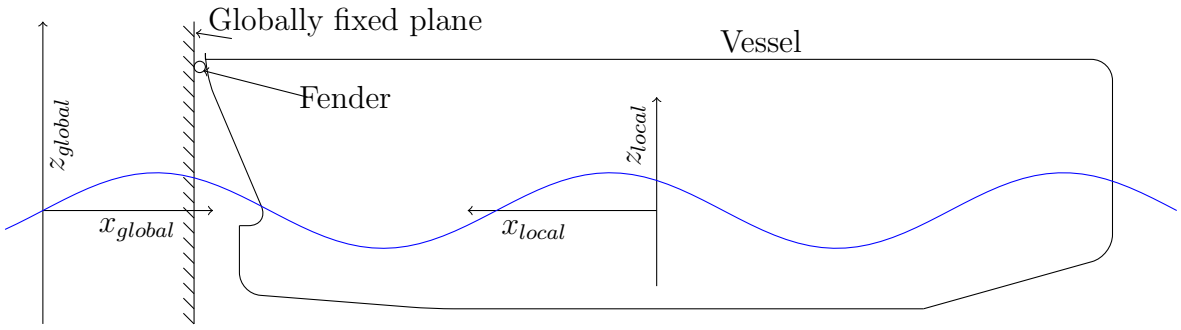

Figure 3.5: 2-D illustration of wind turbine, fender, vessel, local and global coordinate system.

Fender modelling

For tugs and service vessels, the D-shaped fender is recommended due to it's high energy absorption according to Longwood (2015). Longwood marine fenders offers a selection of different fenders, and two 8 inch D-shaped fender with 4 inch D-shaped bore is chosen. Longwood does not offer information about the shear stiffness , it is hence assumed the same shear stiffness of 3000 kN/m as used by Wu (2014). With a contact length of 10 cm, the damping and stiffness characteristics of the fender is shown in the following figure. The damping is assumed to be 5% of critical damping. The fenders are giving friction in all directions along the sliding plane.

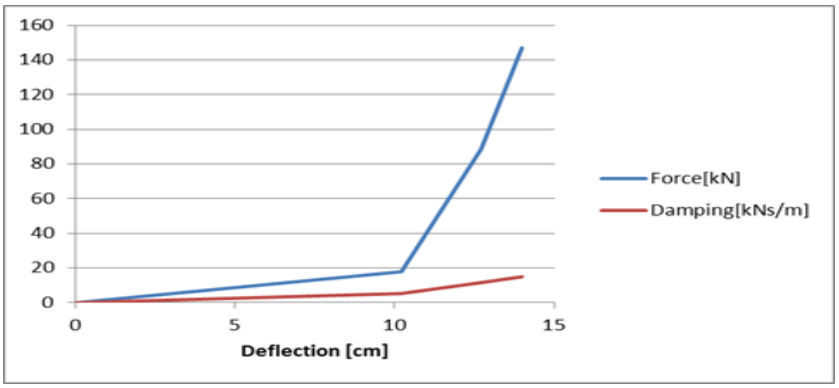

Figure 3.6: Fender characteristics of D-shaped 8 inch fender from Longwood marine fenders.(Damping assumed to be 5% of critical damping)

Vessel modelling

SIMA has the capability to import files of VERES format, hence the linear hydrodynamic properties and mass properties of the vessel are imported directly from VERES. To capture the viscous effects, an imaginary slender element is attached to the vessel as described on page 48 Ormberg (2014). It stretches from (-12,0,-1.3) to (12,0,-1.3). To avoid the inclusion of unwanted effects, neither gravity nor buoyancy is included for this imaginary element, only quadratic drag. To estimate the quadratic drag coefficients, the script Bquad.m found in appendix D was used. The element is simplified to have a uniform drag coefficient in all directions throughout its length.

3.3 Verification

3.3.1 Strategy

In the frequency domain program, limiting significant wave height was calculated for all combinations of 32 peak periods and 5 wave directions for a total of 13 different input conditions. A total of 2080 limiting significant wave heights. This is not possible to do in the time domain within the time frame of a master thesis. Hence, to verify the frequency domain method, specific relevant sea states are analysed and compared with the results obtained with the frequency domain program. This way it can be seen if the method proposed by Wu (2014) is able to catch the physical effects necessary to analyse fender docking of offshore wind turbines with a SWATH vessel. The most important physical differences between the two methods are the following:

- Dynamics in fender(Neglected in Wu (2014))
- Bollard force through center of gravity in SIMA, assumed constant normal onto fender Wu (2014)
- The way of estimating viscous effects
- Single fender point in Wu (2014), two fender points with 40 cm between them in SIMA
- Slip defined as 10 cm deviation in SIMA, any slip defined as slip in Wu (2014)

As SIMA does not have the TMA-spectrum built in, results obtained with JONSWAP will be compared. Four different scenarios is investigated:

1. Response to a harmonic wave of 1 m amplitude and 8 s period
2. Standard deviation of roll and pitch in moderate irregular sea states
3. Investigate what parameters that should be included in an accept criteria
4. Time to first incident where sea state is given by the frequency domain program

Scenario 1 and 2 will indicate if the physical properties in general are similar in the two models. What parameters that needs to be included in an accept criteria will first be investigated in the frequency domain, then in scenario 3 this result will be attempted verified. While scenario 4 might give information about whether the limiting significant wave heights produced by the frequency domain program are realistic or not. After the first slip, the physics of the operation are likely to change, for instance the coordinates of the fender point and the direction of vessel etc. Hence the key variable from the SIMO simulations with respect to scenario 4 is the time before first incident, which is defined as slip in either direction or roll angle exceeding limit.

3.3.2 Statistical approach of time to first incident

The time before first incident,t_{inc}, will be a memoryless variable, i.e the expected time to next incident is independent of how much time has already gone by. Mathematically this can be described, Walpole (2007):

$$P(t_{inc} \geq t) = P(t_{inc} \geq t_0 + t | t_{inc} \geq t_0) \tag{3.54}$$

This makes it reasonable to assume that the time to first slip can be assumed to be exponentially distributed. When comparing the two methods, it would be important knowledge to know if

one is more conservative than the other. When comparing the time to first slip the following two hypotheses are considered.

- H_0: Expected time to first slip is larger in the time domain model, than in the frequency domain method
- H_1: Expected time to first slip is larger in the frequency domain method, than in the time domain model.

The frequency of incidents is a input to the frequency domain program, for a given frequency of incidents, peak period and wave direction it calculates a limiting significant wave height. Exposing the time domain model to the same sea state one can compare the time to first slip from the two models. The expected time to first slip from the frequency domain calculation is simply the inverse of the acceptable frequency of incidents, t_{exp}. Each sea state will be simulated in SIMA with n different wave seeds and one get a mean value of t_{inc}, $\overline{t_{inc}}$. Working under the assumption that t_{inc} is exponentially distributed one can establish a (100-τ)% confidence interval for the expected time to first slip, t_{expinc}, with help of the χ^2 distribution as described in Ross (2009)

$$\frac{2n\overline{t_{inc}}}{\chi^2_{0.5\tau,2n}} < t_{expinc} < \frac{2n\overline{t_{inc}}}{\chi^2_{1-0.5\tau,2n}} \tag{3.55}$$

This way one might be able to verify either H_0 or H_1 within a (100-τ)% level of confidence.

3.4 Proposed improved frequency domain method

This method is based on the method described in section 3.2.1, the only difference is that it is no longer assumed that the bollard thrust is in global x-direction. The thrust is now more physically correct assumed to follow the vessels local x-axis. It was developed the last week of this thesis after consideration of the time domain results, and has hence not been used in this thesis. The statical calculation has been verified in SIMO, but it has not been verified otherwise. It can be considered as a suggestion to how one can improve the frequency domain method suggested by Wu (2014).

A new variable is introduced:

L_t= Vertical distance between propeller thrust and fender point.

And then the moment induced by this on the vessel:

M_5=Moment induced by vertical distance between propeller thrust and fender point on the vessel.

To find the constant vertical force one solve the statical coupled equation for pitch and heave, C represents the hydrostatical stiffness matrix and r the response vector.

$$\begin{bmatrix} C_{33} & C_{35} \\ C_{53} & C_{55} \end{bmatrix} * \begin{bmatrix} r_3 \\ r_5 \end{bmatrix} = \begin{bmatrix} F_{zc} \\ M_5 - F_{zc} * x_p \end{bmatrix} \tag{3.56}$$

Then remembering that one can express the translations of the vessel as a function of its rotations as described in 3.2.1 the equation can be rewritten to:

$$\begin{bmatrix} C_{33} & C_{35} \\ C_{53} & C_{55} \end{bmatrix} * \begin{bmatrix} x_p * r_5 \\ r_5 \end{bmatrix} = \begin{bmatrix} F_{zc} \\ M_5 - F_{zc} * x_p \end{bmatrix} \tag{3.57}$$

From line one the following expression is obtained:

$$F_{zc} = C_{33} * x_p * r_5 + C_{35} * r_5 \tag{3.58}$$

Entering this into line two:

$$C_{53} * x_p * r_5 + C_{55} * r_5 = M_5 - x_p(C_{33} * x_p * r_5 + C_{35} * r_5) \tag{3.59}$$

Then solving for the initial pitch angle is an easy task:

$$r_5 = \frac{M_5}{C_{53} * x_p + C_{55} + x_p(C_{33} * x_p + C_{35})} \tag{3.60}$$

Inserting this in 3.58 then yields:

$$F_{zc} = (C_{33} * x_p + C_{35}) * \frac{M_5}{C_{53} * x_p + C_{55} + x_p(C_{33} * x_p + C_{35})} \tag{3.61}$$

This force will be added to the slip criterias described in section 3.2.1. It should be noted that as long as the fender point is above the propeller thrust, F_{zc} will be a negative value, i.e point downwards increasing the probability of upwards slip. Force contribution from the static pitch angle calculated in 3.60 will be neglected in this proposed method. In the standard case used in this thesis the angle was found to be 0.007 radians, 0.4 deg, giving a force contribution of 1.4

kN. If it is found to matter, it can easily be implemented.

Then forces induced by oscillating pitch and yaw motion needs to be addressed. Assuming small angles these forces can be written:

$$F_z = F_b * r(5) \tag{3.62}$$

$$F_y = F_b * r(6) \tag{3.63}$$

Including the new forces one get the new downwards, upwards, rightwards and leftwards slip criterias:

$$J_3(t) + F_{zc} - F_b * r(5) < \mu * (F_b + J_1(t)) \tag{3.64}$$

$$J_3(t) + F_{zc} - F_b * r(5) > -\mu * (F_b + J_1(t)) \tag{3.65}$$

$$J_2(t) - F_b * r(6) < \mu * (F_b + J_1(t)) \tag{3.66}$$

$$J_2(t) - F_b * r(6) > -\mu * (F_b + J_1(t)) \tag{3.67}$$

Now introducing a new version of the slip variables presented in chapter three:

$$\eta(t) = J_3(t) - \mu J_1(t) - F_b * r(5) \tag{3.68}$$

$$\alpha(t) = -(J_3(t) + \mu J_1(t)) + F_b * r(5) \tag{3.69}$$

$$\chi(t) = J_2(t) - \mu J_1(t) - F_b * r(6) \tag{3.70}$$

$$\psi(t) = -(J_2(t) + \mu J_1(t)) + F_b * r(6) \tag{3.71}$$

One get new convenient limits for slip:

$$\eta(t) < \mu * F_b - F_{zc} \tag{3.72}$$

$$\alpha(t) < \mu * F_b + F_{zc} \tag{3.73}$$

$$\chi(t) < \mu * F_b \tag{3.74}$$

$$\psi(t) < \mu * F_b \tag{3.75}$$

These variables will still be stationary, ergodic , Gaussian with zero mean. Hence the Rayleigh distribution is suitable to describe the peaks, using the standard deviation which can be found from the new transfer functions of $\eta(t)$,$\alpha(t)$, $\chi(t)$ and $\psi(t)$.

$$\eta_{transf}(\omega, \beta) = J_3(\omega, \beta) - \mu J_1(\omega, \beta) - F_b * r_5(\omega, \beta) \tag{3.76}$$

$$\alpha_{transf}(\omega,\beta) = -(J_3(\omega,\beta) + \mu J_1(\omega,\beta)) + F_b * r_5(\omega,\beta) \tag{3.77}$$

$$\chi_{transf}(\omega,\beta) = J_2(\omega,\beta) - \mu J_1(\omega,\beta) - F_b * r_6(\omega,\beta) \tag{3.78}$$

$$\psi_{transf}(\omega,\beta) = -(J_2(\omega,\beta) + \mu J_1(\omega,\beta)) + F_b * r_6(\omega,\beta) \tag{3.79}$$

Here $r_5(\omega,\beta)$ and $r_6(\omega,\beta)$ is the respective transfer function of pitch and yaw. How one find the standard deviation and probability for slip during one cycle follows the exact procedure described in 3.2.1. The final expression becomes:

$$P_{inc} = 1-(1-e^{\frac{-\theta_{max}^2}{2\sigma_{roll}^2}})*(1-e^{\frac{-(\mu*F_b-F_{zc})^2}{2\sigma_\eta^2}})*(1-e^{\frac{-(\mu*F_b+F_{zc})^2}{2\sigma_\alpha^2}})*(1-e^{\frac{-(\mu*F_b)^2}{2\sigma_\chi^2}})*(1-e^{\frac{-(\mu*F_b)^2}{2\sigma_\psi^2}}) \tag{3.80}$$

Chapter 4

Results

4.1 Frequency domain

As this thesis is not about design of a SWATH vessel, the importance of the results lies in the comparison of the accessibility found with different input parameters rather than the value itself. The different subsections contains results for different values of one input parameters while the other ones are kept constant at their standard values. Analysis is done for three different values for the input parameters investigated. The standard values are given in the following table. Each simulation lasts about 3 minutes. The availability is what availability the system would have had in the period from 1957-2010 on Dogger Bank location 2, given by the NORA10 hindcast.

μ [-]	F_b [kN]	θ_{max}[deg]	h[m]	R_{acc} [-]	X_{acc}[m]	Viscous effects
0.8	200	10	30	0.03966	12.24	Yes, $\xi_A = 1m$

Table 4.1: Standard input values

4.1.1 Friction coefficient and bollard push force

$\mu * F_b[kN]$	A_{jon}	A_{tma}	A_{2spec}	$disA$	A_{jonW}	A_{tmaW}	A_{2specW}
80	0.101	0.107	0.169	0.27	0.049	0.053	0.100
140	0.348	0.358	0.469	0.05	0.225	0.236	0.326
280	0.528	0.533	0.668	0.02	0.378	0.385	0.519

Table 4.2: Results for varying bollard push force

One can observe that the availability depend significantly on the product of friction coefficient and bollard push force. Applying the TMA-spectrum yields slightly better availability than what is obtained with the JONSWAP spectrum. While dividing the sea state into swell and wind generated part yields significantly better availability. For less bollard push, the number of sea states approved by the one spectrum method and disapproved by the two spectra method increases.

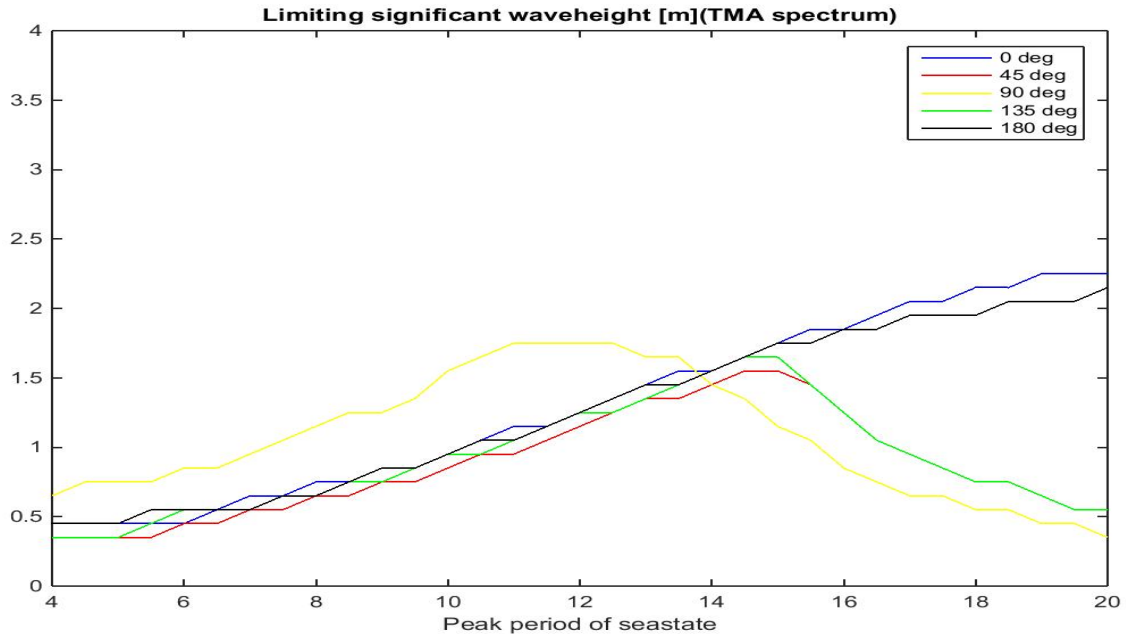

Figure 4.1: Limiting significant wave height for 100 kN bollard push force and 0.8 as friction coefficient, obtained with TMA-spectrum.

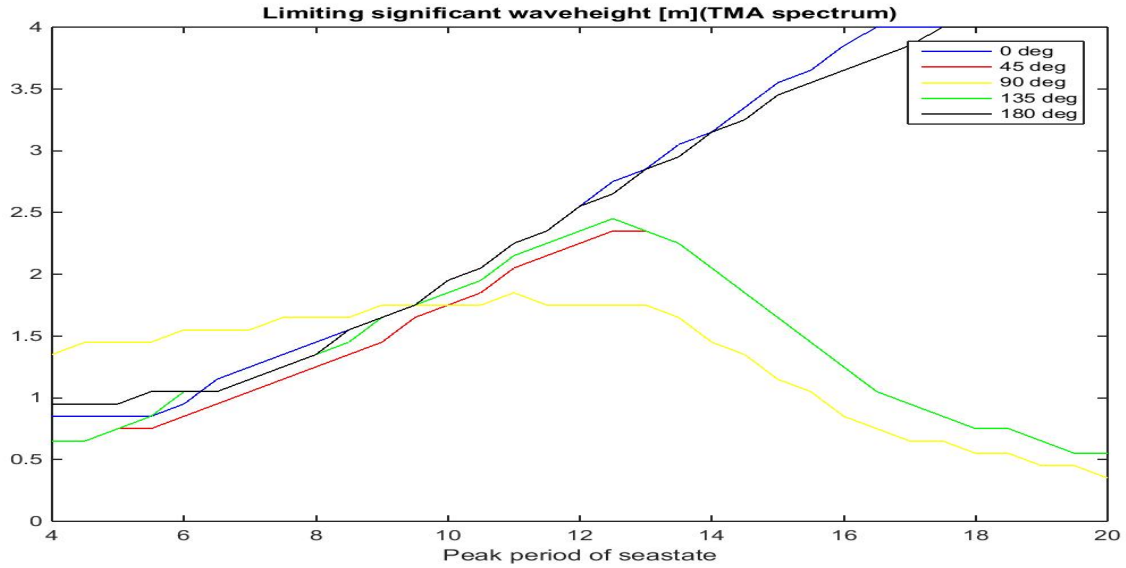

Figure 4.2: Limiting significant wave height for 200 kN bollard push force and 0.8 as friction coefficient, obtained with TMA-spectrum.

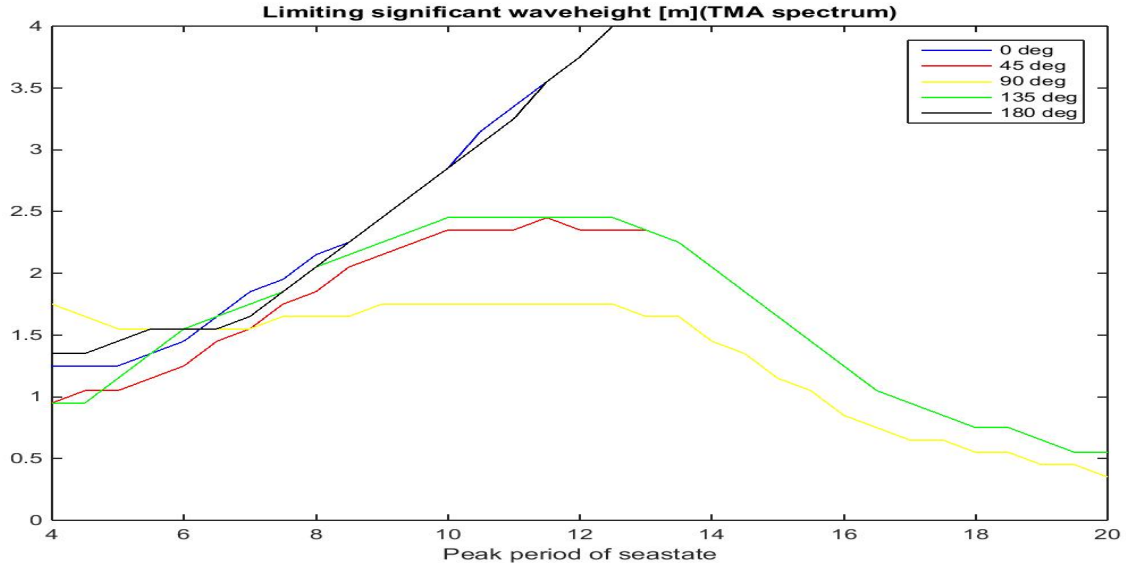

Figure 4.3: Limiting significant wave height for 300 kN bollard push force and 0.8 as friction coefficient, obtained with TMA-spectrum.

One can observe that the limiting significant wave height do depend strongly on peak period

and to some extension the direction of the waves. It is also observed that the improvement in availability is largest for the wave directions 0 and 180 degrees for increasing bollard push force.

4.1.2 Maximum roll angle

$\theta_{max}[deg]$	A_{jon}	A_{tma}	A_{2spec}	$disA$	A_{jonW}	A_{tmaW}	A_{2specW}
5	0.317	0.328	0.388	0.07	0.193	0.207	0.248
10	0.348	0.358	0.469	0.05	0.225	0.236	0.326
15	0.348	0.359	0.501	0.05	0.225	0.238	0.368

Table 4.3: Results for varying maximum roll angle

One can observe difference in availability between 5 and 10 degrees as maximum roll angle, while the difference in availability between 10 and 15 degrees as maximum is quite small. Slightly larger effect for the two spectrum calculation.

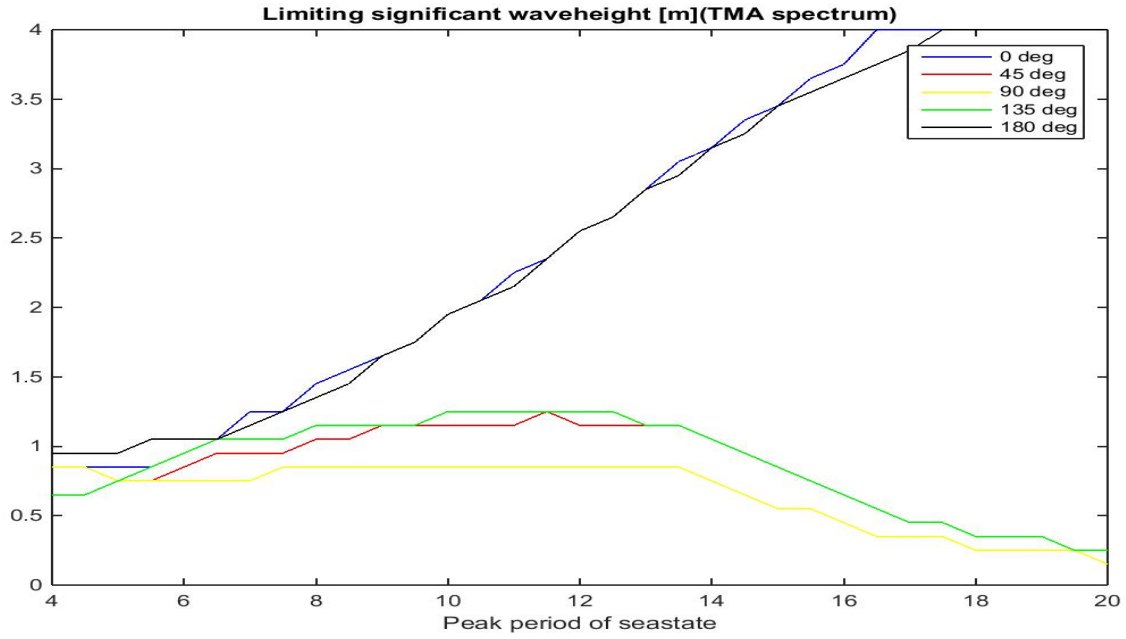

Figure 4.4: Limiting significant wave height with 5 [deg] as maximum roll angle.

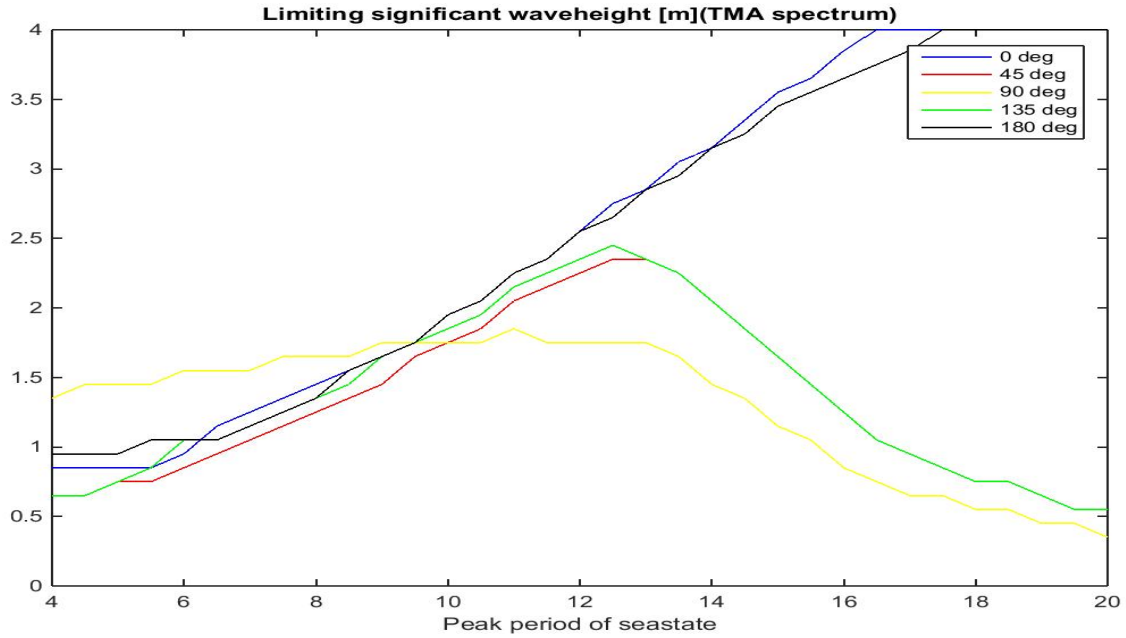

Figure 4.5: Limiting significant wave height with 10 [deg] as maximum roll angle.

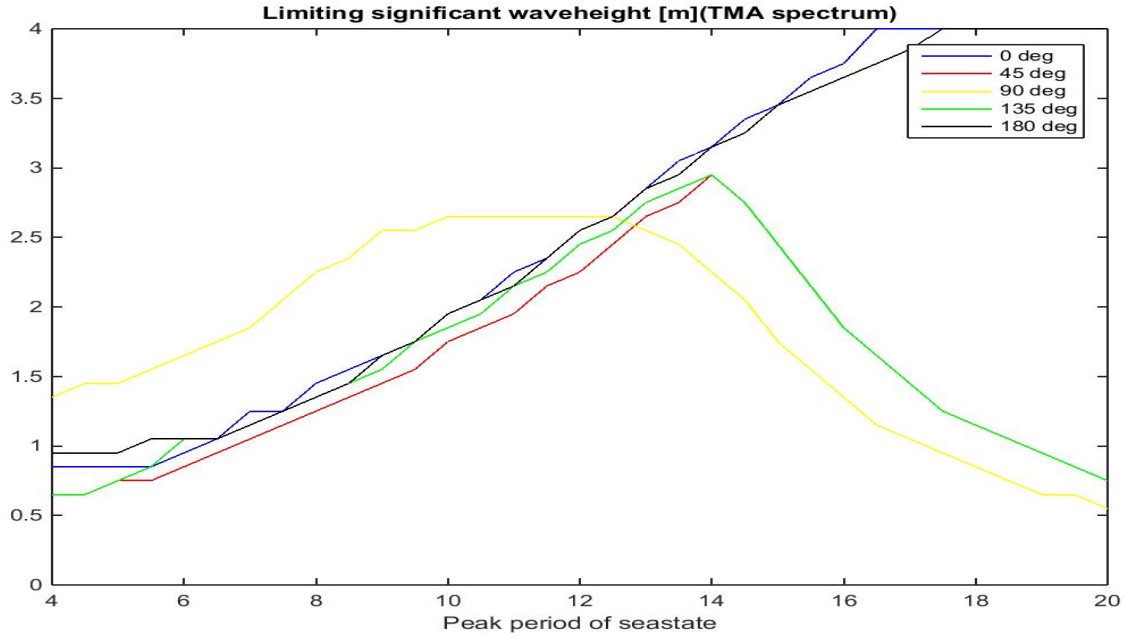

Figure 4.6: Limiting significant wave height with 15 [deg] as maximum roll angle.

It is observed that the change of maximum allowed roll angle do not effect the sea states with wave direction 0 and 180 degrees. 45 and 135 degrees are effected, especially in the range of peak periods between 8 and 16 seconds. The sea state with beam sea is the most effected by changes in the maximum allowed roll angle.

4.1.3 Acceptable probability of failure during access

$P_{facc} * 10^{-4}[-]$	A_{jon}	A_{tma}	A_{2spec}	$disA$	A_{jonW}	A_{tmaW}	A_{2specW}
0.2	0.281	0.290	0.382	0.07	0.167	0.179	0.251
12.0	0.348	0.358	0.469	0.05	0.225	0.236	0.326
268.1	0.420	0.425	0.554	0.03	0.286	0.294	0.408

Table 4.4: Results for varying acceptable probability of failure during access

The acceptable probability of slip during one access operation effects the availability to some extent. The best guess allows for 60 times larger acceptable probability of slip during access than the most conservative estimate, and yields about 19% improved availability.

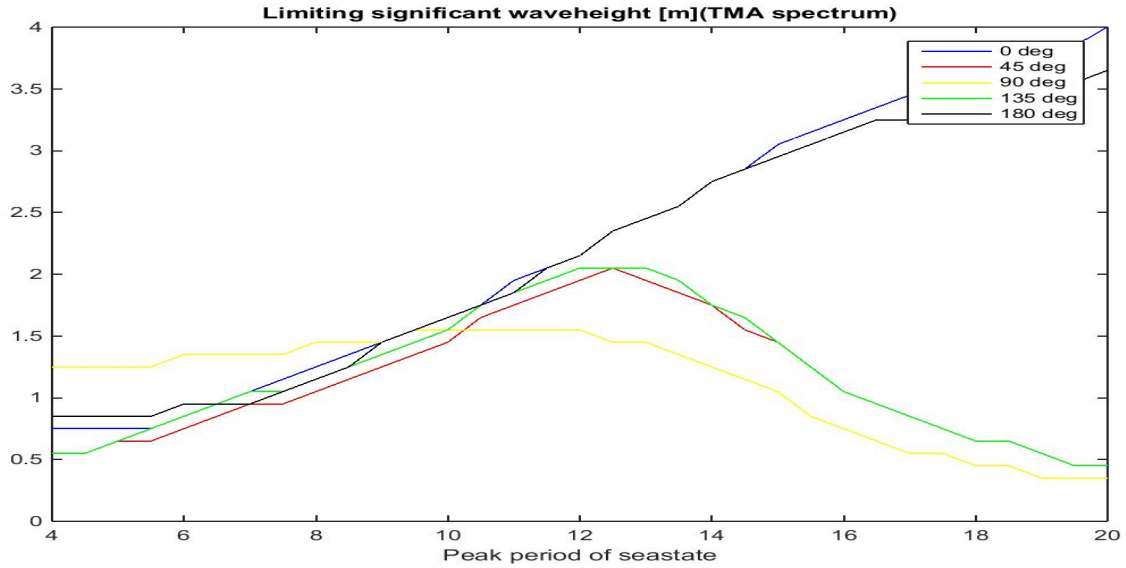

Figure 4.7: Limiting significant wave height with 0.00002 as acceptable probability of fender slip during one access operation.

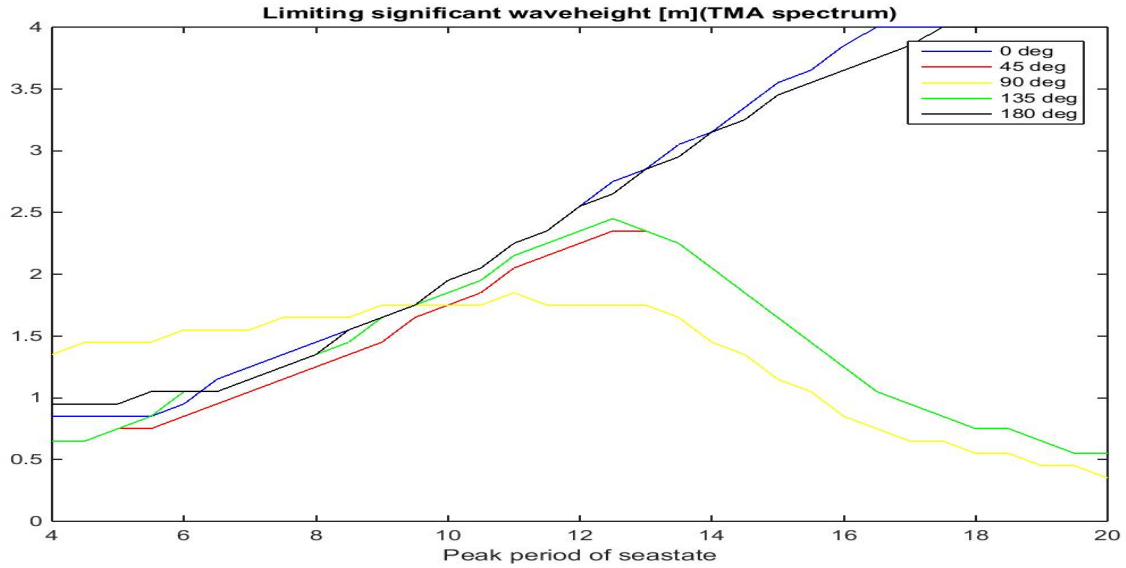

Figure 4.8: Limiting significant wave height with 0.00119 as acceptable probability of fender slip during one access operation.

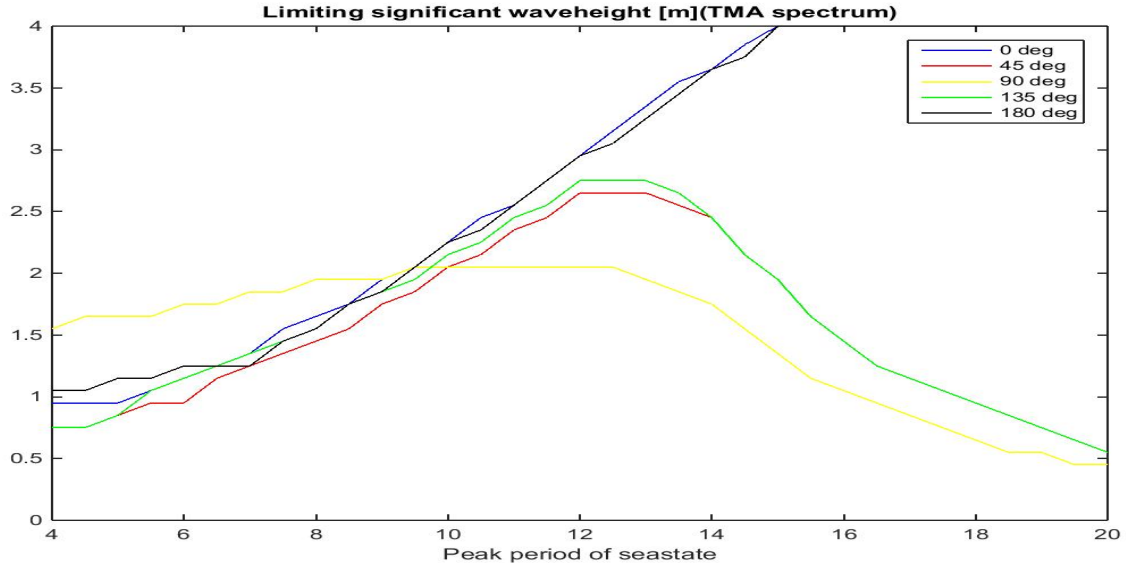

Figure 4.9: Limiting significant wave height with 0.02681 as an acceptable probability of fender slip during one access operation.

One can observe that the change in limiting significant wave height is quite similar for all

wave directions.

4.1.4 Water depth

Water depth [m]	A_{jon}	A_{tma}	A_{2spec}	$disA$	A_{jonW}	A_{tmaW}	A_{2specW}
15	0.348	0.370	0.497	0.04	0.225	0.247	0.353
30	0.348	0.358	0.469	0.05	0.225	0.236	0.326
60	0.348	0.350	0.462	0.05	0.225	0.229	0.318

Table 4.5: Results for varying water depth

The effect of water depth do influence the availability, the difference in availability between 15 and 60 meters water depth is 7.5% .

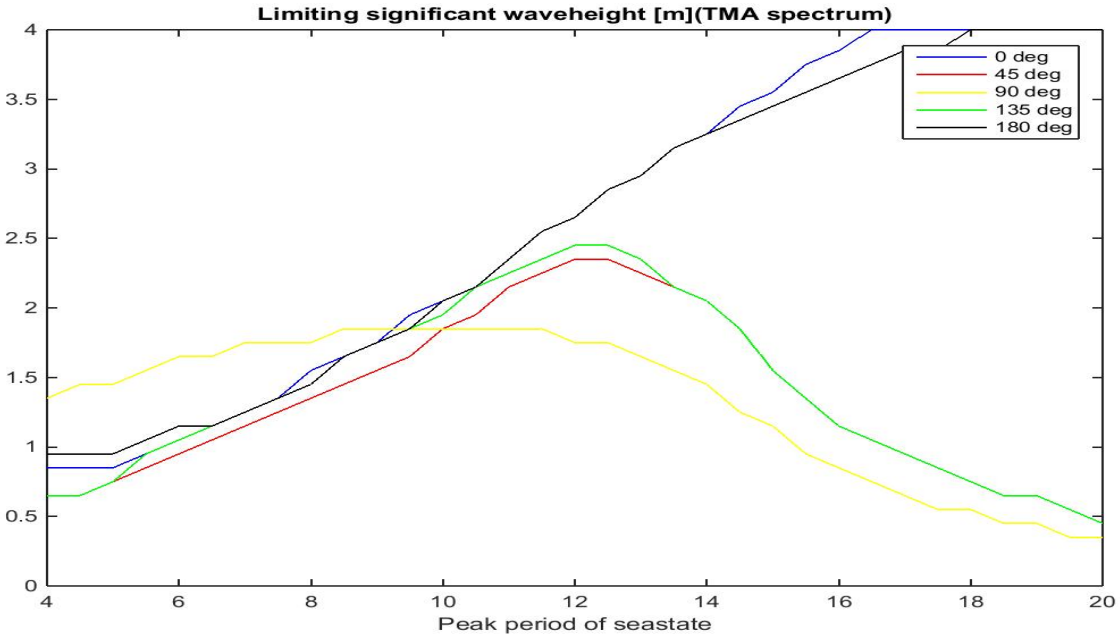

Figure 4.10: Limiting significant wave height at 15 m water depth

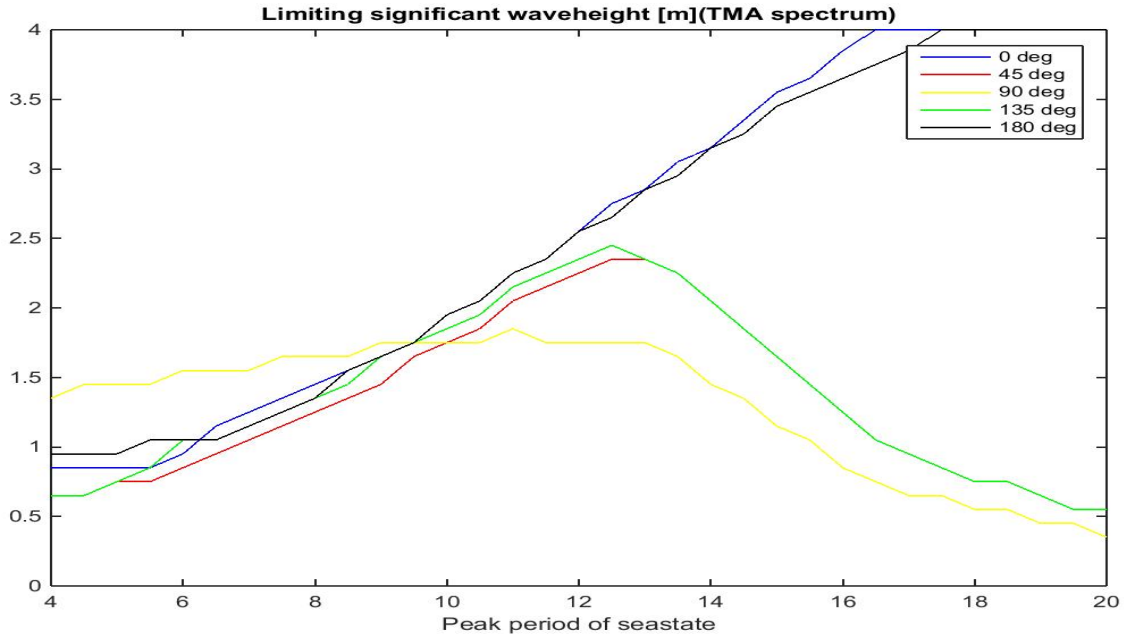

Figure 4.11: Limiting significant wave height at 30 m water depth

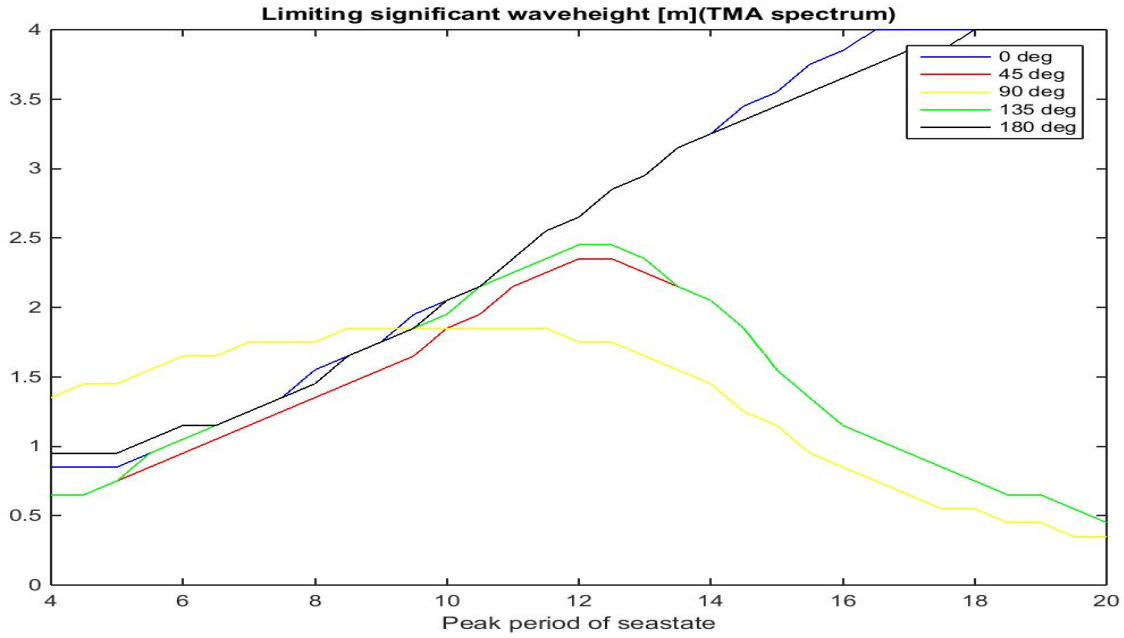

Figure 4.12: Limiting significant wave height at 60 m water depth.

One can see that water depth effects all wave directions similarly.

4.1.5 X-coordinate of fender

X_{acc}	A_{jon}	A_{tma}	A_{2spec}	$disA$	A_{jonW}	A_{tmaW}	A_{2specW}
11.24	0.339	0.345	0.456	0.06	0.215	0.225	0.313
12.24	0.348	0.358	0.469	0.05	0.225	0.236	0.326
13.24	0.365	0.370	0.483	0.04	0.240	0.247	0.339

Table 4.6: Results for varying X-coordinate of Fender

The X-coordinate of the fender do somewhat effect the availability, moving the fender point 2 m from 11.24 to 13.24 gives a a improvement in availability of 6%.

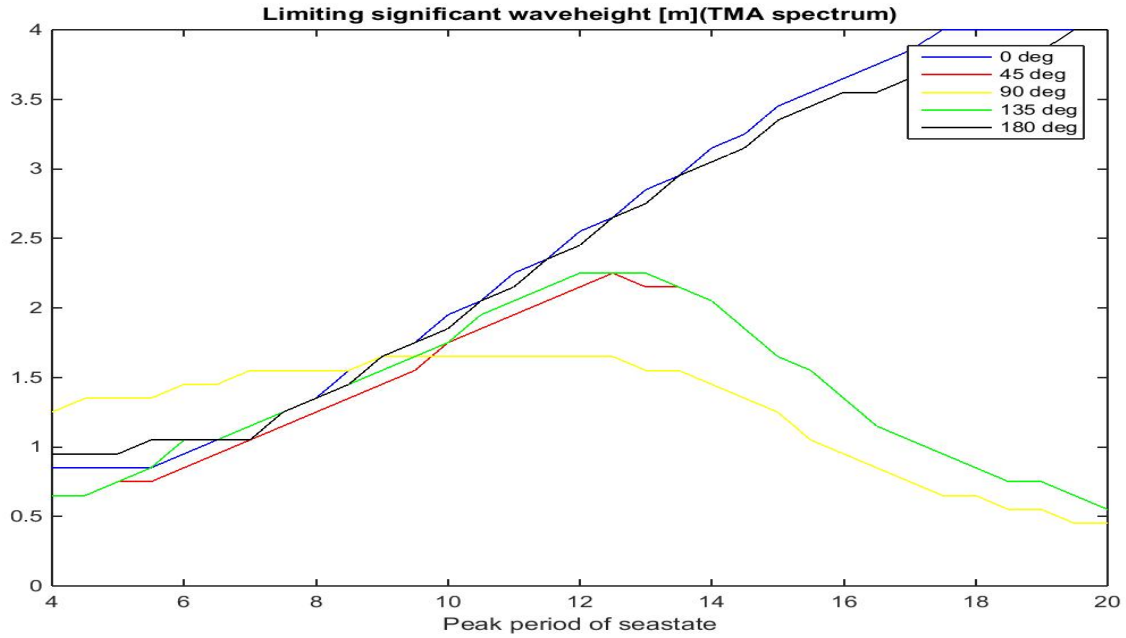

Figure 4.13: Limiting significant wave height, X-coordinate of fender = 11.24

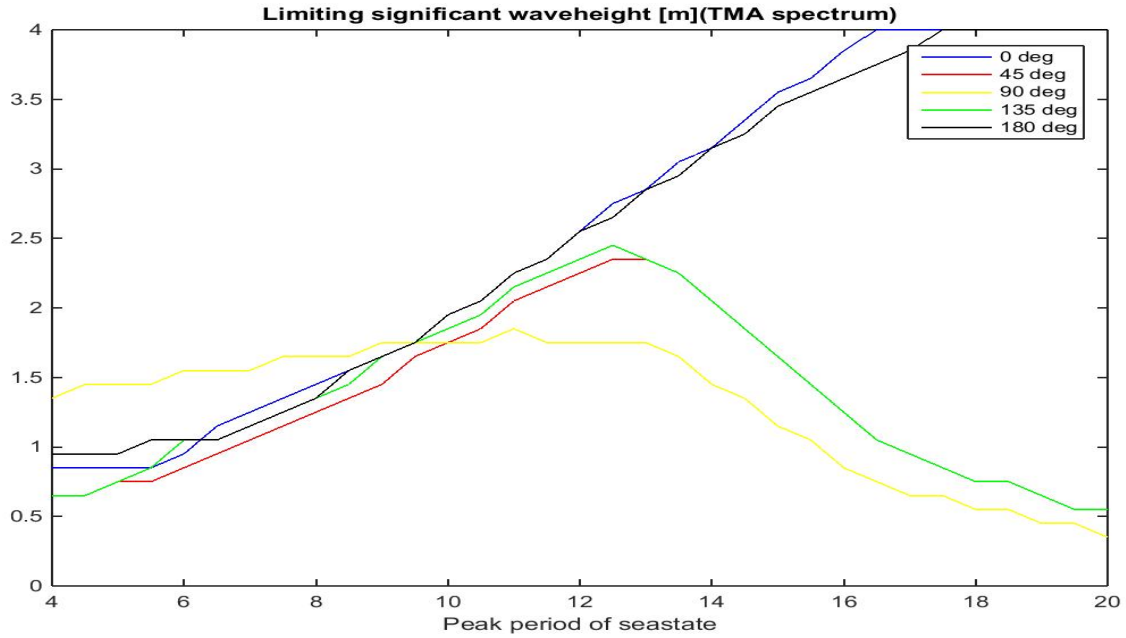

Figure 4.14: Limiting significant wave height, X-coordinate of fender = 12.24

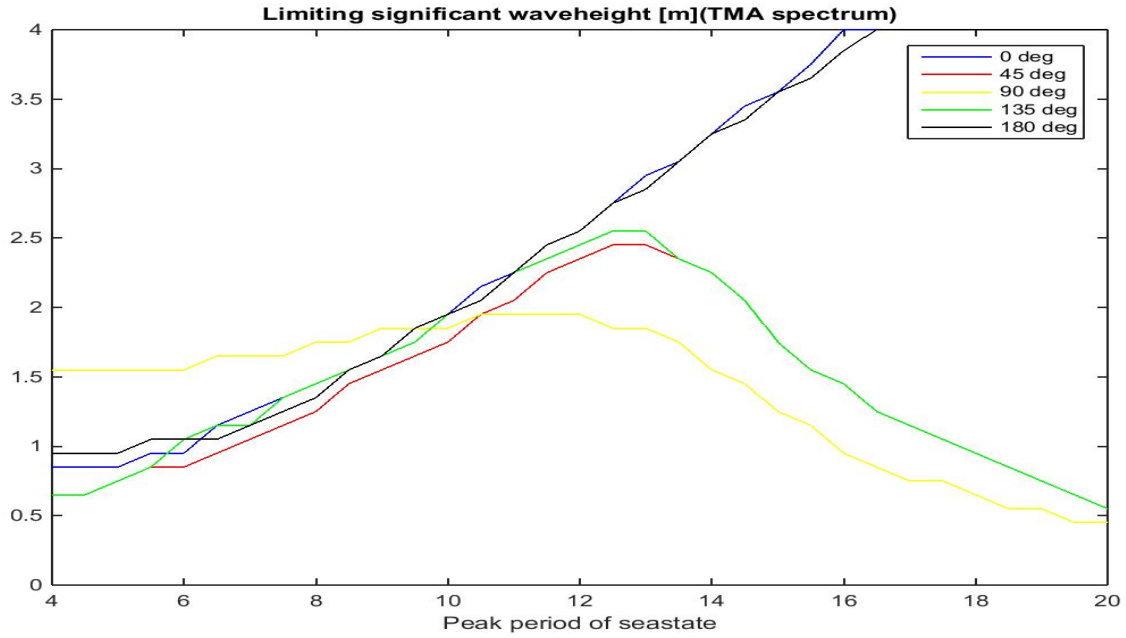

Figure 4.15: Limiting significant wave height, X-coordinate of fender = 13.24

One can observe that the availability is somewhat more effected in beam sea than in the other directions.

4.1.6 Viscous effects

Viscous effects	A_{jon}	A_{tma}	A_{2spec}	$disA$	A_{jonW}	A_{tmaW}	A_{2specW}
NO	0.321	0.330	0.379	0.13	0.200	0.208	0.248
YES, $\xi_A = 1m$	0.348	0.358	0.469	0.05	0.225	0.236	0.326
YES, $\xi_A = 2m$	0.332	0.339	0.466	0.05	0.213	0.222	0.325

Table 4.7: Results for including viscous effects with different assumed wave amplitude

One can see that the introduction of viscous effects improves the availability. A improvement of 24% between no viscous effects and viscous effects included with 1 meter wave amplitude assumed. Assuming 2 meter wave amplitude instead gives slightly decreased availability, a change of less than 1%.

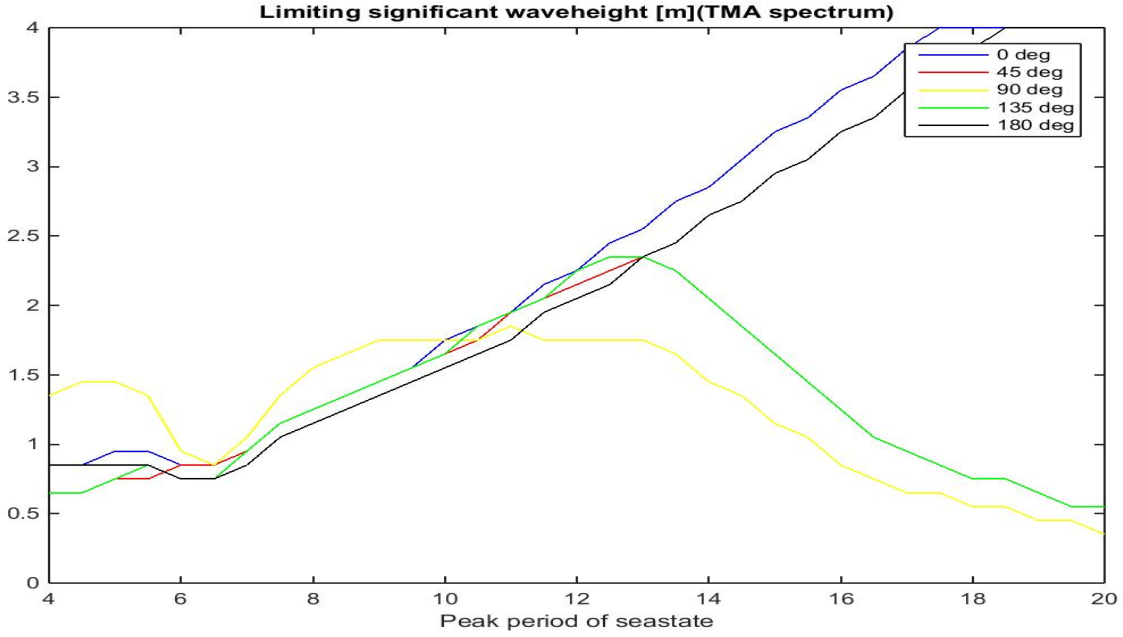

Figure 4.16: Limiting significant wave height, only viscous roll damping

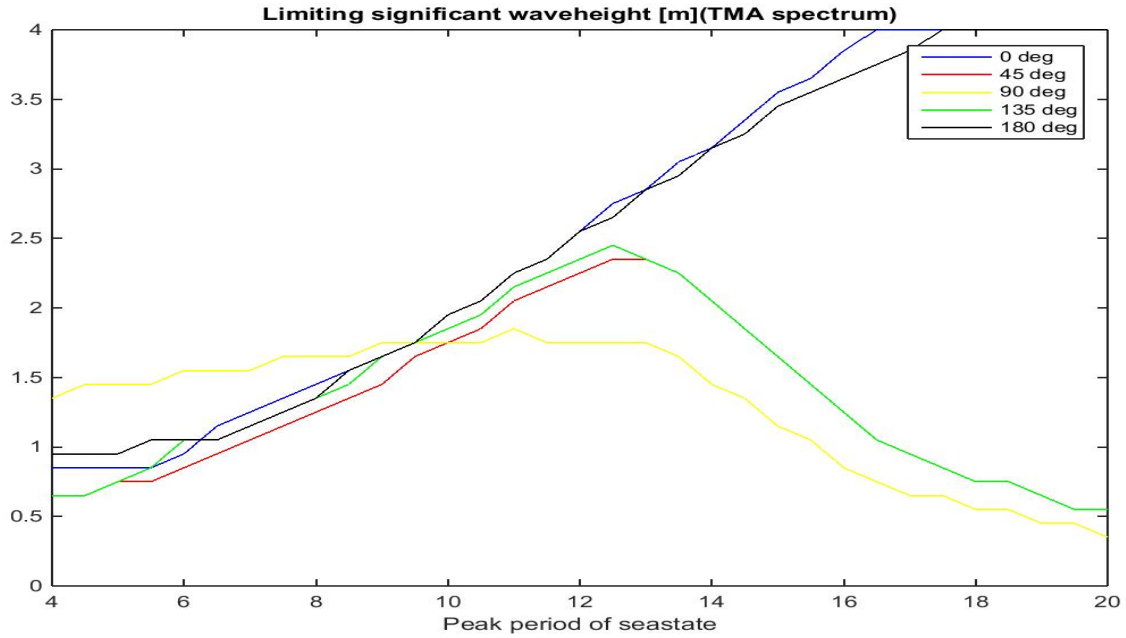

Figure 4.17: Limiting significant wave height with viscous damping in roll, pitch and heave and a drag force term in heave. Assumed wave amplitude 1 m.

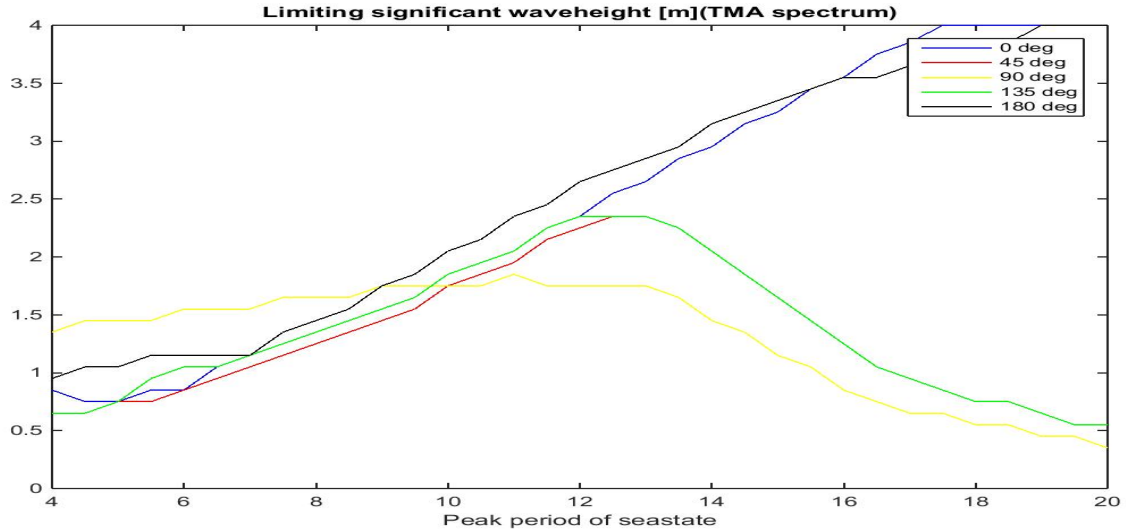

Figure 4.18: Limiting significant wave height with viscous damping in roll, pitch and heave and a drag force term in heave. Assumed wave amplitude 2 m.

It is observed that the beam sea for low peak periods experiences the largest improvement

of limiting significant wave height with the introduction of viscous effects. Plots showing the magnitude of viscous damping and heave excitation force compared to their linear counterparts can be found in appendix A.

4.2 Verification in Time Domain

4.2.1 Response to a harmonic wave

Sea state			Time domain		Frequency domain	
$\zeta_a[m]$	$T[s]$	$\beta[deg]$	$Roll_{amp}[deg]$	$Pitch_{amp}[deg]$	$Roll_{amp}[deg]$	$Pitch_{amp}[deg]$
1	8	0	0	3.9	0	4.3
1	8	45	5.5	4.0	3.9	4.4
1	8	90	7.7	4.0	5.1	4.5

Table 4.8: Response to a harmonic wave of 1 m amplitude and 8 s period

One can observe that the roll response is larger in the SIMA simulations, while the pitch response is somewhat larger in the frequency domain calculations.

4.2.2 Standard deviations of vessel coupled to turbine

The standard deviations calculated in the frequency domain are compared with the standard deviations measured in the time domain for some selected moderate sea states. The time domain simulations have a length of at least 1000 s.

Sea state			Time domain results		Frequency domain results	
$H_s[m]$	$T_p[s]$	$\beta[deg]$	$\sigma_{roll}[deg]$	$\sigma_{pitch}[deg]$	$\sigma_{roll}[deg]$	$\sigma_{pitch}[deg]$
1	5	0	0.0	0.7	0.0	0.5
1	7	0	0.0	0.9	0.0	1.0
1	9	0	0.0	1.0	0.0	1.0
1	5	45	1.6	0.6	1.2	0.5
1	7	45	1.6	1.0	1.1	1.1
1	9	45	1.6	1.0	1.0	1.1
1	5	90	1.8	0.5	1.3	0.5
1	7	90	2.0	1.0	1.3	1.3
1	9	90	2.1	1.0	1.3	1.1

Table 4.9: Standard deviation in roll and pitch measured in SIMO and calculated in frequency domain

One can observe that the standard deviations in pitch in general correlate quite well, while in roll the standard deviations are significantly larger in the time domain simulations.

4.2.3 Parameters to be included in accept criteria

The results from the frequency domain suggests that the limiting significant wave height is not a constant value, but a function of peak period and direction of the sea state. This is put to the test by exposing the model to a constant significant wave height and then vary either peak period or sea state direction to observe the effect, the following table show the effect on time to slip for different wave directions when the significant wave height and peak period is held constant. Only time to slip is considered, no roll angle limit. If no slip is recorded, the time to slip is set to 10 000.

Sea state			Time to slip for wave seeds 1-4				Mean
$H_s[m]$	$T_p[s]$	$\beta[deg]$	1	2	3	4	$\overline{t_{inc}}[s]$
1.2	7	0	10 000	10 000	10 000	10 000	10 000
1.2	7	45	3930	628	263	1182	1501
1.2	7	90	1121	646	312	760	710

Table 4.10: Time to slip from simulations in time domain with constant H_s and T_p, varying β.

The result suggest that the limiting significant wave height do depend on the direction of the sea state, the effect is more pronounced than in the frequency domain calculation. The frequency domain calculations suggest that limiting significant wave height for beam sea might be higher than for head sea given T_p=7 s, disagreeing with this the SIMA-simulations suggests the vessel is far more robust in head sea than in beam and quartering seas for T_p=7 s. The following table show the effect on time to slip for different peak periods when the significant wave height and wave direction is held constant.

Sea state			Time to slip for wave seeds 1-4				Mean
$H_s[m]$	$T_p[s]$	$\beta[deg]$	1	2	3	4	$\overline{t_{inc}}[s]$
2	5	0	393	101	178	365	259
2	7	0	2933	2036	261	768	1500
2	9	0	10 000	6206	265	767	4310

Table 4.11: Time to slip from simulations in time domain with constant H_s and β , varying T_p.

One can observe that the results suggests that the limiting significant wave height do depend on peak period of the sea state.

In the frequency domain significantly better availability was achieved by dividing the sea state into one swell part and one wind generated part, to test for the same effect in the time domain, the SIMA model is exposed to two common misaligned sea states at Dogger Bank found from the NORA10 hindcast. The time to slip from having the same sea state described by two spectra and by one spectrum is compared. The sea states are described in the following table.

Case	Sea state			=	Sea state described with two spectra					
[-]	$H_s[m]$	$T_p[s]$	$\beta[deg]$	=	$H_sW[m]$	$T_pW[s]$	$\beta_w[deg]$	$H_sS[m]$	$T_pS[s]$	$\beta_s[deg]$
1	1.65	7.2	20	=	1.3	5	0	1	10	45
2	1.65	7.2	39	=	1.3	5	0	1	10	90

Table 4.12: Sea states investigated to consider benefits of dividing the sea state into swell and wind generated parts

Doing simulations with 4 wave seeds, the following results were obtained.

Case	Wave seed				Mean [s]
[-]	1	2	3	4	$\overline{t_{inc}}[s]$
1, one spectrum	1396	7061	1322	6228	4002
1, two spectra	6823	8614	10 000	8167	8401
2, one spectrum	396	257	377	170	300
2, two spectra	2753	2402	1969	2318	2360

Table 4.13: Effect of dividing the sea state into swell and wind generated parts

One can observe that the results from dividing the sea state into swell and wind generated part, do indeed effect the result. For the two sea states investigated here, the single spectrum calculation is conservative. However, not enough sea states have been investigated to conclude with whether the single spectrum approach is conservative in general.

4.2.4 Time before first incident

One expected slip every 3600 seconds and the JONSWAP spectrum is used as input to calculate the limiting significant wave heights for some selected sea states with the MATLAB program. Hence, the value to compare with from the frequency domain calculation is 3600 seconds.

For every sea state, 8 simulations with different wave seeds of duration up to 10 000 seconds has been done in SIMO to investigate the time before first incident. The first 100 seconds of the simulations is not considered, if slip occurs here , the simulation will be redone with up to three different wave seeds. If no valid value can be obtained for three different seeds the time to incident is set to zero. If no incident is recorded the value is set to 10 000. A incident is defined as when the fender point of the vessel moves more than 10 cm away from its original position, or the roll angle exceeds 10 degrees. A total simulation of one sea state with 8 wave seeds has a duration of about 45 minutes on a lap top with a modern Intel i7 2.7 GHz processor. Values exceeding 3600 seconds(the value predicted by the frequency domain program) are coloured green, while values under 3600 seconds are coloured red.

Sea state			Time to slip[s] for waveseeds 1-8							
$H_s[m]$	$T_p[s]$	$\beta[deg]$	1	2	3	4	5	6	7	8
1.15	5	0	10 000	10 000	10 000	10 000	10 000	10 000	10 000	10 000
1.65	7	0	10 000	3018	10 000	10 000	6914	10 000	2049	10 000
2.25	9	0	3906	262	763	800	6914	5776	450	962
1.05	5	45	523	140	326	163	509	424	720	266
1.45	7	45	350	142	0	143	300	421	378	264
2.05	9	45	101	138	0	101	168	103	102	267
1.95	5	90	0	0	0	0	0	0	0	0
2.15	7	90	127	0	0	0	0	0	0	149
2.25	9	90	0	107	0	0	356	151	101	149

Table 4.14: Time to incident from simulations in time domain.

One can observe large deviations between the two methods, only for head sea states the values obtained in SIMA is of the same order of magnitude as those used in the frequency domain. Within a 90% confidence interval the following table show if H_0(Frequency domain method conservative) or H_1(non-conservative) was confirmed in the simulations for each sea state.

Sea state			Mean	Lower limit	Upper limit	H_0 or H_1 confirmed?
$H_s[m]$	$T_p[s]$	$\beta[deg]$	$\overline{t_{inc}}[s]$	[s]	[s]	[-]
1.15	5	0	10 000	6 100	20 000	H_0
1.65	7	0	7 742	4645	9290	H_0
2.25	9	0	2 479	1487	4958	Neither
1.05	5	45	383	140	326	H_1
1.45	7	45	250	153	500	H_1
2.05	9	45	122	74	244	H_1
1.95	5	90	0	0	0	H_1
2.15	7	90	28	17	56	H_1
2.25	9	90	108	65	216	H_1

Table 4.15: Hypotheses testing, showing the 90% confidence interval for t_{expinc}

One can observe that which method is the conservative varies with sea state. It can easily be seen that the vessel is far more vulnerable to beam and quartering sea in the time domain simulations than it was predicted by the frequency domain program.

Chapter 5

Discussion

5.1 Effect of concept specific parameters

5.1.1 Bollard push force and friction coefficient

In the frequency domain the effect on availability of the system for varying bollard push force, maximum allowed roll angle and longitudinal distance between the fender point and center of gravity was investigated. The availability of the access system was found to be sensitive with respect to bollard push force. A 50% increase from 200 kN to 300 kN lead to a 49% increase in availability. If one take a look at the expression for risk of slip during one cycle, equation 3.36, it is easy to understand that the availability calculated in the frequency domain heavily depends on the product of friction coefficient and the bollard push force.

$$P_{slip} = e^{\frac{-(\mu * F_b)^2}{2\sigma^2}} \tag{3.36}$$

The practical consequence of this is that the bollard push force on a access vessel using fender docking, should be maximised with respect to the load capacity of the access platform and practical limitations such as maximum engine size. Increasing bollard push force leads to increased availability which ultimately results in a reduction of downtime costs, on the other hand to build stronger access platforms and have vessel with stronger engines have a cost too. Hence, for the construction of a new offshore wind farm, the design of access platform and choice of access vessel should be considered together and optimized with respect to the total cost.

5.1.2 Distance from fender point to center of gravity

When investigating the effect of varying the distance between the fender point and center of gravity of the vessel, it was found that increasing distance led to somewhat improved availability. 3% improvement when increasing the distance 1 from 12.24 m to 13.24. The interesting here is not necessary the quantity of the improvement, but that it is a factor that matters to some extent and hence is a factor the designers of access vessels should have in mind.

5.1.3 Maximum roll angle

Given single point fender docking, as is assumed in Wu (2014), the access operation is not vulnerable to roll motion. Still, to transfer personnel safely to the wind turbine some sort of gangway has to be used and the roll motion can not be unlimited. Increasing maximum roll angle was found to increase the availability of the access system up to 10 degrees, increasing the maximum roll angle further than 10 degrees did not change the availability significantly. A increase from 10 to 15 degrees lead to an increase of the availability of only 0.3%, while increasing the maximum from 5 to 10 degrees gives the significant improvement of 9%.

The interpretation of this is that for sea states causing roll angles exceeding 10 degrees, there will any ways be a too high risk for slip. This tells us that increasing the maximum roll angle the gangway system can handle pays off until a level of 10 degrees is reached, further increasing the roll robustness will not lead to increased availability of the access system and hence not pay off.

5.2 Effect of acceptable risk

If for every sea state there where either 100% chance for success or 100% chance for failure, the limiting significant wave height would not depend on the risk of failure one consider to be acceptable. As ocean waves are a stochastic process this is not the case, it does not make sense talking about a limiting significant wave height without knowing what risk is inherent in this value. When investigating the effect of varying acceptable probability of failure on the availability of the access system(i.e the limiting significant wave height), it was found that the availability to some extent depend on the acceptable probability of failure.

The most conservative estimate which has a 60 times smaller acceptable probability for failure during one access operation than the best estimate yields a 19 % reduction in availability.

While the non-conservative estimate accepting one annual fatality during access in the European offshore wind industry, having 22 times as large acceptable probability of failure than the best estimate, yields 19% improved availability. This shows us that when comparing limiting significant wave height between access concepts, a value typically stated by the manufacturers of the vessel, one need to know what risk level is assumed to make a fair comparison.

5.3 Parameters to be included in the accept criteria

The standard in the industry today is to have a single limiting H_s independent of the direction and peak period of the sea state. As can be seen from for instance figure 4.2, the results from the frequency domain calculations suggests that the limiting significant wave height depend on both peak period and wave direction. The results from the SIMA simulations verifies this. The consequence of this is that the accept criteria for starting the access operation should be a limiting H_s as a function of peak period and wave direction.

Another consequence, is that what access concept is the best choice depend on the wave environment at the specific wind farm location. One might imagine that a access vessel can be designed to maximize its performance in the actual wave environment where it will operate. However, this demands that the offshore wind farm owner is willing to share weather data they have paid for with manufacturers, which might prove problematic.

Sperstad (2014) investigates the effect of single and multi-parameter accept criteria for access on the total O&M cost and optimal fleet size by use of a strategic maintenance and logistics model. Where the multi-parameter approach contained T_p and β in addition to H_s. It was found that the two approaches could give relatively similar results, but only if the single limiting significant wave height was obtained using the information generated by the multi-parameter criteria together with the relevant weather data. This supports the view stated earlier in this section that the limiting H_s should be considered as a function of T_p and β.

5.4 Analysing the access operation

5.4.1 Finite water depth

Introducing finite water depth to the description of the wave environment, gave 3% better availability for the SWATH concept investigated with standard inputs on Dogger Bank location 2

where the water depth is around 30 m.In the case of 15 m water depth, the improvement in availability was found to be 6%. The effect decreases rapidly with water depth and was found to be 0.5% for 60 m. The effect of finite water depth is taken into account by applying the TMA spectrum instead of the JONSWAP spectrum commonly used in the offshore petroleum industry to describe the wave environment. As the TMA spectrum is based on JONSWAP, it can be implemented without much effort as described in DNV-RP-C205 .

Even though 3% improvement as in this case not is radical, using a more physically correct spectrum is a low hanging fruit that should be picked. The TMA spectrum is more physically correct as it takes into account the effect of dissipation of wave energy due to the existence of a bottom boundary layer, stated by Fonseca (2012). SIMA do not at the moment have the TMA spectrum built in, an eventual implementation should be very simple as the JONSWAP spectrum is already built in. As shallow water operations becomes more relevant with the growth of the offshore wind industry, I expect this to change.

5.4.2 Effect of dividing the sea state into swell and wind generated part

A wave environment might consist of waves of different origin coming in from different directions. From the frequency domain calculations , significantly higher availability of the access system was obtained when dividing the sea state into a swell and a wind generated part. 31% increase in all-year availability and a 38% increase in winter availability. As the vessel was far more vulnerable to beam and quartering sea in the SIMA simulations, one might think that the effect is less favorable than found in the frequency domain. Nevertheless, results obtained in SIMA suggest that there is a significant difference between dividing the sea state and not to do so. Not enough cases were investigated in SIMA to verify whether the effect is favorable with regards to availability or not, but it is verified that there is a difference.

Before an investment decision is made on choice of access system, one should in principle compare the different systems with the type of analysis closest to reality. Which would be to divide the sea state into swell and wind generated part. One could compare different access systems by their performance in the most common aligned and misaligned sea states at the wind farm location. The problem with this is that the manufacturers would have to distribute detailed information about their vessels design, technical and hydrodynamical properties, valuable information one cannot expect commercial companies to give away freely.

Even if it proves difficult using the divided sea state approach in the comparison of access concepts, in the every day operations of the wind farm when the properties of the access concept is well known this approach should be applied. This is of two reasons, one is the potential increase of the availability of the access system. The second reason is to take care of the safety of the technicians. In the frequency domain calculations standard case, 5% of the sea states approved by the one spectrum approach was deemed to risky by the divided sea state approach. In the 25 years lifetime of an offshore wind farm this means that using the one spectrum approach, a significant amount of access operations will be done with a risk level not found acceptable.

5.4.3 Viscous effects

It was found necessary to include viscous effects due to very large extreme values in the RAO's for pitch and heave around the natural period. As can be seen from the figures in appendix A, the linear damping in the wave frequency area is quite small for both heave and pitch. The results shows that viscous effects matter, a improvement of the availability of 24% was found when including viscous effects with assumed wave amplitude 1 m. However, it is conservative to neglect them. The pitch response to a harmonic wave was quite similar in the MATLAB program and the SIMA simulation. This suggests that the way of linearising viscous effects in the MATLAB program do not change the physics of the situation significantly. Nevertheless, to linearize a quadratic effect is a simplification which inevitably will lead to some error. More conventional hull forms than the quite special SWATH are likely not be effected by viscous effects to the same extent.

5.5 Comparison with catamaran work boats

According to EWEA (2014), modern catamaran work boats as extensively used in the industry today, is able to do access in H_s up to 1.5 m. As can be seen from the following figure, this would lead to a availability of about 50% at Dogger Bank location 2. The SWATH concept investigated here, with the standard input, was found to have a availability of 47%. 6% less than a catamaran work boat.

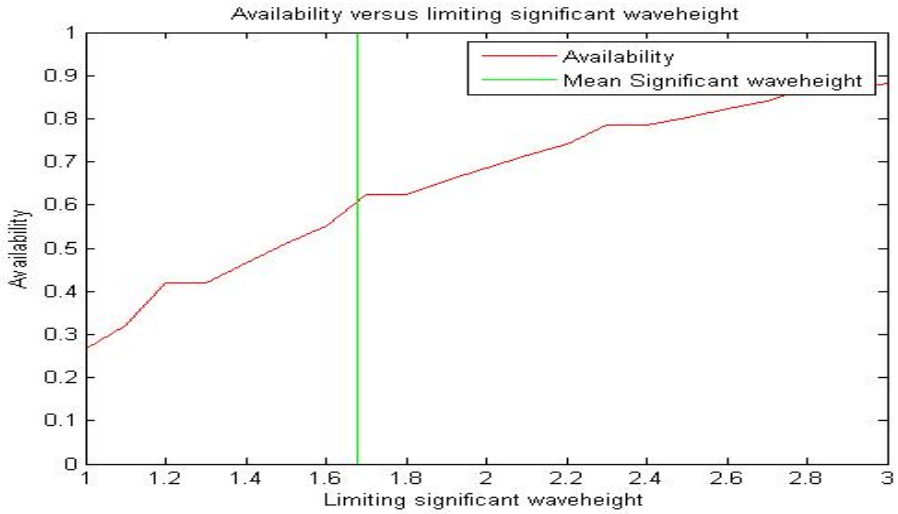

Figure 5.1: Availability versus significant wave height at Dogger Bank location 2

However, one should have in mind that the value of 1.5 m H_s, typically stated by the manufacturers, do not contain any information of dependency on T_p and β nor what risk is inherent in the value. Together with the fact that wind farm owners reports of work boats not being able to perform as promised in all sea states, this suggest that this value is optimistic. As well, as this is not a design thesis and not many design iterations were done, a optimized SWATH vessel surely would outperform the SWATH vessel investigated here.

5.6 Verification of frequency domain method

5.6.1 General

The method proposed by Wu (2014) has not been verified in this thesis. The results from the SIMA simulations do not correspond with the results from the frequency domain calculations. When comparing the response to a moderate harmonic wave and the standard deviations for moderate sea states, the results corresponded fairly well. However, when exposing the model to the less moderate sea states generated in the frequency domain program by expecting one slip every 3600 s, the results did not correspond. In general the SIMA model was more robust in head seas and more vulnerable in beam and quartering seas than predicted by the frequency domain calculations.

The interesting question is then why do the results not correspond. One possibility is of course that either the SIMA model, the MATLAB program or both contains errors such that they are simply wrong. All though that the results from moderate sea states corresponded fairly well suggests otherwise. There have not been time to a thorough analysis of why the deviations are so large, but a little time was spent investigating the possible error sources.

5.6.2 Reasons for failed verification

In Wu (2014) it is assumed that the propeller thrust force is constant working along the global x-axis normal onto the fender, while in the SIMA model it is more physically correct set to be working along the local x-axis of the vessel. Two observations makes this the main suspect as the main reason for the large deviations. One, that when trying to remove the error sources one by one it gave the largest improvement in the results. And two, that in the SIMA simulations almost exclusively upwards slips were observed. This was not predicted by the frequency domain calculations, where upwards slip was the least common slip mode. To change the force to work along the local x-axis, as explained below, specifically increases the risk of upwards slip. This suggest that the assumption of bollard thrust in global x-direction is the main reason behind the large deviations. It should be noted though, that other reasons may matter significantly as well. For instance does not the frequency domain program have any viscous excitation in sway.

The fact that the propeller thrust works along the local x-direction yields two effects that increases the chance for slip. The bollard thrust have a force contribution in both Z and Y direction in the fender as a function of pitch and yaw angle. As well, a moment around the Y-axis is induced by the propeller thrust and the vertical distance between the propeller thrust and fender point. This creates a constant vertical force in the fender,F_{zc}, that the vertical force in the fender will oscillate around. This force can be found by solving the statical heave pitch problem, how to do this is shown in the end of chapter three. The static calculations and the fact that the vertical fender force will oscillate around this value is verified by static and dynamic analysis in SIMA. A plot of the vertical force in one of the two fenders in a moderate sea state is shown below.

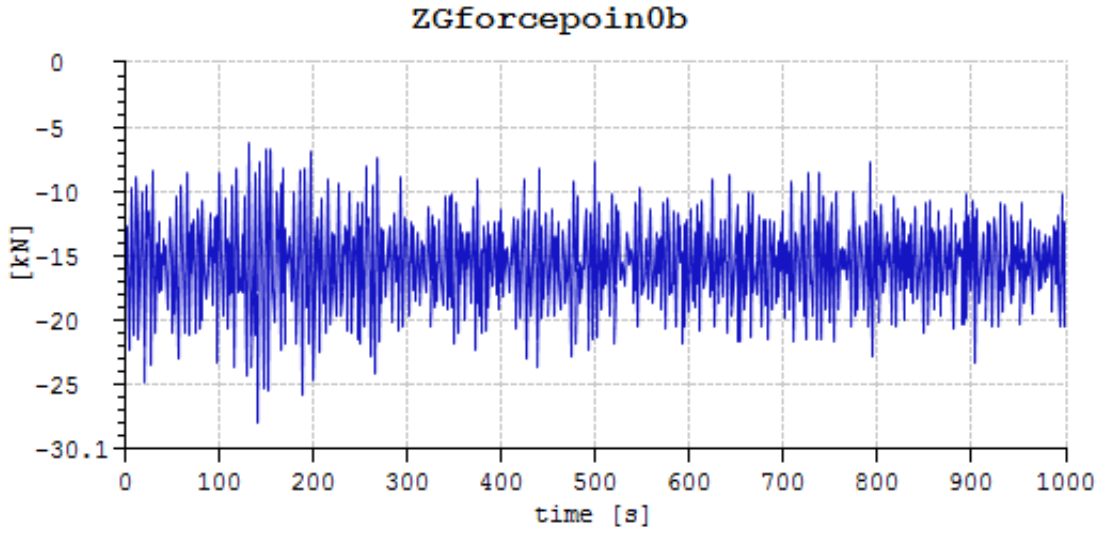

Figure 5.2: Vertical force in left fender,H_s=1 m, T_p=10 s and β=0 deg.

For the standard case investigated here a downwards force from the fender was found to be of magnitude 29.5 kN. Remembering the limit for upwards slip:

$$\alpha(t) < \mu * F_b \tag{3.22}$$

Then including the constant vertical force:

$$\alpha(t) < \mu * F_b - F_{zc} \tag{5.1}$$

It is easy to see that if F_{zc} not is negligible compared to $\mu * F_b$, the risk of upwards slip is increased. In our standard case with a $\mu * F_b$ of 160 kN and a F_{zc} of 29.5 kN, a reduction of the limit for upwards slip of 18.5 % is obtained, a significant amount. The risk of downwards slip is reduced in the same way, this might be the reason why the SIMA model is more robust in head sea than what was predicted in the frequency domain. It should be noted that one might manage to avoid this effect, by counteracting the induced moment with for instance the use of a ballast system.

The force in horizontal and vertical direction induced in the fender by yaw an pitch motions will increase the risk for slip in all directions. The force in Z and Y direction with $r(t)$ as the ship response vector can be written:

$$F_z = F_b * sin(r(5)) \tag{5.2}$$

$$F_y = F_b * sin(r(6)) \tag{5.3}$$

To quantify this, with a yaw or pitch angle of 5 degrees one get a force contribution of 17 kN. That is significant compared to 160 kN. The next interesting question would then be if it is possible to include these two effects in a frequency domain method. The static force is not problematic to implement. Assuming that both pitch and yaw are small angles, have zero mean, are ergodic narrow banded and normally distributed the forces induced in the fender from the pitch and yaw motion as well can be included in the slip criterias described in chapter three. To propose a way of doing this is somewhat beside the scope of this thesis, but a suggestion is made and can be found in the end of chapter three .

Chapter 6

Conclusion and proposals for further work

6.1 Conclusion

The topic of this thesis is the marine operation to access an offshore wind turbine to transfer technicians and parts. Compared to marine operations in the offshore petroleum industry, there are similarities, but also some fundamental differences that require a different mindset. Where operations in the petroleum industry often are few, but large and complex, the operations in the offshore wind industry are repetitive and less complex. The repetitive nature of offshore wind marine operations makes the benefits of finding a optimal solution rather than just a good solution, more significant than in the offshore petroleum industry. In the case of access, the access vessels may spend their entire life cycle in a geographically very limited area. This gives the new opportunity to optimize a vessel with respect to one location.

One obstacle for optimizing the access solutions, is the restricted flow of information between the players in the offshore wind industry. The different participants in the supply chain do not have access to the necessary information to make their part as good as possible. To optimize a access vessel, the yard need information about both the wave environment and the design of access platform. To analyse what is the best possible choice of access solution, the wind farm owner needs detailed technical and hydrodynamic information of the different vessels. This problem is not easily solved. It is understandable that commercial companies are not giving away their intellectual property, even though increased openness would have been beneficial for the industry as a hole. If anything, it shows the value for the wind farm owner to have broad

in-house expertise.

Looking back at the introduction, three focus points for this thesis were mentioned. One of them was to explore the potential of small water plane area solutions for access of offshore wind turbines. The SWATH concept investigated showed that it is possible to design a vessel to perform better in certain type of sea states. Catamaran work boats is considered to be able to make access in H_s up to 1.5 m according to EWEA (2014), this would lead to a availability of about 50% at Dogger Bank location 2. However, one should have in mind that the limiting H_s for work boats is typically given by manufacturers, without information of risk level nor dependency of peak period and wave direction of sea state. Together with the fact that wind farm owners reports of work boats not being able to perform as promised in all sea states, this suggest that this value is optimistic.

Nevertheless, the SWATH concept investigated here is not able to beat a availability of 50%. One should though have in mind that not many design iterations were done and that a optimized SWATH design surely would outperform the concept investigated here. To sum up, it is found that it is possible to design a SWATH to perform in a specific wave environment, but it is not proved that it would outperform a classical catamaran work boat.

Another focus point was to investigate what parameters that should be included in a accept criteria for starting the access operation. It was found that the limiting significant wave height depend on both peak period and wave direction. Hence it is recommended to step away from the industry standard of considering limiting H_s as constant value, to consider limiting H_s as function of wave direction and peak period. The effect of dividing the sea state into swell and wind generated sea was also investigated, it might prove problematic to use this in the comparison of different access concepts, but it was found beneficial to use this in the everyday operation of the offshore wind farm.

The last focus point was to verify the method proposed by Wu (2014) by time domain simulation in SIMO by the use of SIMA. It is concluded that in its current form the method is too simplified and yields results of limited value. It is shown in chapter 5 why the assumption of bollard thrust along the global x-axis effects the results significantly. A frequency domain method including these effects is proposed in 3.4. However, it might very well be that the problem of fender docking simply is too strongly non-linear to be assessed in the frequency domain.

One should have in mind that as discussed in Jimenez (2007), the friction coefficient of rubber do not follow the classic Coulomb's and Amonton's friction laws. The friction coefficient depend on contact pressure, temperature and sliding speed. In addition, as more closely discussed in Groetting (2014), both the assumption of linear waves and the validity of calculating frequency dependent terms with strip theory or panel methods are questionable. This is due to the shallow water and small size of the vessels. As well, the hydrodynamical interaction between the turbine and the vessel is not accounted for neither in the frequency domain nor the SIMA model in this thesis. All in all, both models have room for improvements.

6.2 Proposals for further work

As offshore wind farms move further offshore, it seems that larger vessels with active motion compensating units are gaining popularity. If vessels using fender docking will still be used in large quantities for offshore wind farms, the industry would benefit from better knowledge of the operation. First of all, governing authorities should find a acceptable probability of failure during one access operation, such that future accept criterias can be based on scientific analysis and not depend on the willingness to take risk of each captain.

To improve the understanding of fender docking, a first step would be to obtain a better understanding of the fender. The analysis in SIMO were quite sensitive to small changes in both dynamic and static friction coefficient. Hence to know how temperature, sea water, slip speed and pressure effects the friction coefficient is a key factor in modelling fender docking.

It would be of interest to make a more complex time domain model including for instance diffraction effects from the wind turbine and a more advanced fender. Then this should be validated with model testing or sea trials. One major challenge with this is to obtain the necessary information about the wind turbine, the access platform and the access vessel including the fender. To solve this problem one could imagine a cooperation between a wind farm service vessel owner and a wind farm owner.

When a complex time domain model has been validated, other more simplified time domain models and frequency domain methods would have something to be validated against. Then it would be interesting to try to verify frequency domain methods, for instance the improved method proposed here in 3.4. The benefits of finding a reliable frequency domain method are without a doubt large, it would be a efficient tool for design of access vessels and for wind farm

owners to compare access concepts.

Bibliography

Brekken, T. (2012). Hovedtrekk ved dodsulykkene. *Kompass Tema nr. 3 2013*.

Cengel, Y. A. and Cimbala, J. M. (2010). *Fluid mechanics fundamentals and applications*. McGraw Hill.

Cockburn, C. L. (2010). Accessing the far shore wind farm. *THE ROYAL INSTITUTION OF NAVAL ARCHITECTS*.

Corbetta, G. and Mbistrova, A. (2015). The european offshore wind industry - key trends and statistics 2014. *EWEA*.

DNV (2010). *RULES FOR CLASSIFICATION OF HIGH SPEED, LIGHT CRAFT AND NAVAL SURFACE CRAFT, PART 3 CHAPTER 4 STABILITY AND WATERTIGHT INTEGRITY*. DNV.

EWEA (2014). http://www.wind-energy-the-facts.org/availability-reliability-and-access.html. *http://www.wind-energy-the-facts.org/*.

Faltinsen, O. (1990). *Sea loads on ships and offshore structures*. Cambridge.

Fathi, D. (2004). *VERES USER MANUAL*. MARINTEK.

Fonseca, N. (2012). Finite depth effects on the wave energy resource and the energy captured by a point absorber. *Ocean Engineering*.

Forbes, C. e. (2010). *Statistical distributions*. Hoboken.

Groetting, H. (2014). Access of offshore wind turbines. Project thesis.

Jimenez, M. (2007). The influence of contact pressure on the dynamic friction coefficient in cylindrical rubber-metal contact geometries. *Springer*.

Longwood (2015). Longwood marine fender catalog.

Nielsen, B. (2014). *Conversation with Brian Nielsen 2014, a Statkraft maintenance engineer at Smoela wind farm.*

Ormberg, H. (2014). *SIMO THEORY MANUAL*. Marintek.

Ross, S. M. (2009). *Introduction to probability and statistics for engineers and scientists*. Associated Press.

Sperstad, I. B. (2014). A comparison of single- and multi-parameter wave criteria for accessing wind turbines in strategic maintenance and logistics models for offshore wind farms. *EERA DeepWind 2014, 11th Deep Sea Offshore Wind RD Conference*.

Starfelt, N., Wikdahl, C. E., and Ab, E. (2005). Economic analysis of various options of electricity generation- taking into account health and environmental effects.

Tveiten, C. K. (2011). Hse challenges related to offshore renewable energy. *SINTEF*.

Vada, T. K. (2013). Hydrodynamic analysis of offshore structures. *DNV Software, whitepaper*.

Walpole, R. E. (2007). *Probability and Statistics for engineers and scientists*. Pearson International Edition.

Wu, M. (2014). Numerical analysis of docking operation between service vessels and offshore wind turbines. *Ocean Engineering91(2014)*.

Appendix A

Viscous damping coefficients and excitation forces

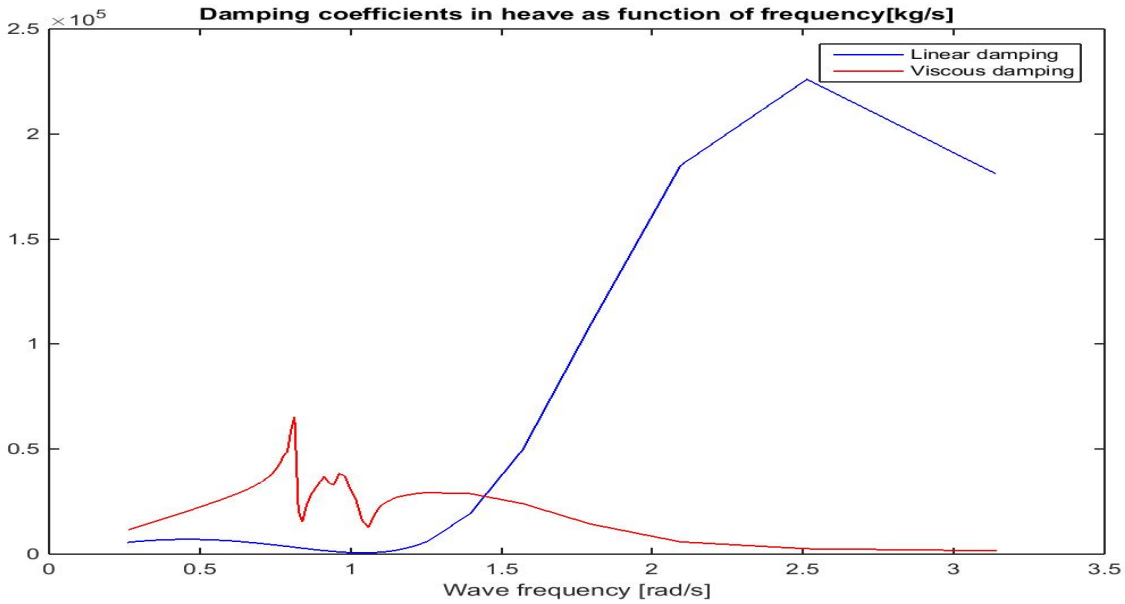

Figure A.1: Damping coefficients in heave, assumed wave amplitude 1 m.

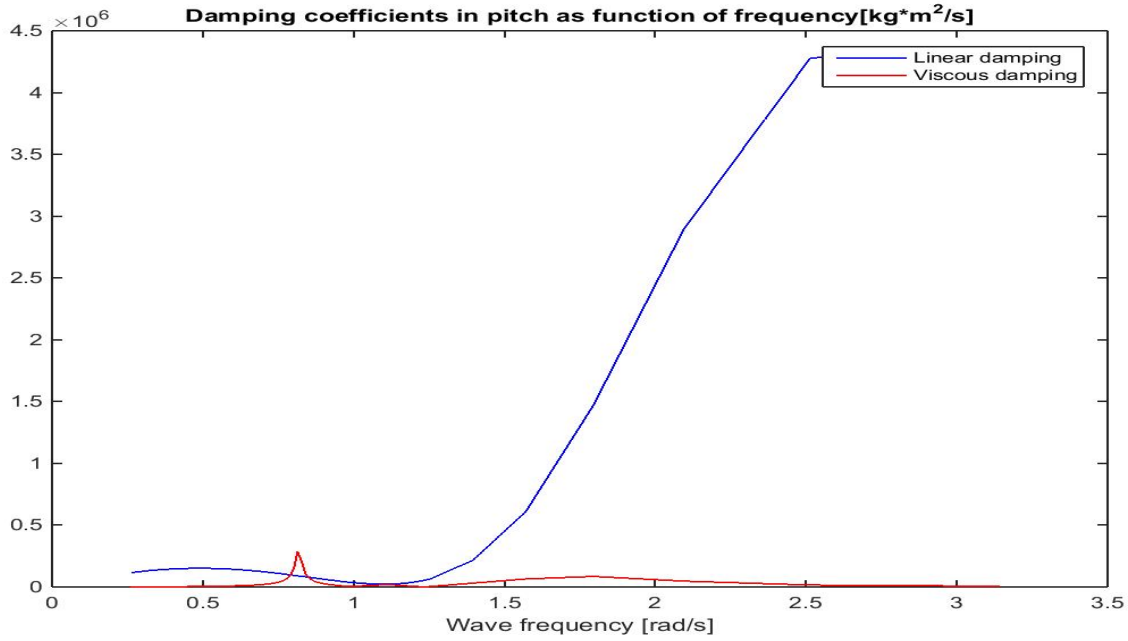

Figure A.2: Damping coefficients in pitch, assumed wave amplitude 1 m.

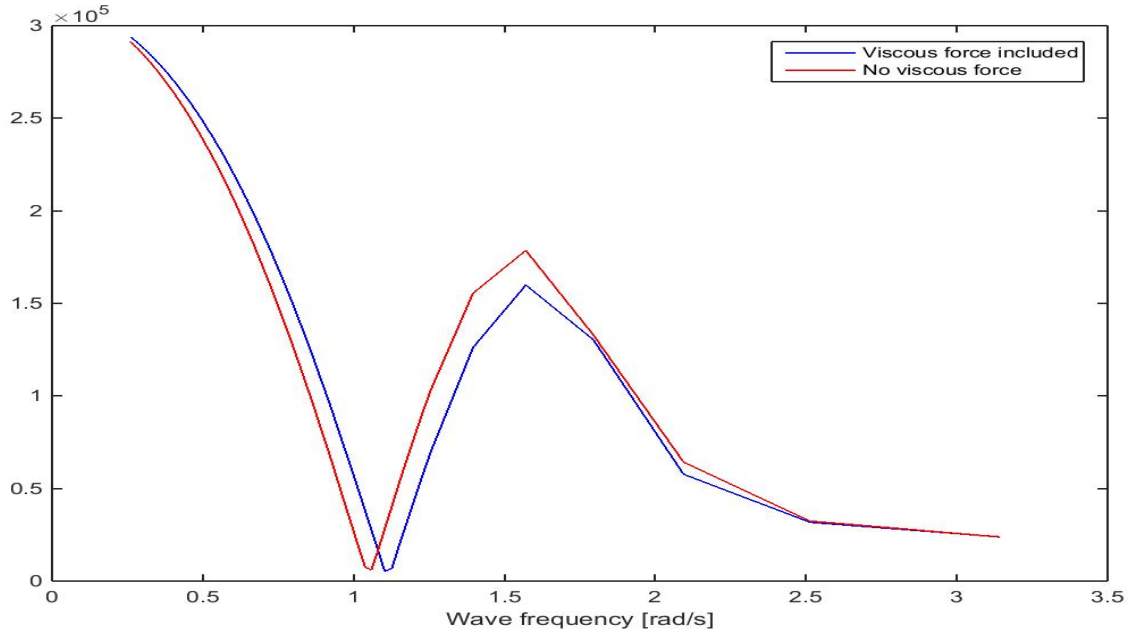

Figure A.3: Heave excitation force, assumed wave amplitude 1 m.

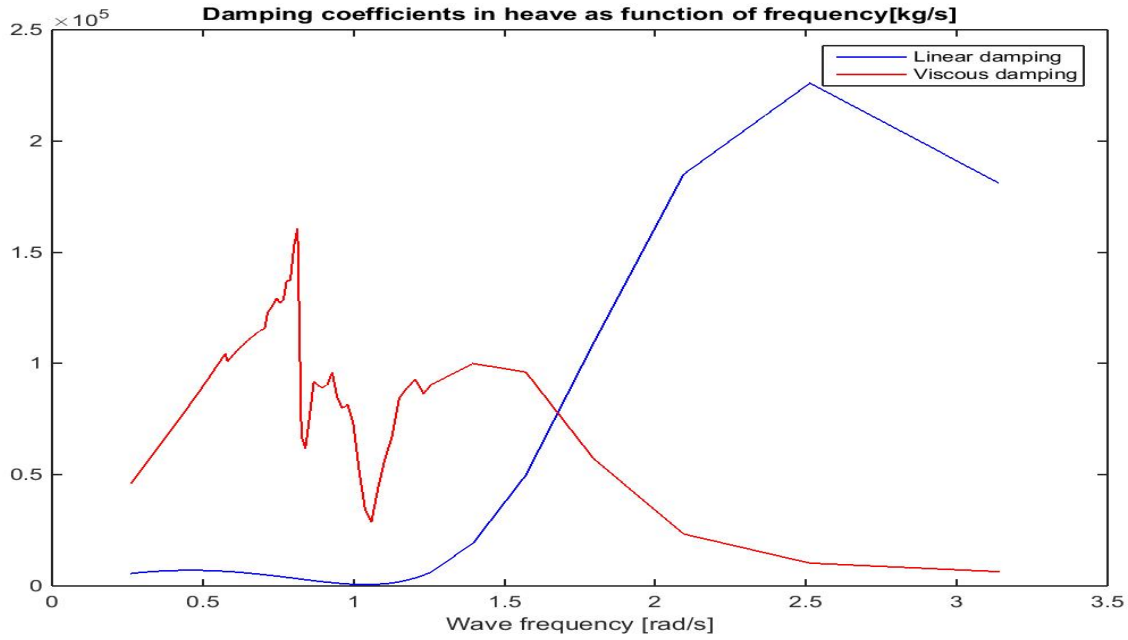

Figure A.4: Damping coefficients in heave, assumed wave amplitude 2 m.

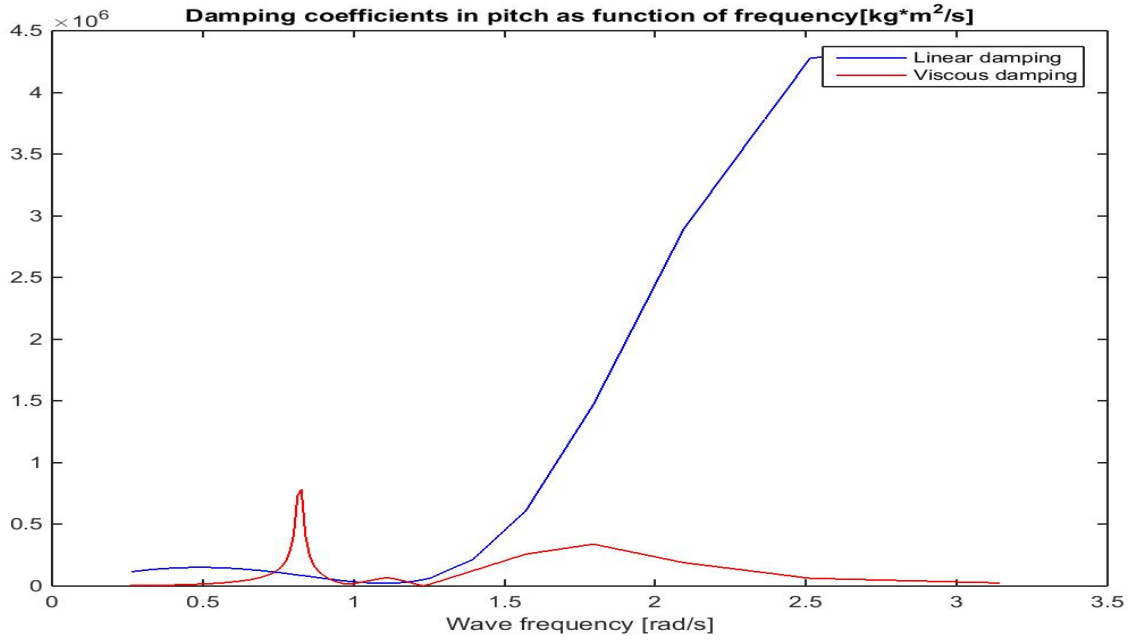

Figure A.5: Damping coefficients in pitch, assumed wave amplitude 2 m.

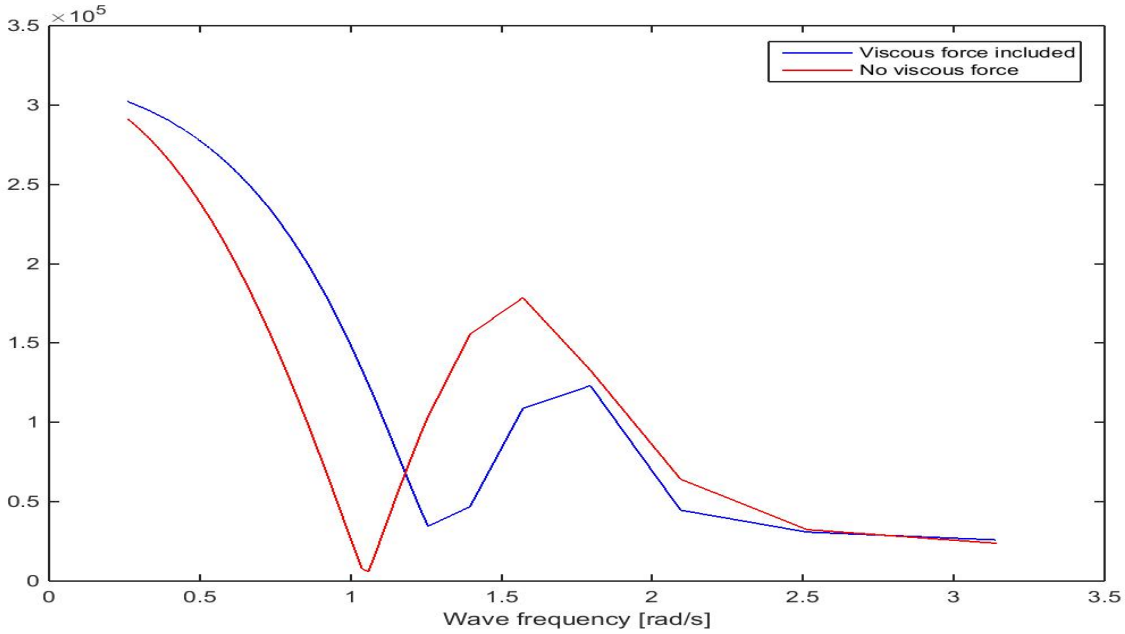

Figure A.6: Heave excitation force, assumed wave amplitude 2 m.

Appendix B

MATLAB program

The flow in the program can shortly be described as the following.

1. The hydrodynamical basis of the vessel is read by the function readveres.m
2. Viscous damping is calculated in viscdamp.m using the RAO's from VERES directly.
3. viscousF.m calculates the viscous excitation force in heave.
4. fendertransf.m calculates the transfer functions of the vessel and forces in the fender when coupled to the wind turbine.
5. limHs2.m finds the limiting significant wave height for each combination of peak period and wave direction. Using the function stdev.m to calculate the standard deviations and specter.m to calculate wave spectrums.
6. availability.m goes through the weather data from NORA10 and compares with the limiting significant wave heights calculated by limHs2.m , output is what the availability would have been the time period between 1957 to 2010.
7. doublespec.m reads each sea state from NORA10 and calculates for each sea state, whether access can be done or not.
8. Then the results obtained is presented in the file result.dat and various graphical outputs.

This is illustrated in the following flowchart.

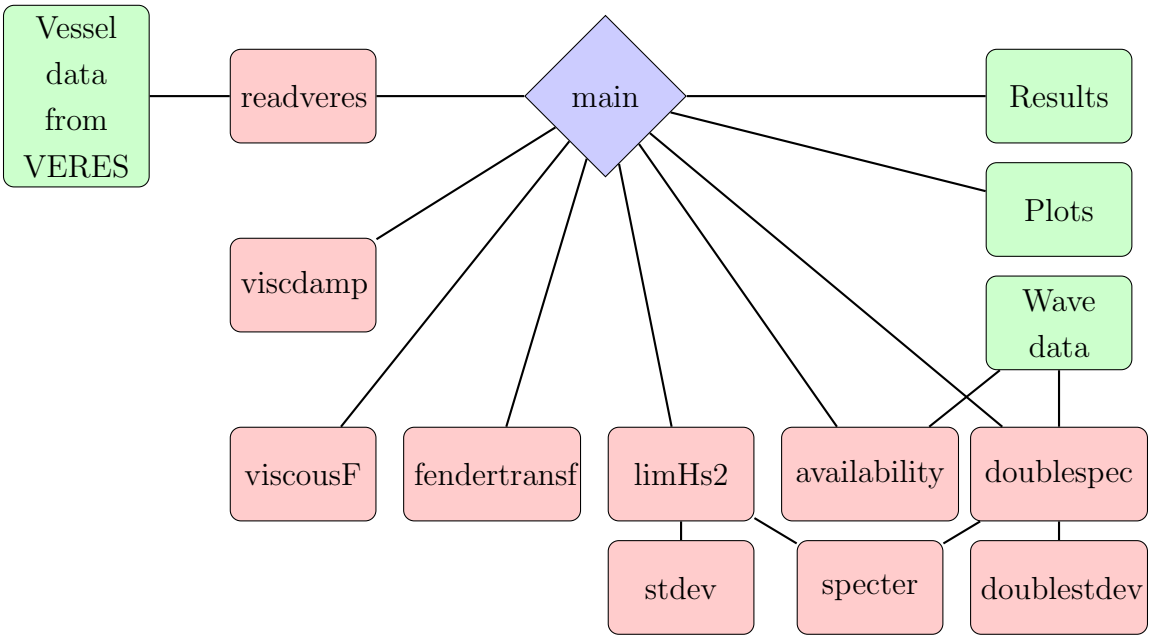

Figure B.1: Flow chart of the frequency domain program

```
%-------------------------------------------------------------------%
% main.m                                                            %
%-------------------------------------------------------------------%
%Script for calculating the limiting significant waveheight as%
%a function of peak period and wave direction and return      %
%useful statistics and graphics when compared to weather data.%
%-------------------------------------------------------------------%
% Author: Heine Groetting                                           %
%-------------------------------------------------------------------%
% Last edit: 19/04-15                                               %
%-------------------------------------------------------------------%
% Input:                                                            %
% name          - VERES hydrodynamic data file name                 %
% Racc          - Acceptable risk for failure during one access%
% Wavestat.dat - Metoccean file from Dogger Bank location 2   %
% Fbollard      - Available bollard force available for vessel %
% AccP          - Point of access, coordinate system have      %
%                 origo in water plane, right handed          %
%                 and positive x direction towards stern      %
% gma           - Parameter for the JONSWAP spectrum          %
% my            - Friction coefficient for vessel turbine     %
%                 fender interaction                          %
```

```
% h            - Water depth [m]                                  %
% Hsmax        - Maximum Hs one would like to consider [m]        %
% Rollmax      - Maximum roll angle acceptable [deg]              %
% Needs to be hardcoded into main.m                               %
%-----------------------------------------------------------------%
% Output:                                                         %
% result.dat - File containing key results                        %
% plots      - Folder containing plots describing the LHS         %
%              ,excitation forces and RAOS                        %
%-----------------------------------------------------------------%
% Self written functions:                                         %
% [A, B, C, M, Frao, beta , omega,RAOS]=readveres(name);          %
% [Stma Sjon Spm]= specter(Hs,Tp, h,omega, gma)                   %
% []=plotter(Frao, beta, omega, LHS_TMA,LHS_JON,Heta,...          %
% Hneta,Rtransf,J1,J2,J3,RAOS)                                    %
% [LHS_TMA LHS_JON dwTMA upTMA dwJON upJON]=limHs2(Heta,...       %
% Hneta,Racc,gma,h,omega,beta,Fbollard...                         %
% ,my,Hsmax,Rollmax,Rtransf,SHeta, SHneta)                        %
% [avblty_TMA avblty_JON avblty_JON_W avblty_TMA_W TMA_vector]    %
% =availabily(LHS_TMA,LHS_JON)                                    %
% Standev = stdev(Hw,S,omega);                                    %
% Standev = doublestdev(HwW,SW,HwS,SS,omega,beta)                 %
% [avblty_2spc_W avblty_2spc diffdec]=doublespec(Racc,Heta...     %
% Hneta,h,my,Fbollard,omega,gma,beta,...                          %
% Rtransf,Rollmax,TMA_vector,SHeta, SHneta)                       %
% [Heta Hneta Rtransf J1 J2 J3 SHeta SHneta]=fendertransf...      %
%(A,M,C ,B,Frao,omega,beta,AccP,my)                               %
%[Bvisc]=viscdamp(my,A,B,C,M,RAOS,omega,Frao,viscKsi,h)           %
%[Fv]=viscousF(my,omega,Frao,beta,viscKsi)                        %
%-----------------------------------------------------------------%
clc
clear all
close all
format long
tic
%************** INPUT *********************************%
name='inputs/input_35_26.out';
AccP=[-12.24 0 3.8];
my=0.8; % Friction Coefficient
Fv=0;
viscKsi=1; % Assumed wave amplitude for calaculation of viscous damping and forces
h=30; % Water depth
```

```
Racc=12*10^(-4); % Acceptable probability for failure during one access
gma=3.3; % Gammafactor (JONSWAP)
gmaS=5; % Gammafactor for representing swell
Fbollard=2*10^5;%[N]
plotting=0; %If plotting shall be done
dividedseacalc=0;% If divided sea state calculation shall be done
Hsmax=4; % MAximum Hs considered
Rollmaxdeg=10; %[deg]
Rollmax=Rollmaxdeg*pi/180; % Translating to [rad]
viscouseffects=1; % Parameter to determine weather viscous effects
                  % in heave and pitch should be accounted for( Roll already is)
%*****************************************************%

[A, B, C, M, Frao, beta , omega,RAOS]=readveres(name);
if viscouseffects
   [Bvisc]=viscdamp(my,A,B,C,M,RAOS,omega,Frao,viscKsi,h);
   B=B+Bvisc;
   [Fv]=viscousF(my,omega,Frao,beta,viscKsi);

end
  [Heta Hneta Rtransf J1 J2 J3 SHeta SHneta Ptransf]=fendertransf(A,M,C,B,Frao,omega,beta,A

[LHS_TMA LHS_JON ]=limHs2(Heta,Hneta,...
    Racc,gma,h,omega,beta,Fbollard,my,Hsmax,Rollmax,Rtransf,SHeta, SHneta);
[avblty_TMA avblty_JON avblty_JON_W avblty_TMA_W TMA_vector]=availability(LHS_TMA,LHS_JON);


if plotting
plotter(Frao, beta, omega, LHS_TMA,LHS_JON,Heta, Hneta,Rtransf,J1,J2,J3,RAOS);

end

if dividedseacalc
[avblty_2spc_W avblty_2spc diffdec]=doublespec(Racc,Heta,Hneta,h,my,...
    Fbollard,omega,gma,beta,Rtransf,Rollmax,TMA_vector,gmaS,SHeta, SHneta);
end
t=toc
[a]=resultprint(avblty_2spc_W,avblty_2spc,diffdec,...
    avblty_TMA,avblty_JON,avblty_JON_W,avblty_TMA_W,t,Rollmaxdeg,Hsmax,my,Fbollard,Racc,Acc


%-----------------------------------------------------------%
```

```
% readveres.m                                                          %
%---------------------------------------------------------------------%
% Function for reading file from Veres of type input.out              %
% Frequency dependent added mass and damping terms , mass mat-%
% rix , hydrostatic stiffness matrix together with transfer           %
% function for excitation forces for different frequencies            %
% and directions is read from the file generated by VERES to          %
% be used in a function written later that will calculate the %
% limiting significant waveheight for access of a offshore            %
% wind turbine.                                                       %
%---------------------------------------------------------------------%
% Author: Heine Groetting                                             %
%---------------------------------------------------------------------%
% Last edit: 27/02-15                                                 %
%---------------------------------------------------------------------%
% Input:                                                              %
% A VERES result file of format input.out                             %
%---------------------------------------------------------------------%
% Output:                                                             %
% N is number of frequencies investigated and M is number of          %
% of directions.                                                      %
% M - 6x6 mass matrix                                                 %
% C - 6x6 hydrostatic stiffness matrix                                %
% A - 6*Nx6 added mass matrices                                       %
% B - 6*Nx6 damping matrices                                          %
% Frao - 6*NxM                                                        %
% omega - Nx1 vector containing frequencies                           %
% beta - Mx1 vector containing headings                               %
% RAOS - 6*Nx6 responce amplitude operator                            %
%---------------------------------------------------------------------%

function [A, B, C, M, Frao, beta , omega,RAOS]=readveres(name)
A=[];
B=[];
C=[];
M=[];
Frao=[];
RAO=[];
fid=fopen(name,'r');

run=1;
teller=1;
```

```
while run
temp=fgetl(fid);
teller=teller+1;
if strcmpi(temp,'     WAVE ENVIRONMENT')
    for i=1:4
        dummy=fgets(fid);
    end
    temp2=fgetl(fid);
    temp3=strsplit(temp2,'=');
    Nfreq=str2double(temp3(2))% NUMBER OF FREQUENSIES INVESTIGATED
    %A=zeros(Nfreq*6,6);
    %B=zeros(Nfreq*6,6);
    for i=1:2
        dummy=fgets(fid);
    end
    temp2=fgetl(fid);
    temp3=strsplit(temp2,'=');
    Nhead=str2double(temp3(2))% NUMBER OF HEADINGS INVESTIGATED
    for i=1:10
        dummy=fgets(fid);
    end
    for i=1:Nfreq
    temp2=strsplit(fgetl(fid));
    temp3=str2double(temp2);
    omega(i)=temp3(3);
    Wnum(i)=temp(5); %%% Wave numbers
    end
    for i=1:7
        dummy=fgets(fid);
    end

    temp2=str2double(strsplit(fgetl(fid)));
    beta=temp2(2:(Nhead+1));



end

if strcmpi(temp,'     Mass matrix:')
    for i=1:6
    temp2=strsplit(fgetl(fid));
    temp3=str2double(temp2);
```

```
86      M(i,:)=temp3(2:7); %READING MASS MATRIX
87      end
88      for i=1:3
89          dummy=fgets(fid);
90      end
91      for i=1:6
92      temp2=strsplit(fgetl(fid));
93      temp3=str2double(temp2);
94      C(i,:)=temp3(2:7); %READING HYDRODYNAMIC STIFFNESS MATRIX
95      end
96  end
97  if strcmpi(temp,'     ADDED MASS AND DAMPING MATRICES')
98       for i=1:Nhead
99           for j=1:Nfreq
100              for n=1:11
101              dummy=fgets(fid)  ;
102              end
103              temp1=(j-1)*6;
104              for n=1:6
105              temp2=temp1+n;
106              temp3=strsplit(fgetl(fid));
107              temp4=str2double(temp3);
108              A(temp2,:)=temp4(2:7);
109              end
110              dummy=fgets(fid);
111              dummy=fgets(fid);
112              for n=1:6
113              temp2=(j-1)*6+n;
114              temp3=strsplit(fgetl(fid));
115              temp4=str2double(temp3);
116              B(temp2,:)=temp4(2:7);
117              end
118              for n=1:14
119              dummy=fgets(fid)  ;
120              end
121              temp3=strsplit(fgetl(fid));
122              temp4=str2double(temp3);
123              Frao(1+temp1,i)=complex(temp4(2),temp4(3));
124              Frao(2+temp1,i)=complex(temp4(4),temp4(5));
125              Frao(3+temp1,i)=complex(temp4(6),temp4(7));
126              for n=1:5
127              dummy=fgets(fid)  ;
```

```
128             end
129             temp3=strsplit(fgetl(fid));
130             temp4=str2double(temp3);
131             Frao(4+temp1,i)=complex(temp4(2),temp4(3));
132             Frao(5+temp1,i)=complex(temp4(4),temp4(5));
133             Frao(6+temp1,i)=complex(temp4(6),temp4(7));
134             for n=1:18
135             dummy=fgets(fid)  ;
136             end
137
138         end
139     end
140
141 end
142 if strcmpi(temp,'     NON-DIMENSIONAL MOTION TRANSFER FUNCTION')
143    for n=1:22
144       dummy=fgets(fid) ;
145    end
146    %%%%%%%%%%%%%%%%%%%%%%  0 deg %%%%%%%%%%%%%%%%%%%%%%
147    for n=1:Nfreq
148            temp3=strsplit(fgetl(fid));
149            temp4=str2double(temp3);
150             RAOS(n,1)=temp4(3);
151             RAOS(n,2)=temp4(5);
152             RAOS(n,3)=temp4(7);
153
154    end
155    for n=1:5
156       dummy=fgets(fid)  ;
157    end
158   for n=1:Nfreq
159            temp3=strsplit(fgetl(fid));
160            temp4=str2double(temp3);
161             RAOS(n,4)=temp4(3);
162             RAOS(n,5)=temp4(5);
163             RAOS(n,6)=temp4(7);
164
165   end
166    for n=1:27
167           dummy=fgets(fid)  ;
168    end
169    %%%%%%%%%%%%%%%% 45 deg %%%%%%%%%%%%%%%%%%%
```

```
170       for n=1:Nfreq
171            temp3=strsplit(fgetl(fid));
172            temp4=str2double(temp3);
173             RAOS(Nfreq+n,1)=temp4(3);
174             RAOS(Nfreq+n,2)=temp4(5);
175             RAOS(Nfreq+n,3)=temp4(7);
176
177    end
178    for n=1:5
179       dummy=fgets(fid)  ;
180    end
181   for n=1:Nfreq
182            temp3=strsplit(fgetl(fid));
183            temp4=str2double(temp3);
184             RAOS(Nfreq+n,4)=temp4(3);
185             RAOS(Nfreq+n,5)=temp4(5);
186             RAOS(Nfreq+n,6)=temp4(7);
187
188   end
189    for n=1:27
190           dummy=fgets(fid)  ;
191    end
192   %%%%%%%%%%%%%%%%%%%%%%%%%%%% 90 deg %%%%%%%%%%%%%%%%%%%%%%%%
193         for n=1:Nfreq
194            temp3=strsplit(fgetl(fid));
195            temp4=str2double(temp3);
196             RAOS(2*Nfreq+n,1)=temp4(3);
197             RAOS(2*Nfreq+n,2)=temp4(5);
198             RAOS(2*Nfreq+n,3)=temp4(7);
199
200    end
201    for n=1:5
202       dummy=fgets(fid)  ;
203    end
204   for n=1:Nfreq
205            temp3=strsplit(fgetl(fid));
206            temp4=str2double(temp3);
207             RAOS(2*Nfreq+n,4)=temp4(3);
208             RAOS(2*Nfreq+n,5)=temp4(5);
209             RAOS(2*Nfreq+n,6)=temp4(7);
210
211   end
```

```
212
213     run=0; % QUITING WHILE LOOP
214 end
215
216
217 end
218
219 fclose(fid)
220
221
222
223
224
225 end
```

```
1  %--------------------------------------------------------------%
2  % fendertransf.m                                               %
3  %--------------------------------------------------------------%
4  % Function that calculates the relevant transfer functions    %
5  % as a function of frequency and wave heading                 %
6  %--------------------------------------------------------------%
7  % Author: Heine Groetting                                      %
8  %--------------------------------------------------------------%
9  % Last edit: 27/02-15                                          %
10 %--------------------------------------------------------------%
11 % Input:                                                       %
12 % M     - 6x6 mass matrix                                     %
13 % C     - 6x6 hydrostatic stiffness matrix                    %
14 % A     - 6*Nx6 added mass matrices                           %
15 % B     - 6*Nx6 damping matrices                              %
16 % Frao  - 6*NxM                                               %
17 % omega - Nx1 vector containing frequensies                   %
18 % beta  - Mx1 vector containing headings                      %
19 % AccP  - Point of access                                     %
20 % my    - Friction coefficient between vessel and turbine     %
21 %--------------------------------------------------------------%
22 % Output:                                                      %
23 % Heta   - Transfer function for eta, variable that describes %
24 %          limit for downward slip. Function of frequency and %
25 %          wave direction. Nfreq x Nhead                      %
26 % SHneta  -Transfer function for sneta, variable thatdescribes%
```

```
%          limit for sideways slip . Function of frequency and%
%          wave direction. Nfreq x Nhead                       %
% SHeta   -Transfer function for seta, variable thatdescribes %
%          limit for sideways slip. Function of frequency and %
%          wave direction. Nfreq x Nhead                       %
% Hneta  - Transfer function for neta, variable that describes%
%          limit for upward slip . Function of frequency and  %
%          wave direction. Nfreq x Nhead                       %
% Rtransf- Transfer function for roll angle. Function of       %
%          frequency and wave direction. Nfreq x Nhead         %
% J1     - Transfer function for normal force in fender        %
% J2     - Transfer function for sideways force in fender      %
% J3     - Transfer function for vertical force in fender      %
%-------------------------------------------------------------%
function [Heta Hneta Rtransf J1 J2 J3 SHeta SHneta Ptransf]=fendertransf(A,M,C,B,Frao,omega

Heta=[];
Hneta=[];
Rtransf=[];
P1=[];% Joint force in x,y,z direction. Consists of J1,J2 and J3
J1=[];
J2=[];
J3=[];
Xacc=AccP(1);
Yacc=AccP(2);
Zacc=AccP(3);

Q=[0 -Zacc Yacc; Zacc 0 -Xacc; -Yacc Xacc 0];
RQ=-Q;
Nfreq=length(omega);
Nhead=length(beta);
if Fv==0
    Fv=zeros(6*Nfreq,Nhead);
end
teller=1;
img=1i;
for i=1:Nhead
    temp1=(i-1)*6;
    for j=1:Nfreq
    temp2=(j-1)*6;
    tempA=A((temp2+1):(temp2+6), 1:6); % Added mass matrix for given frequency
    tempB=B((temp2+1):(temp2+6), 1:6); % Damping matrix for given frequency
```

```
69      tempFraov=Fv((temp2+1):(temp2+6), i);
70      tempFraov=real(tempFraov).*cosd(imag(tempFraov))+real(tempFraov).*sind(imag(tempFraov))
71      tempFrao=Frao((temp2+1):(temp2+6), i); % Excitation force Rao for given frequency and c
72      tempFrao=real(tempFrao).*cosd(imag(tempFrao))+real(tempFrao).*sind(imag(tempFrao)).*imq
73      G=-omega(j)^2*(M+tempA)+omega(j)*tempB*1i+C;
74      H=(G(1:3,1:3)*Q+G(1:3,4:6))*inv(G(4:6,1:3)*Q+G(4:6,4:6)-Q*G(1:3,1:3)*Q-Q*G(1:3,4:6));
75      P1=H*(tempFrao(4:6)-Q*tempFrao(1:3))- tempFrao(1:3);
76      Heta(j,i)=P1(3)-my*P1(1);
77      Hneta(j,i)=-(P1(3)+my*P1(1));
78      R2=inv(G(4:6,1:3)*Q+G(4:6,4:6))*(tempFrao(4:6)+Q*P1);
79      Rtransf(j,i)=R2(1);
80      Ptransf(j,i)=R2(2);
81      SHeta(j,i)=P1(2)-my*P1(1);
82      SHneta(j,i)=-(P1(2)+my*P1(1));
83      J1(j,i)=P1(1);
84      J2(j,i)=P1(2);
85      J3(j,i)=P1(3);
86      end
87  end
88
89
90  end
```

```
1   %--------------------------------------------------------------%
2   % limHs2.m                                                     %
3   %--------------------------------------------------------------%
4   % Function that calculates limiting significant waveheight as %
5   % function of wave frequency and direction                     %
6   %--------------------------------------------------------------%
7   % Author: Heine Groetting                                      %
8   %--------------------------------------------------------------%
9   % Last edit: 17/03-15                                          %
10  %--------------------------------------------------------------%
11  % Input:                                                       %
12  % Heta    - Transfer function for eta, variable that describes%
13  %           limit for downward slip. Function of frequency and%
14  %            wave direction. Nfreq x Nhead                     %
15  % Hneta   - Transfer function for neta,variable that describes%
16  %           limit for upward slip . Function of frequency and %
17  %           wave direction. Nfreq x Nhead                     %
18  % SHneta  -Transfer function for sneta, variable thatdescribes%
```

```
%          limit for sideways slip . Function of frequency and%
%          wave direction. Nfreq x Nhead                       %
% SHeta   -Transfer function for seta, variable thatdescribes %
%          limit for sideways slip. Function of frequency and %
%          wave direction. Nfreq x Nhead                       %
% Racc    - Acceptable probability for failure during one     %
%           seastate                                          %
% gma     - Peakness factor for JONSWAP spectrum              %
% h       - Water depth [m]                                   %
% omega   - Wave frequencies                                  %
% beta    - Wave headings                                     %
% Fbollard- Bollard force[N]                                  %
% my      - Friction coefficient for fender                   %
% Hsmax   - Maximum significant wave height considered        %
% Rollmax - Maximum acceptable roll angle                     %
% Rtransf - Roll transfer function                            %
%-------------------------------------------------------------%
% Output:                                                     %
%  LHS_TMA - Matrix containing limiting significant waveheight%
%            as function of peak frequency and wave heading   %
%            calculated by use of the TMA spectrum            %
%  LHS_JON - Same as LHS_TMA but with use of JONSWAP          %
%-------------------------------------------------------------%
function [LHS_TMA LHS_JON ]=limHs2(Heta,Hneta,Racc,gma,h,omega,beta,Fbollard,my,Hsmax,Rolln
LHS_TMA=[];
LHS_JON=[];
Tp=[2:0.5:20];
lim=my*Fbollard;
for j=1:length(beta) % wave headings
for i=1:length(Tp)

  Nsycle=1800/Tp(i); % Approximation of number of cycles during one access operation
  %%%%%% WORKING UNDER THE 0.5HOUR OPERATION ASSUMPTION %%%%%%%%
  Racc_1cycle=Racc/Nsycle ; % Acceptable probability of slip per cycle
  runTMA=1;
  runJON=1;
  run=1;
  Hs=0.1;
while run~=0;
 [Stma Sjon Spm]=specter(Hs,Tp(i), h,omega, gma) ;
     TMAstdv_eta=stdev(Heta(:,j),Stma,omega);
     TMAstdv_neta=stdev(Hneta(:,j),Stma,omega);
```

```
61      TMAstdv_seta=stdev(SHeta(:,j),Stma,omega);
62      TMAstdv_sneta=stdev(SHneta(:,j),Stma,omega);
63      TMAstdv_roll=stdev(Rtransf(:,j),Stma,omega);
64      JONstdv_eta=stdev(Heta(:,j),Sjon,omega);
65      JONstdv_neta=stdev(Hneta(:,j),Sjon,omega);
66      JONstdv_seta=stdev(SHeta(:,j),Sjon,omega);
67      JONstdv_sneta=stdev(SHneta(:,j),Sjon,omega);
68      JONstdv_roll=stdev(Rtransf(:,j),Sjon,omega);
69
70      TMAdw_probfail=exp(-lim^2/(2*TMAstdv_eta^2));
71      TMAup_probfail=exp(-lim^2/(2*TMAstdv_neta^2));
72      TMA_rollfail=exp(-Rollmax^2/(2*TMAstdv_roll^2));
73      TMAle_probfail=exp(-lim^2/(2*TMAstdv_seta^2));
74      TMAri_probfail=exp(-lim^2/(2*TMAstdv_sneta^2));
75      JONdw_probfail=exp(-lim^2/(2*JONstdv_eta^2));
76      JONup_probfail=exp(-lim^2/(2*JONstdv_neta^2));
77      JON_rollfail=exp(-Rollmax^2/(2*JONstdv_roll^2));
78      JONle_probfail=exp(-lim^2/(2*JONstdv_seta^2));
79      JONri_probfail=exp(-lim^2/(2*JONstdv_sneta^2));
80      TMA_probfail=1-(1-TMAup_probfail)*(1-TMAdw_probfail)*(1-TMAle_probfail)*...
81          (1-TMAri_probfail)*(1-TMA_rollfail);
82           JON_probfail=1-(1-JONup_probfail)*(1-JONdw_probfail)*(1-JONle_probfail)*...
83          (1-JONri_probfail)*(1-JON_rollfail);
84  if runTMA
85      if  TMA_probfail>Racc_1cycle
86      runTMA =0;
87      LHS_TMA(i,j)=Hs-0.05;
88      run=run-0.5;
89
90      end
91
92
93   end
94
95  if runJON
96      if  JON_probfail>Racc_1cycle
97      runJON =0;
98      LHS_JON(i,j)=Hs-0.05;
99      run=run-0.5;
100     end
101 end
102 Hs=Hs+0.1;
```

```
103 if Hs>=Hsmax %%%%% *Introducing  a maximum Hs%%%%%
104     run=0;
105    if runTMA
106        LHS_TMA(i,j)=Hs;
107        runTMA =0;
108    end
109    if runJON
110        LHS_JON(i,j)=Hs;
111        runJON =0;
112    end
113 end
114 
115 end
116 end
117 end
118 end
```

```
1  %-------------------------------------------------------------%
2  % doublespec.m                                                %
3  %-------------------------------------------------------------%
4  % Function that calculates the availability dividing the      %
5  % seastate in one swell and other wind generated part         %
6  % with respect to nora hindcast stored in wavedat.dat         %
7  %-------------------------------------------------------------%
8  % Author: Heine Groetting                                     %
9  %-------------------------------------------------------------%
10 % Last edit: 27/02-15                                         %
11 %-------------------------------------------------------------%
12 % Input:                                                      %
13 %  Heta        - Transfer function for limiting downwards slip%
14 %  Hneta       - Transfer function for limiting upwards slip  %
15 %  SHeta       - Transfer function for limiting left slip     %
16 %  SHneta      - Transfer function for limiting right slip    %
17 %  wavedat.dat - Wave data for Dogger Bank location 2         %
18 %  Racc        - Acceptable probability for failure per access%
19 %  h           - Water depth                                  %
20 %  omega       - Frequencies of Heta and Hneta                %
21 %  my          - Friction coefficient between fender and mill %
22 %  Fbollard    - Amount of bollard thrust                     %
23 %  beta        - Vector with the wave headings considered     %
24 %  Rtransf     - Transfer function for roll motion            %
```

```
%  Rollmax     - Maximum acceptable roll angle                 %
%  TMA_vector  - Vector containing if access can be made       %
%                according to the calculation with the TMA     %
%                spectrum                                      %
%-------------------------------------------------------------%
% Output:                                                      %
% avblty_2spc_W   - Winter availability obtained               %
% avblty_2spc     - Overall availability                       %
% diffdec         - Part of seastates found acceptable by use  %
%                   of the TMA spectrum that was not approved  %
%                   by the  two spectrum method                %
%-------------------------------------------------------------%


function [avblty_2spc_W avblty_2spc diffdec]=doublespec(Racc,Heta,Hneta,h,my,Fbollard,omega
A=load('wavedat.dat'); % A becomes a matrix containing the wave data
Hs=A(:,1); % Vector containing the signinficant waveheights
Tp=A(:,2);  % Vector containing the peak periods
Mdir=A(:,3); % Vector containing the mean direction
HsS=A(:,4); % Vector containing the significant waveheight of swell part of waves
TpS=A(:,5);  % Vector containing the the peak periods of swell
MdirS=A(:,6); % Mean direction of swell
HsW=A(:,7); % Vector containing the significant waveheight of windsea
TpW=A(:,8); % Vector containing the peak periods of wind sea
MdirW=A(:,9); % Mean direction of windsea
month=A(:,10); % Month of record
Nseas=length(Hs); % Number of seastates

Avteller=0;
UAteller=0;
Wteller=0;
AWteller=0;
lim=my*Fbollard;
roll_teller=0;
dw_teller=0;
up_teller=0;
gmaW=1;
diffdec=0;
for i=1:Nseas
  Nsycle=1800/Tp(i); % Approximation of number of cycles during one access operation
  Racc_1cycle=Racc/Nsycle ; % Acceptable probability of slip per cycle
```

```
67
68 [Swind Sjon Spm]=specter(HsW(i),TpW(i), h,omega, gmaW);
69 [Sswell Sjon Spm]=specter(HsS(i),TpS(i), h,omega, gmaS);
70     if or((MdirS(i)>=338),(MdirS(i)<=23))
71     betacordS=1;% _Head sea
72     elseif or((MdirS(i)>=293),(MdirS(i)<=68))
73     betacordS=2; %Quartering head sea
74     elseif or((MdirS(i)>=247),(MdirS(i)<=113))
75     betacordS=3;% Beam sea
76     elseif or((MdirS(i)>=203),(MdirS(i)<=158))
77     betacordS=4; % Quartering following sea
78     else
79     betacordS=5; % Following sea
80     end
81
82     if or((MdirW(i)>=338),(MdirW(i)<=23))
83     betacordW=1;% _Head sea
84     elseif or((MdirW(i)>=293),(MdirW(i)<=68))
85     betacordW=2; %Quartering head sea
86     elseif or((MdirW(i)>=247),(MdirW(i)<=113))
87     betacordW=3;% Beam sea
88     elseif or((MdirW(i)>=203),(MdirW(i)<=158))
89     betacordW=4; % Quartering following sea
90     else
91     betacordW=5; % Following sea
92     end
93    stdev_eta=doublestdev(Heta(:,betacordW),Swind,Heta(:,betacordS),Sswell,omega,beta);
94    stdev_neta=doublestdev(Hneta(:,betacordW),Swind,Hneta(:,betacordS),Sswell,omega,beta);
95    stdev_roll=doublestdev(Rtransf(:,betacordW),Swind,Rtransf(:,betacordS),Sswell,omega,beta
96    stdev_seta=doublestdev(Heta(:,betacordW),Swind,SHeta(:,betacordS),Sswell,omega,beta);
97    stdev_sneta=doublestdev(Hneta(:,betacordW),Swind,SHneta(:,betacordS),Sswell,omega,beta);
98    dw_probfail=exp(-lim^2/(2*stdev_eta^2));
99    up_probfail=exp(-lim^2/(2*stdev_neta^2));
100   roll_probfail=exp(-Rollmax^2/(2*stdev_roll^2));
101   left_probfail=exp(-lim^2/(2*stdev_seta^2));
102   right_probfail=exp(-lim^2/(2*stdev_sneta^2));
103   probfail=1-(1-dw_probfail)*(1-up_probfail)*(1-roll_probfail)*...
104       (1-left_probfail)*(1-right_probfail);
105    if or(month(i)==12,month(i)<4);
106    Wteller=Wteller+1;
107    end
108
```

```
109       if  probfail>Racc_1cycle
110           UAteller=UAteller+1;
111           if TMA_vector(i)
112               diffdec=diffdec+1;
113           end
114       else
115           Avteller=Avteller+1;
116
117               if or(month(i)==12,month(i)<4);
118               AWteller=AWteller+1;
119               end
120
121       end
122
123 end
124 avblty_2spc_W=AWteller/Wteller;
125 avblty_2spc=Avteller/Nseas;
126
127 diffdec=diffdec/sum(TMA_vector);
128
129 end
```

```
1  %-------------------------------------------------------------%
2  % availability.m                                              %
3  %-------------------------------------------------------------%
4  % Function that calculates the availability for a given LHS   %
5  % with respect to weather data stored in wavedat.dat          %
6  %-------------------------------------------------------------%
7  % Author: Heine Groetting                                     %
8  %-------------------------------------------------------------%
9  % Last edit: 17/03-15                                         %
10 %-------------------------------------------------------------%
11 % Input:                                                      %
12 %  LHS_TMA     - Matrix containing limiting significant      %
13 %                waveheight as function of peak frequency    %
14 %                and wave heading calculated by use of the   %
15 %                TMA spectrum                                %
16 %  LHS_JON     - Same as LHS_TMA but with use of the JONSWAP %
17 %                spectrum instead                            %
18 %  wavedat.dat - Wave data for Dogger Bank location 2        %
19 %-------------------------------------------------------------%
```

```
% Output:                                                        %
% avblty_TMA   - Availability with use of the JONSWAP spectrum%
% avblty_JON   - Availability with use of the JONSWAP spectrum%
% avblty_TMA_W - Availibilty in December, January              %
%                    February,  Mars                           %
% avblty_JON_W - Availibilty in December, January              %
%                    February,  Mars                           %
% TMA_vector   - Vector of length Nseas containg 1 if the      %
%                    seastate was ok and 0 if not              %
%-----------------------------------------------------------------%


function [avblty_TMA avblty_JON avblty_JON_W avblty_TMA_W TMA_vector]=availabily(LHS_TMA,LH
A=load('wavedat.dat'); % A becomes a matrix containing the wave data
Hs=A(:,1); % Vector containing the signinficant waveheights
Tp=A(:,2);  % Vector containing the peak periods
Mdir=A(:,3); % Vector containing the mean direction
HsS=A(:,4); % Vector containing the significant waveheight of swell part of waves
TpS=A(:,5);  % Vector containing the the peak periods of swell
MdirS=A(:,6); % Mean direction of swell
HsW=A(:,7); % Vector containing the significant waveheight of windsea
TpW=A(:,8); % Vector containing the peak periods of wind sea
MdirW=A(:,9); % Mean direction of windsea
month=A(:,10); % Month of record
l=length(Hs);
JONteller=0;
TMAteller=0;
Wteller=0;
JONWteller=0;
TMAWteller=0;

for i=1:l
    temp=round(Tp(i)+0.5)-0.5;
    Tpcord=temp/0.5-6;
    if Tpcord<1
        Tpcord=1;
    end

    if or((Mdir(i)>=338),(Mdir(i)<=23))
    betacord=1;% _Head sea
    elseif or((Mdir(i)>=293),(Mdir(i)<=68))
```

```
62      betacord=2; %Quartering head sea
63      elseif or((Mdir(i)>=247),(Mdir(i)<=113))
64      betacord=3;% Beam sea
65      elseif or((Mdir(i)>=203),(Mdir(i)<=158))
66      betacord=4; % Quartering following sea
67      else
68      betacord=5; % Following sea
69      end
70      if Hs(i)<=LHS_TMA(Tpcord,betacord)
71          TMAteller=1+TMAteller;
72          TMA_vector(i)=1;
73      else
74          TMA_vector(i)=0;
75      end
76
77      if Hs(i)<=LHS_JON(Tpcord,betacord)
78          JONteller=1+JONteller;
79      end
80      if or(month(i)==12,month(i)<4);
81          Wteller=Wteller+1;
82          if Hs(i)<=LHS_TMA(Tpcord,betacord)
83          TMAWteller=1+TMAWteller;
84          end
85
86          if Hs(i)<=LHS_JON(Tpcord,betacord)
87          JONWteller=1+JONWteller;
88          end
89      end
90
91  end
92
93  avblty_TMA=TMAteller/l;
94  avblty_JON=JONteller/l;
95  avblty_JON_W=JONWteller/Wteller;
96  avblty_TMA_W=TMAWteller/Wteller;
```

```
1  % Function that calculates additional quadratic damping in    %
2  % heave and pitch, linearize it and and returns an additional %
3  % damping matrix.                                             %
4  % viscdamp.m
5  %-------------------------------------------------------------%
```

```
% Author: Heine Groetting                                              %
%--------------------------------------------------------------------%
% Last edit: 17/03-15                                                 %
%--------------------------------------------------------------------%
% Input:                                                              %
% M     - 6x6 mass matrix                                             %
% C     - 6x6 hydrostatic stiffness matrix                            %
% A     - 6*Nx6 added mass matrices                                   %
% B     - 6*Nx6 damping matrices                                      %
% Frao  - 6*NxM                                                       %
% omega - Nx1 vector containing frequensies                           %
% beta  - Mx1 vector containing headings                              %
% AccP  - Point of access                                             %
%--------------------------------------------------------------------%
% Output:                                                             %
% Bvisc= Additional viscous damping matrix                            %
%--------------------------------------------------------------------%
function [Bvisc]=viscdamp(Xg,A,B,C,M,RAOS,omega,Frao,ksiA,h)
a=Xg;
viscplot=1;
[HxP WxP x]=Swathdesign(a);
Cd=1.1;   % # Cengel and Cimbala for this kind of form and aspect ratio
amp=ksiA;  % This value has to be assumed, and result will depend on this!
Nfreq=length(omega);
img=1i;
Bvisc=zeros(6*Nfreq,6);
RAOS2=RAOS(1:Nfreq,:);
Nponts=length(WxP);
DX=x(2)-x(1);

rho=1025;%% Density of seawater
g=9.81;
teller=0;
for i=1:Nfreq

    temp=(i-1)*6;
    diff=1;
    krav=0.1;
    tempA=A((temp+1):(temp+6), 1:6); % Added mass matrix for given frequency
    tempB=B((temp+1):(temp+6), 1:6); % Damping matrix for given frequency
    tempFrao=amp*Frao((temp+1):(temp+6), 1); % Excitation force Rao for given frequency
    B33(i)=0;
```

```
48      B55(i)=0;
49      RAO=inv(-omega(i)^2*(tempA+M)+omega(i)*img*tempB+C)*tempFrao;
50      RAOold=RAO;
51      teller=0;
52      while diff>krav
53
54
55      Mamp=abs(RAO(3))*amp;
56      Cdstar=0.5*rho*Cd*Mamp*8*omega(i)/(3*pi);%%% Linearization, ref Faltinsen page 97
57      for j=1:Nponts
58          b33(j)=2*Cdstar*WxP(j)*DX;% two pontoons
59
60      end
61      B33(i)=sum(b33);
62      tempB(3,3)=B(temp+3, 3)+B33(i);
63      RAOnew=inv(-omega(i)^2*(tempA+M)+omega(i)*img*tempB+C)*tempFrao;
64      diff=abs(abs(RAOnew(3))-abs(RAO(3)));
65      teller=teller+1;
66      RAO=RAOnew;
67      end
68      Bvisc(temp+3,3)=B33(i);
69      diff=1;
70      krav=0.05;
71      while diff>krav
72
73      k=wavenum(omega(i),h);
74      Mamp=k*abs(RAO(5))*amp;
75      Cdstar=0.5*rho*Cd*Mamp*8*omega(i)/(3*pi);%%% Linearization, ref Faltinsen page 97
76      for j=1:Nponts
77          b55(j)=2*Cdstar*WxP(j)*DX*x(j)^3;
78      end
79      B55(i)=sum(b55);
80      tempB(5,5)=B(temp+5, 5)+B55(i);
81      RAOnew=inv(-omega(i)^2*(tempA+M)+omega(i)*img*tempB+C)*tempFrao;
82      diff=abs(abs(RAOnew(5))-abs(RAOold(5)));
83      teller=teller+1;
84      w=omega(i);
85      RAOold=RAOnew;
86      end
87
88
89
```

```
    Bvisc(temp+5,5)=B55(i);
    RAOS2(i,1:6)=abs(RAOnew);

end



end
```

```
%-------------------------------------------------------------%
% viscousF.m                                                  %
%-------------------------------------------------------------%
% Function that estimates viscous excitation force in heave   %
%-------------------------------------------------------------%
% Author: Heine Groetting                                     %
%-------------------------------------------------------------%
% Last edit: 2/05-15                                          %
%-------------------------------------------------------------%
% Input:                                                      %
% Frao    - Excitation force RAO                              %
% omega   - Wave frequencies                                  %
% beta    - Wave headings                                     %
% Xg      - Poition of COG compared to LPP/2                  %
%-------------------------------------------------------------%
% Output:                                                     %
% Fv      - Viscous excitation force in heave as depending in %
%           frequency and direction. 6*NxM matrix             %
%-------------------------------------------------------------%
function [Fv]=viscousF(Xg,omega,Frao,beta,ksiA)
a=Xg;
viscplot=0;
[HxP WxP x]=Swathdesign(a);
Nfreq=length(omega);
Nhead=length(beta);
Cd=1.1;
rho=1025;%% Density of seawater
g=9.81;
```

```
Nponts=length(WxP);
DX=x(2)-x(1);
z=-1.5;
h=30;
img=1i;
Fv=zeros(6*Nfreq,Nhead);
for n=1:Nhead
for i=1:Nfreq
    temp=(i-1)*6;
    if omega(i)>1.57

    end
    k(i)=wavenum(omega(i),h);

    Wavelength(i)=2*pi/k(i);
   kx=cosd(beta(n))*k(i);
   ky=sind(beta(n))*k(i);
   F3amp=0;
    for j=1:Nponts
        WspeedAmpleft=ksiA*omega(i)*(sinh(k(i)*(z+h))/sinh(k(i)*h))*cos(-kx*x(j)-ky*4);
        WspeedAmpright=ksiA*omega(i)*(sinh(k(i)*(z+h))/sinh(k(i)*h))*cos(-kx*x(j)+ky*4);
        Cdstarleft=ksiA*0.5*rho*Cd*WspeedAmpleft*8*omega(i)/(3*pi);
        Cdstarright=ksiA*0.5*rho*Cd*WspeedAmpright*8*omega(i)/(3*pi);
        F3amp(j)=(Cdstarleft+Cdstarright)*WxP(j)*DX;%        % Taking into account varying
        % lin=linearization factor
    end
    Fv(temp+3,n)=sum(F3amp)/ksiA-img*90; % Taking care of the phase
    F3(i,n)=sum(F3amp);
end
end

end
```

```
%-------------------------------------------------------------%
% stdev.m                                                     %
% Function that calculates the standard deviation of a        %
% of a transfer function and a load spectrum, working under   %
% the assumption that the stochasticprocess is ergodic, normal%
% distributed and narrow banded.                              %
%-------------------------------------------------------------%
% Author: Heine Groetting                                     %
```

```
%-------------------------------------------------------------%
% Last edit: 27/02-15                                         %
%-------------------------------------------------------------%
% Input:                                                      %
% Hw  - Transfer function                                     %
% S   - Spectra                                               %
% omega - Corresponding frequency values                      %
%-------------------------------------------------------------%
% Output:                                                     %
% Standev  - The standard deviation                           %
%-------------------------------------------------------------%

function Standev = stdev(Hw,S,omega);
Hw=(transpose(Hw));
integ=abs(Hw.*Hw.*S);
variance=trapz(omega,integ);
Standev=sqrt(variance);
%fig=figure(7)
%plot(omega,Hw,'r')
%figure (8)
%plot(omega, S,'blue')
%figure(9)
%plot(omega,integ,'green')



end
```

```
%-------------------------------------------------------------%
% doublestdev.m                                               %
% Function that calculates the standard deviation of two load %
% spectrums and two fransfer functions linearly working under %
% the assumption that the stochasticprocess is ergodic, normal%
% distributed and narrow banded.                              %
%-------------------------------------------------------------%
% Author: Heine Groetting                                     %
%-------------------------------------------------------------%
% Last edit: 16/03-15                                         %
%-------------------------------------------------------------%
% Input:                                                      %
```

```
% HwW  - Transfer function 1                                    %
% SW   - Spectra      1                                         %
% HwS  - Transfer function  2                                   %
% SS   - Spectra   2                                            %
% omega - Corresponding frequency values                        %
% beta  - Corresponding headings                                %
%---------------------------------------------------------------%
% Output:                                                       %
% Standev  - The standard deviation                             %
%---------------------------------------------------------------%

function Standev = doublestdev(HwW,SW,HwS,SS,omega,beta);
HwW=(transpose(HwW));
integW=abs(HwW.*HwW.*SW);
HwS=(transpose(HwS));
integS=abs(HwS.*HwS.*SS);
integ=integW+integS;
variance=trapz(omega,integ);
Standev=sqrt(variance);




end
```

```
%---------------------------------------------------------------%
% specter.m                                                     %
%---------------------------------------------------------------%
% Function that generates a TMA and a JONSWAP spectrum given    %
% Hs, Tp and depth. Spectras are defined as in RP C205 by DNV   %
%---------------------------------------------------------------%
% Author: Heine Groetting                                       %
%---------------------------------------------------------------%
% Last edit: 17/03-15                                           %
%---------------------------------------------------------------%
% Input:                                                        %
% Tp - Peak period                                              %
% Hs - Significant waveheight                                   %
% h  - Occean depth                                             %
% gma - gammafactor in the JONSWAP spectrum                     %
```

```
% omega - wave frequencies                                          %
%-------------------------------------------------------------------%
% Output:                                                           %
% Stma - TMA specter                                                %
% Sjon - JONSWAP specter                                            %
% Spm  - PM specter                                                 %
%-------------------------------------------------------------------%
function [Stma Sjon Spm]=specter(Hs,Tp, h,omega,gma)

Stma=[]; % TMA spetrum
Sjon=[]; % JONSWAP spectrum
Spm=[]; % PM spectrum
Agamma=1-0.287*log(gma); % Normalizing factor, log means natural algorithm in MATLAB
wP=2*pi/Tp;
w=omega;
krav=10^-6; % Accuracy in the wave number iteration
diff=1;  % just to get the wave number iteration started
g=9.81;  % Acceleration of gravity

for i=1: length(w)

    if w(i)< wP
        sigma=0.07; % Width parameter of JONSWAP Spectrum
    else
        sigma=0.09;
    end
    Spm(i) = (5/16)*Hs^2*wP^4*(w(i)^-5)*exp(-1.25*(w(i)/wP)^-4);

    Sjon(i)=Agamma*Spm(i)*gma^(exp(-0.5*((w(i)-wP)/(sigma*wP))^2));

    %********** Wave number iteration ***************%
    k=w(i)^2/g;
    while diff>krav

    knew=w(i)^2/(g*tanh(k*h)); % The dispersion relation
    diff=abs(knew-k);
    k=knew;
    end
    TMA= (cosh(k*h))^2/((cosh(k*h))^2+w(i)^2*h/g);
    Stma(i)=Sjon(i)*TMA;
    %************************************************%

```

```
58 end
59
60
61 end
```

Appendix C

Script for writing input file to VERES

```
%-------------------------------------------------------%
% Swathdesign.m                                         %
%-------------------------------------------------------%
%  Function for creating a geometry file to be          %
%  used in VERES. Input is a SWATH main particulars     %
%  and output is a .mgf file for application in  VERES  %
% ------------------------------------------------------ %
% Written by: Heine Groetting                            %
% Last edit: 22/02-15                                    %
% ------------------------------------------------------ %
% Input: -Hard coded main characteristics of SWATH       %
%-------------------------------------------------------%
% Output: - mgf file for input in Veres                  %
%         - x, containing x-coordinates of the           %
%           different sections.                          %
%         - HxP, containing height of pontoon as         %
%           function of x-coordinate                     %
%         - WxP, width of pontoon as function            %
%           of x-coordinate                              %
%%%%%%%%%%%%%%%%%%%%%%%%%%%%%%%%%%%%%%%%%%%%%%%%%%%%%%%%

function [HxP WxP x]=Swathdesign(a);
%---------Defining main particulars-----------------------------%
Lpp= 23 ;% [m] Length between perpendiculars
B= 10.6; % [m] Beam of vessel
Lwl= 24; % [m] Lengt in waterline
```

```
Dswath= 2.6; % [m]  Draft in SWATH mode
Dcat=   1.6 ; % [m] Draft in catamaran mode
Depth= 6.4 ;  %  [m]Depth of vessel
SWF=0.35; % [-] Width of strut as a fraction of width of pontoon
Lps=0.9; % [-] Length of struts as part of length of pontoons
Ns=31; % [-] Number of sections
Np=20; % [-]  Numer of points per section
WP=2.6; % [m] Width of Pontoon at the widest
HP= 2.2; % [m] Height of Pontoon at highest
HPB=1.8; % [m] Height of pontoon at bow
HPS=1.2; % [m] Height of pontoon at stern
YP= (B-WP)*0.5;   % [m] Horizontal distance from centerline to centerline of pontoon
DX=Lwl/(Ns-1); % [m] Length between sections
BowInc=6 ; % [m] Distance where the pontoon is inclined in the bow;
SternInc=5; % [m] Distance where the pontoon is inclined in the stern;
SternHPS=3;   % [m] Distance where the pontoon have HPS;
NSternInc=floor(SternInc/DX); % [-] Number of sections pontoon inclined in stern
NBowInc=floor(BowInc/DX);% [-] Number of sections pontoon inclined in bow
%-------------------------------------------------------------%


HxP=[]; % [m] Height of pontoon as a function of section
WxS=[]; % [m] Width of strut as a function of section
WxP=[]; % [m] Width of pontoon as a function of section
Zcord=zeros(Np,Ns); % [m] (Np,Ns) Matrix containing z coordinate for point n section m
Ycord=Zcord; % [m] (Np,Ns) Matrix containing y coordinate for point n section m

%
teller=1;
for i=1:Ns
     x(i)=-Lwl*0.5+ (i-1)*DX;

     if x< -0.5*Lwl+BowInc
    HxP(i)=HPB+(Lwl*0.5+x(i))*(HP-HPB)/BowInc;

     else
         if x< -0.5*Lwl+(Lwl-SternInc-SternHPS);
       HxP(i)=HP;

         else

             if  x< -0.5*Lwl+(Lwl-SternHPS);
```

```
            HxP(i)=HP-(x(i)-(Lwl*0.5-SternInc-SternHPS))*(HP-HPS)/SternInc;
            teller=teller+1;
            else
                HxP(i)=HPS;
            end
        end
    end
    if x(i)>=0;
    WxP(i)=0.5*WP*sqrt(1-(x(i)/(0.5*Lwl))^2);
    else
    WxP(i)=0.5*WP*cos(pi*x(i)/Lwl);
    end

    WxS(i)=SWF*WxP(i);
    teller2=1;
     for j=1:(Np*0.5)
        if j == (Np*0.5)
            Zcord(j,i)=HP-HxP(i);
            Ycord(j,i)=YP;
            Zcord(Np,i)=Depth;
            Ycord(Np,i)=0;

        elseif j==1
            Zcord(j,i)=Depth;
            Ycord(j,i)=YP+WxS(i);
            Zcord(Np-j,i)=Zcord(j,i);
            Ycord(Np-j,i)=YP-WxS(i);
        elseif j==2
            Zcord(j,i)=HP;
            Ycord(j,i)=YP+WxS(i);
            Zcord(Np-j,i)=Zcord(j,i);
            Ycord(Np-j,i)=YP-WxS(i);
        elseif j==3
            Zcord(j,i)=HP;
            Ycord(j,i)=YP+(WxP(i)-0.02);
            Zcord(Np-j,i)=Zcord(j,i);
            Ycord(Np-j,i)=YP-(WxP(i)-0.02);
        else
            temp1= 0.5*(Np-8);
            temp2=HxP(i)/(temp1+1);
            temp3=temp2* teller2;
            Zcord(j,i)=HP-temp2* teller2;
```

```
111                 Ycord(j,i)=YP+ WxP(i)*sqrt(1-(temp3/HxP(i))^2);
112                 Zcord(Np-j,i)=Zcord(j,i);
113                 Ycord(Np-j,i)=YP- WxP(i)*sqrt(1-(temp3/HxP(i))^2);
114                 teller2=teller2+1;
115             end
116
117
118
119
120         end
121
122
123
124
125
126 end
127
128
129
130 %%%%%%%%%%%%%%%%%%%%%%%%%%%%%%%%%%%%%%%%%%%%%%%%%%%%%%%%%%%%%%%%%%%%%%%
131
132 fid=fopen('swath_35.mgf', 'w');
133     fprintf(fid, 'VERES GEOMETRY FILE\n');
134     fprintf(fid, 'SWATH OFFSHORE WINDTURBINE SERVICE VESSEL\n');
135     fprintf(fid, ' Draught between 2.6 and 1.6\n');
136     fprintf(fid, 'Author: Heine Groetting\n');
137     fprintf(fid, '%f \n', Lpp);
138 for i=1:Ns
139
140     fprintf(fid, '%i \n', Ns+1 -i); % SECTION number, beginning in the bow
141     fprintf(fid, '%f \n', x(i)); % Printing x position
142     fprintf(fid, '%i \n', Np); % Number of points per section
143
144     for j=1:Np
145      fprintf(fid, '%f %f\n', Ycord(j,i), Zcord(j,i));
146
147     end
148
149
150
151
152
```

```
153
154 end
155
156 fclose(fid);
157 WxP=2*WxP;
158
159 end
```

Appendix D

Script for calculation of drag coefficients

```
%%%%%%%%%%%%%%%%%%%%%%%%%%%%%%%%%%%%%%%%%%%%%%%%%%%%%%%%
% Script for calculating quadratic force   coefficients%
% of a SWATH, specific for design made by Swathdesign.m%
%------------------------------------------------------%
% input:                                               %
%      HxP- height of pontoon as function of x-position%
%      WxP- Width of pontoon as function of x position %
%      x  - x-positions of sections of SWATH           %
%------------------------------------------------------%
% output:                                              %
%         Bq- Diagonal quadratic force matrix          %
%             Coupled terms neglected , given in       %
%             kN s^2/m^2 and kNs^2/m                   %
%         Cdx- Drag coefficient in x direction         %
%         Cdy- Drag coefficient in y direction         %
%         Cdz- Drag coefficient in z direction         %
%%%%%%%%%%%%%%%%%%%%%%%%%%%%%%%%%%%%%%%%%%%%%%%%%%%%%%%%
% Author: Heine Groetting                              %
%------------------------------------------------------%
% Last edit: 02/06-2015                                %
%------------------------------------------------------%
a=1;
rho=1.025;
[HxP WxP x]=Swathdesign(a);
```

```
Bq=zeros(6,6);
dx=abs(x(1)-x(2));
Nsec=length(x);
L=x(Nsec)-x(1);
HxPm=max(HxP);
WxPm=max(WxP);
Cd1=0.1; %%% Drag coefficients from CENGEL and CIMBALA 2010
Cd2=1.2;
Cd3=1.1;
Bq(1,1)=2*(WxPm*0.35*0.4+HxPm*WxPm)*Cd1*0.5*rho;
Bq(2,2)=2*(L*2.6)*Cd2*0.5*rho;
    for j=1:Nsec
        B33(j)=dx*Cd3*WxP(j)*0.5*rho*2;
        B55(j)=dx*abs(x(j)^3)*WxP(j)*Cd3*0.5*rho*2;
    end
    Bq(3,3)=sum(B33);
    Bq(5,5)=sum(B55);
Cdx=Bq(1,1)/24
Cdy=Bq(2,2)/24
Cdz=Bq(3,3)/24
```